EFFECT OF FABRIC STRUCTURE ON LIQUID TRANSPORT, INK JET DROP SPREADING AND PRINTING QUALITY

A Thesis
Presented to
The Academic Faculty

By

Shamal Kamalakar Mhetre

In Partial Fulfillment
Of the Requirements for the Degree
Doctor of Philosophy in
Polymer, Textile and Fiber Engineering

Georgia Institute of Technology

May, 2009

EFFECT OF FABRIC STRUCTURE ON LIQUID TRANSPORT, INK JET DROP SPREADING AND PRINTING QUALITY

Approved by:

Dr. Radhakrishnaiah Parachuru, Advisor
School of Polymer, Textile and Fiber Engineering
Georgia Institute of Technology

Dr. Wallace Carr
School of Polymer, Textile and Fiber Engineering
Georgia Institute of Technology

Dr. Fred Cook
School of Polymer, Textile and Fiber Engineering
Georgia Institute of Technology

Dr. Dong Yao
School of Polymer, Textile and Fiber Engineering
Georgia Institute of Technology

Dr. Yehia El Mogahzy
School of Polymer & Fiber Engineering
Auburn University

Date Approved: 05 January 2009

To the everlasting affection and support of

my dad, Mr. Kamalakar Mhetre,

my mom, Mrs. Asha Mhetre

and my sister, Sheetal

ACKNOWLEDGEMENTS

First and foremost, I would like to express my gratitude to my advisor, Dr. Radhakrishnaiah Parachuru who had full faith in me and gave me an opportunity to work with him. He gave me freedom to come up with ideas for my work and helped me surmount problems as and when they arose. It was a wonderful experience working with him. I would like to thank - Drs. Carr, Cook, Yao and Mogahzy for serving on my thesis advisory committee and for providing valuable inputs and suggestions at different stages of progress of the thesis.

I would like to express my sincere thanks to Dr. Deverakonda Sarma of Trident Company, Brookfield, CT, for providing samples of pigment ink which were used in ink jet printing and liquid sorption experiments. I would also like to thank Cotton Incorporated, Raleigh, NC. Mount Vernon Mills, Trion, GA, and Saraswati Polytex Ltd., Ahmedabad, India, for supplying specially engineered cotton and polyester fabrics for the thesis work.

Finally I would like to express my appreciation and gratitude to all my friends and associates for the encouragement and support extended by them during the course of the thesis work.

TABLE OF CONTENTS

LIST OF TABLES

LIST OF FIGURES

SYMBOLS

P	Capillary pressure
γ	*S*urface tension of liquid
θ	Contact angle
r	Radius of pore
ρ	Density
g	Acceleration due to gravity
h *or* L	Height of liquid inside capillary
L_{eq}	Equilibrium wicking height
η	Viscosity of the liquid
T_0	Thickness at zero pressure
T_m	Thickness at a pressure of 50 g/cm^2
K	Wicking coefficient or wicking rate
ϕ_c	Porosity
t	Time
ΔK	% Gain in wicking rate of longitudinal yarn
ΔL_{eq}	% Gain in equilibrium wicking height
w	Weight of liquid absorbed in fabric
A	Area of drop spreading
K_D	Drop spreading rate
D	Drop spreading distance
W_L	Weight of liquid retianed by fabric
L_F	Length of fabric

W_F Width of fabric

T_F Thickness of fabric

V_d Drop volume

ϕ^* Effective porosity

E_{lw} Excess line width on transverse threads

SUMMARY

Sorption is an important performance property of apparel fabrics. Different techniques have been developed and used to characterize and compare the liquid transport or sorption properties of textile structures. The influence of different chemical treatments and finishes on absorption properties of yarns and fabrics has also been studied using these techniques. Although liquid transport studies have been carried out on different fabrics, the influence of fabric structural features has not been fully explored. Further, almost all of the previous liquid transport studies consider textile assemblies as single capillaries, even though these materials consist of capillaries that vary in diameter and length and are interconnected in a complex manner. The phenomenon of liquid migration during sorption from one yarn to another yarn and back to the first yarn is often overlooked despite the fact that it is an important part of the sorption process in fabrics. This work focused on the effect of fabric structure and yarn-to-yarn liquid migration on the overall liquid transport behavior of fabrics. Sorption of liquid from an unlimited reservoir as well as sorption of a limited quantity of liquid by fabrics representing different structural parameters has been studied. Absorption of liquid from an unlimited reservoir is studied by the weight balance and image analysis techniques and the results obtained for the two techniques are compared. Sorption of a limited quantity of liquid is studied by performing drop spreading experiments on fabrics. The spreading and wicking of micron sized drops deposited on fabric surfaces during ink jet printing is also studied. The nature of influence exerted by the fabric structure related variables on the spreading behavior of ink drops and how exactly the spreading influences printing quality has been

investigated. The influence of spreading behavior on dithering of ink was studied by printing solid figures on experimental fabrics. Further, an attempt was made to relate the quality of lines printed on fabrics to the observed sorption behavior of ink from limited and unlimited supply sources.

Results showed that wicking in fabrics is determined by the wicking rates of yarns, thread spacing, and more importantly by the rate at which liquid migrates from longitudinal to transverse threads and again from transverse threads back to longitudinal threads. Comparison of wicking results obtained by weight balance and image analysis methods showed that weight balance method cannot be used in place of image analysis method, especially when measuring the wicking properties of more open fabrics. While drop spreading rates were dependent on fabric structure, the relation between drop spreading rate and fabric structure was found to be very complex in nature. In general, thin and compact cotton fabrics showed the highest values for drop spreading rate. Higher drop spreading rates were also observed in thin polyester fabrics. Drop spreading rates were found to be influenced primarily by the phenomenon of liquid migration from yarn to yarn.

Ink jet printing of experimental fabrics with pigment ink showed that fabrics whose yarns are characterized by narrow and continuous surface capillaries give raise to excessive drop spreading and higher line widths. Thus yarn surface characteristics were found to play a greater role than fabric construction parameters in determining the quality of ink jet printing.

CHAPTER 1
INTRODUCTION

Textile fabrics play an important role in the day to day life of every human being. They are used not only as clothing materials but also in many life saving end uses and a host of industrial applications. Their applicability for many end uses is determined by their liquid transport properties. Many techniques have been developed and used to characterize and compare the liquid transport properties of textile structures. Although liquid transport studies have been carried out on different fabrics, the influence of fabric structural features has not been fully explored. The phenomenon of liquid migration during sorption from one yarn to another yarn and back to the first yarn is often overlooked even though it is believed to be an important part of the sorption process in fabrics. Therefore the main goal of this research is to understand the effect of fabric structure and yarn-to-yarn liquid migration on the overall liquid transport behavior of fabrics.

The technology of ink jet printing has evolved rapidly in the last decade or so and it is now a well established technique for the printing of textile fabrics. Ink jet printing system essentially involves the delivery of ink to a medium in the form of small droplets. Among different inks, pigment ink has become more popular because of its ability to give fuller and brighter shades without the need for any pretreatments. Pigment ink is directly applied on the fabric and then the ink is cured by the application of hot air or by UV treatment. Because there is no pretreatment of the fabric involved, the printing quality of pigment inks can significantly depend on the fabric structure. How the fabric structure related variables influence the spreading of ink drops and how exactly spreading

influences printing quality is investigated in this research. The spreading of drops on different fabrics has been studied under a microscope and the relationship between spreading behavior and printing quality has been investigated by printing lines on fabrics. Further, an attempt was made to relate the quality of lines printed on fabrics to the observed sorption behavior from an unlimited reservoir and also to the observed drop spreading behavior.

Review of studies conducted by different researchers on liquid transport through yarns and fabrics is presented in section 2.1., along with a comprehensive review of the capillary theory of absorption and liquid flow. Ink jet printing technology and the results of previous printing studies on textile fabrics are reviewed in section 2.2. Scope of the project and the specific objectives the thesis are described in Chapter 3. The experimental plan is described in Chapter 4. Findings of the thesis are presented in Chapters 5 and 6.

CHAPTER 2
LITERATURE REVIEW

2.1 Liquid Transport in Yarns and Fabrics

Investigation of kinetics of liquid transport through fabrics is important not only from the point of view of end use performance of fabrics in everyday apparel and specially engineered apparel products, but also to maintain efficiencies and functional requirements of the multiple wet processes of scouring, de-sizing, bleaching, dyeing, finishing, etc.

Rate of absorption of liquids by fabrics is affected by the nature and size of the small capillaries present in textiles. Liquid transport which occurs through the capillaries is called wicking. In wicking, water is transported due to the capillaries present in the fabrics and water is stored in the capillaries that are formed between fibers and yarns. Thus the primary driving forces responsible for the movement of liquid in textile structures are the forces of capillarity which originate from the surface and interfacial tensions at the phase interfaces of the system.

Theory of liquid flow in narrow, closed and continuous capillaries is well developed [1, 2]. According to the theory, capillary forces are governed by the properties of liquid, contact angle and geometric configurations of the pore structures. For an ideal capillary, capillary pressure (P), because of which transport of liquid occurs inside

capillaries, is a function of surface tension of liquid (γ), contact angle (θ) and radius of pore (r_i) and its magnitude is given by the Laplace equation (equation1).

$$P = \frac{2 \times \gamma \times \cos\theta}{r_i} \tag{1}$$

If the capillary pressure (P) is greater than the pressure of a liquid column inside capillary, then liquid is driven upwards due to the net positive force. The pressure of a liquid column inside capillary is $\rho_L gh$ where ρ_L is the density of a liquid g is the acceleration due to gravity and h is the height of liquid inside capillary. Liquid rises until both pressures become equal, at which, the net force driving the liquid becomes zero. Height of the liquid column at this position is called 'equilibrium wicking height' (L_{eq}) and it can be expressed by the following equation,

$$L_{eq} = \frac{2 \times \gamma \times \cos\theta}{r_i \times g \times \rho_L} \tag{2}$$

In classical capillarity theory, the rate of rise of a liquid in a vertical cylindrical capillary tube is given by the following equation developed by Washburn [3]. This equation describes the kinetics of liquid movement in an ideal capillary. Kinetics of wicking in textile structures such as yarns and fabrics is often investigated by fitting the experimental data to famous Lucas-Washburn equation. When the effect of gravity is neglected, at low values of t and when the height of liquid rise (L) is much smaller than L_{eq}, Lucas-Washburn equation is given by,

$$L = \sqrt{\frac{r_i \times \gamma \times \cos\theta}{2 \times \eta}} \times t^{0.5} = K \times t^{0.5} \tag{3}$$

Where, η is the viscosity of the liquid. Parameter K is often referred as wicking coefficient or wicking rate and determined by fitting the experimental data to equation 3.

Capillary theory discussed above forms a fundamental basis for the studies of liquid transport in textile structures since textile structures also comprise large number of capillaries which are formed due to inter-fiber and inter-yarn spaces. These capillaries are however, open, discontinuous, and are connected in a very complex manner. Liquid transport in textile structures has been studied by several methods. These methods are based on three modes of wetting:

(a) Total immersion of the substrate inside liquid

-where time required for a sample to completely sink inside the liquid is measured.

(b) Absorption of a liquid from an unlimited reservoir

- where one end of yarn segment or fabric strip is immersed in a liquid and weight or height of the liquid absorbed in fabric is measured.

(c) Absorption of a limited liquid quantity, such as a drop of a liquid

-where either the time needed for the drop to sink into the fabric or the area covered by the spreading drop is measured.

First method, although simple and quick, is rarely used for research purposes as it gives very limited information about the pore structure and the kinetics of the absorption process. The other two methods have been widely used by researches as they give

relevant information and mimic the spreading process of many industrial operations. The findings of these studies on yarns and fabrics are summarized in the following sections.

2.1.1 Sorption from an Unlimited Quantity of Liquid

2.1.1.1 Sorption in Yarns

Several basic studies have been carried out on liquid transport through yarn from an unlimited reservoir. Researchers have used different techniques to quantitatively analyze the liquid flow through yarns. Commonly used technique consists of observing and measuring the liquid front when liquid is flowing through vertically or horizontally clamped yarn with its one end dipped in an infinite quantity of liquid [4]. In advanced versions of this technique, liquid flow is measured by analysis of CCD images taken during the capillary rise of colored liquid in yams [5]. Another technique is setting liquid-sensitive sensors regularly along the yarn segment [1].

In the last technique, the weight variation of the liquid in the yarn or force exerted by the liquid on yarn can be measured with a sensitive electronic balance [2, 6-8]. Bayramli et al. [9, 10] used it for glass fibers coated in various ways and thus could measure axial capillary flow. However, this technique is too delicate to use with spun staple fiber yarns, because of the flexible nature of the yarns and also due to the fact that wetting force can exceed the effects of capillary forces. Use of this method is more difficult in the case of texturized yarns as they exhibit a tendency to recoil.

All of the above studies have showed that wicking of liquid in yarns follows the Lucas-Washburn equation (equation 3). The experimental data obtained using the above methods is often fitted to equation 3 to determine the wicking coefficient. Capillary

radius can also be determined if the liquid properties -surface tension, viscosity and contact angle for the solid-liquid pair are known.

A small group of researchers have studied the transport of liquid through yarns having complex cross sectional geometry [11, 12]. Unusual and complex geometries arise due to the use of triangular, square, elliptical or criss-cross shaped fibers in yarns instead of usual round shaped fibers. Zhang and coworkers [11] modeled the liquid flow in yarns consisting round, square, triangular and criss-cross shaped fibers using integrated Reed-Wilson and shaped fiber bundle mathematical simulation model (MFB). They determined the parameters such as number of capillaries and average capillary radius by analyzing the fiber bundle cross-sectional images simulated from MFB. The authors observed the highest initial wicking rate in the case of cross fibers followed by double-cross, triangular, square and round fibers. Highest equilibrium height was observed in the case of cross fibers followed by double cross, round, triangular and square shaped fibers.

In a similar study, Rajagopalan and Aneja [12] modeled yarns having circular and elliptical fibers in Polyflow. They used their models to understand the effect of geometric and material parameters on liquid transport. Their models predicted that as the non-roundness of the filament increases, or the void area between the filaments decreases, the maximum liquid height increases while initial rate of wicking decreases.

For twist-less filament yarns, rate of wicking and equilibrium wicking height have been shown to depend upon packing density. Effective capillary radius is lower when packing density is higher. Packing density changes with the tension applied on the yarn. Liu et. al. [13] observed the effect of tension on wicking height in their study on effect of twist on wicking. They observed that initially, wicking height increased rapidly with

tension and then became steady (Figure 1). At certain tension level yarns attained maximum packing density which remained constant on any further addition of tension. Noyni and Brook [4] also observed similar trends in their research.

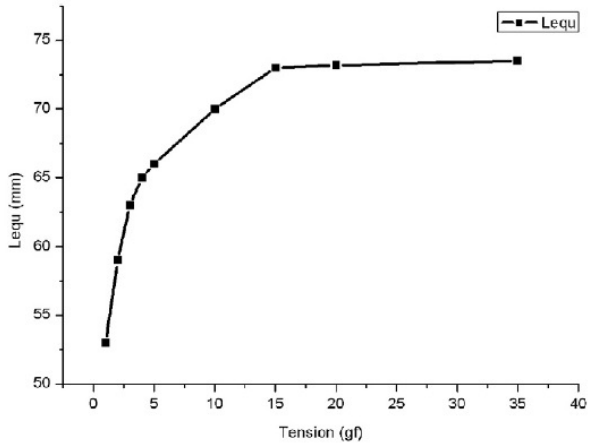

Figure 1: Equilibrium wicking height in twist-less yarn as a function of tension applied on yarn Liu et. al.[13].

While most of the research has been done to understand the kinetics of liquid transport through yarn or fabrics, there are some studies dedicated to modeling of equilibrium wicking height. These studies argue that equilibrium wicking length is important in many applications from practical standpoint of view.

Wiener and his coworkers [14] proposed such a model which was based on the simplified description of the thread structure as shown in Figure 2. This model assumes twist-less continuous filament yarn and along with other usual parameters, it includes parameters such as fineness of fiber, number of fibers at the cross section in the bundle and packing density. At equilibrium the force of gravity is compensated by the resultant

interfacial force. On the basis of this consideration and stated assumptions, the authors expressed the maximum suction height by the following equation (equation 4) .

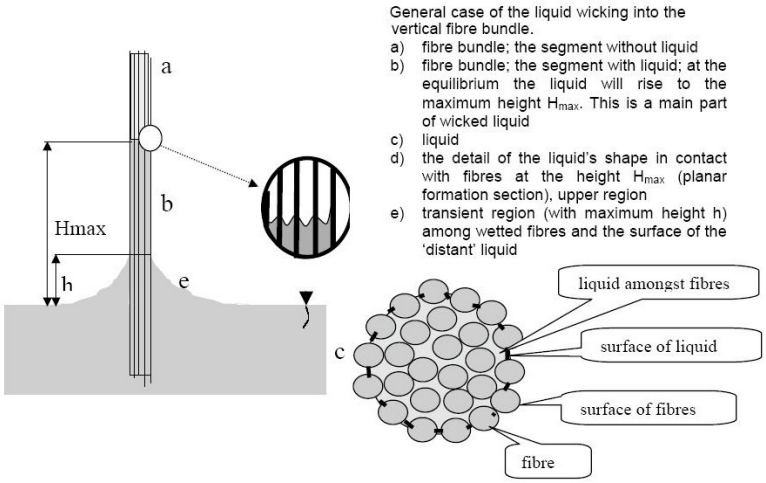

Figure 2: Model assumed by Wiener et. al. [14].

$$H\max = \frac{\sigma_{LG} \times \cos(\Theta) \times 2 \times \mu - \left(\frac{2}{100} \times \sigma_{LG} \times \sqrt{\frac{\mu}{N}} \right) \times (Q \times \cos(\Theta) + P)}{R_V \times (1-\mu) \times g \times \rho} \tag{4}$$

where:

H_{max} - equilibrium suction height, m

N - number of fibers in bundle

R_V - radius of fiber, m

P - part in percent of liquid from surface of bundle, %

Q - part in percent of non-wetted fibers from surface of bundle, %

μ - filling

ρ - density of liquid, $kg.m^{-3}$

σ_{LG} - interfacial tension liquid-air, $N.m^{-1}$

Θ - contact angle

In another study Liu et. al. [13] developed model for wicking in twisted yarns using macroscopic force balance approach and capillary penetration mechanism. Capillary force F_c can be expressed in terms of an upward force F_{cu} arising from the interaction between the liquid and the fibers, and a downward force F_{cd} which arises due to the concave liquid–gas interface as shown in equation 5. Downward force F_{cd} equals $P_l\gamma$ where P_l is perimeter of the yarn and $\gamma$is surface tension of the liquid.

$$F_c = F_{cu} - F_{cd} = F_{cu} - P_l\gamma \tag{5}$$

Further, the authors developed analytical equation for the force component F_{cu}.

$$F_{cu} = \frac{4\pi\varphi H\gamma}{\rho_f \bar{r}_f} \int_0^{r_y} \frac{r\cos(\theta_a + \alpha)}{\sqrt{H^2 + 4\pi^2 r^2}}\, dr \tag{6}$$

where ϕ is packing fraction of fibers in the yarn, r is radius of the fiber helical path, H is pitch length of the helix of the fiber path, ρ_f is density of fiber, θa is advancing contact angle between the liquid and the fiber, r_f is average radius of fiber, L_f is fiber length, r_y is radius of yarn and α is given as.

$$\alpha = \arccos\left(\frac{H}{\sqrt{4\pi^2 r^2 + H}}\right) \tag{7}$$

L_{equ} can be calculated using the following equation.

$$L_{\text{equ}} = \frac{F_{\text{c}}}{\rho_{\text{l}} g A} \tag{8}$$

where ρ_{l} is density of liquid, g is gravitational acceleration and A is area available for liquid flow in yarn cross section.

The authors further expressed wicking time (t) as a function of length of capillary rise in yarn, equilibrium wicking length and a parameter that depends on twist and coefficient as shown in equation 9.

$$t = N\left(L_{\text{equ}} \ln \frac{L_{\text{equ}}}{L_{\text{equ}} - L} - L\right) \tag{9}$$

$$N = \frac{\lambda k}{\rho_{\text{l}} g A} \tag{10}$$

Where L is capillary rise, k is frictional coefficient and λ is twist coefficient.

As can be observed in Figure 3(a) calculated equilibrium length values using equation 8 for yarns with different twist levels matched fairly well with experimental results. Authors attributed discrepancies in the results at low twist levels to the deviation of packing of the fibers from the idealized open-packing. Good agreement between theoretical and experimental results at high twist levels is seen possibly because yarns do achieve idealized packing geometry at high twist levels. In kinematic studies of liquid transport in twisted yarns, the authors observed that parameter N varies linearly with twist level (Figure 3(b)). Thus, from linear model, N can be predicted from known twist level value and with the help of calculated L_{equ}, dynamics of liquid transport in twisted yarns can be predicted.

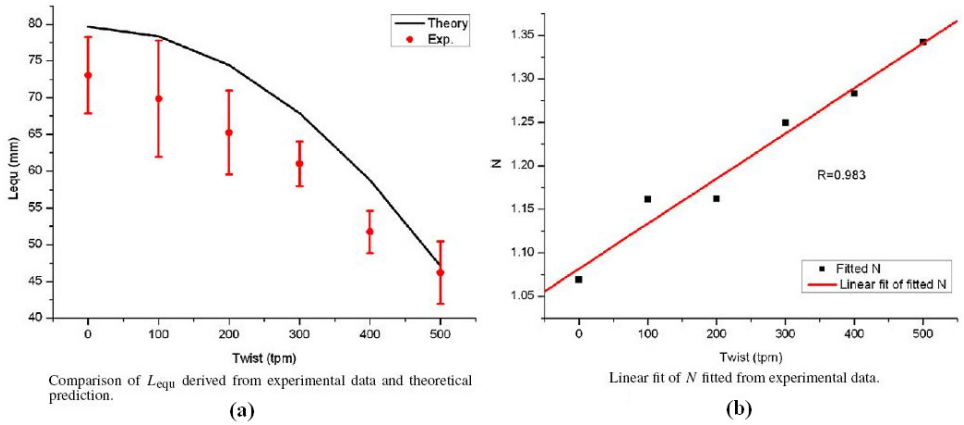

Figure 3: Results of experimental studies on twisted filament yarns; Liu et. al. [13].

Studies carried out on sorption of liquids in fabrics from unlimited reservoir are reviewed in the next section.

2.1.1.2 Sorption in Fabrics

Wicking of liquids in fabrics from an unlimited reservoir is typically studied by immersing one end of vertically hung fabric strip in liquid bath. Measurements can be carried out in different ways. Height of the liquid rise with time can be measured manually using a ruler, using electrical sensors or by the analysis of the images taken during wicking. Alternatively, the weight absorbed by fabrics with time can be measured by electronic micro-weight balances or the force exerted on fabrics can be measured by micro force gauges. In another simpler method, height or weight of the liquid in fabric is measured after certain standard time.

Wicking studies have been widely used to compare the wettability and absorption properties of different types of fabrics. For example, Hollies et.al. [1] studied the wicking of liquids in fabrics and in yarns from those fabrics using electrical sensors. The

fabrics were made from cotton, wool, nylon, polyester and blends of them. The transport of water along fabrics was shown to depend on the laws of capillary action. The authors also found that the rate of travel of water in these capillaries was readily reduced by the presence of randomly arranged fibers in the yarn. Authors concluded that orientation of fibers is more important than the nature of the fiber material in blended fabrics. They further found that the rate of travel of water in a group of wool-type blended fabrics can be well correlated with their thermal resistance properties, and both appeared to depend on the arrangement of the individual fibers in the fabrics. Random arrangement of the fibers in the yarns led to fabrics along which water travels slowly and which also possess increased thermal insulation in the moist state.

In another example, Yoon and Buckley [15] used wicking tests to compare the absorption properties of polyester/cotton knit fabrics. They observed that wicking rate was higher in the wale direction than in the course direction and the rate in an intermediate direction fell within these two limits. They observed substantial variation in wicking behavior as the fiber composition varied in the fabric samples. 100 % cotton and 50/50 blend fabrics showed a very rapid wicking behavior and the wicking rate sharply dropped as the polyester content increased.

When wicking studies are done using weight balance or force balance method, force of wetting can be observed. According to the Wilhelmy principle, when a solid is partially immersed in a liquid, the wetting force *(F_w)* exerted by the liquid on the solid is given by [2]:

$$F_w = P_s \times \gamma_{LV} \times \cos\theta \tag{11}$$

where P_s is the perimeter of the solid along touching boundary of the liquid, γ_{LV} is the surface free energy of the liquid-vapor interface or the surface tension of the liquid, and θ is the contact angle.

Figure 4 shows a typical curve of force vs. time obtained during wicking experiments. Point B in figure indicates the initial force exerted on fabric which is zero. As soon as fabric touches the liquid, force immediately increases from B to C which is mainly due to wetting. Force due to wicking is less dominant at this stage. Gradual increase in force from C to D is however due to the sorption of liquid in fabric due to capillary forces which overcome the viscous, gravitational and inertial forces. When fabric reaches its maximum absorption capacity the steady state region is observed (D to E). During the removal process some increase in force is observed due to buoyancy effects (point F). After complete removal, force drops to point G which remains steady. W_t is the total liquid retention in the vertically hung sample.

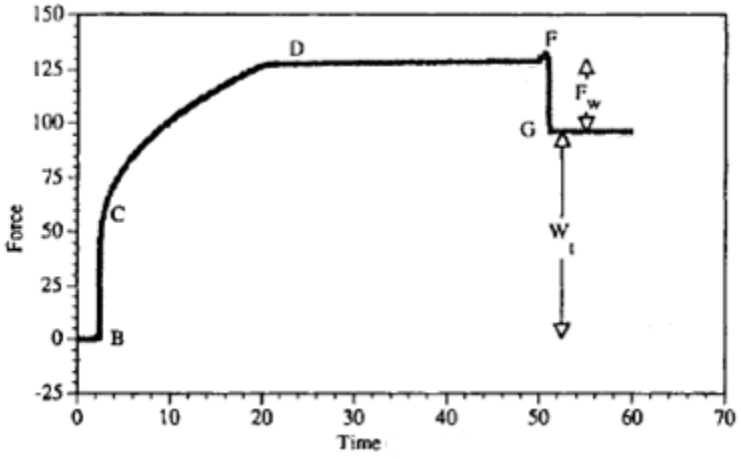

Figure 4: A typical curve of force Vs. time obtained during wicking tests.

It has also been shown by Heish and his coworkers [2, 16] that the wetting characteristics of fabrics do not depend on their configuration i.e. length of fabric, width of fabric, fabric-water interface depth, and fabric direction and it only depends on the material (fiber) properties. This means that wettability of any fabric is the same as the wettability of its constituent fiber and contact angles for fiber-liquid and fabric-liquid are identical. Wicking on the other hand depends on the fabric parameters, specially the parameters which affect the pore size or pore connectivity.

Wicking studies have also been used to study the penetration of resin into composites by Patel and Lee. [17]. They carried out the experiments using the force balance method mentioned above. In their study they monitored the vertical wicking of the liquid into the fiber tows as a function of time, and the weight changes were recorded. They corrected the weights for the buoyancy, and the wetting effects. This correction was obtained at the end of the test, when the weight of the fibrous assembly is constant. The correction was then applied to all the weights from the start of the test. The corrected weight (m_{wick}) values were then converted to the height of the liquid column (h_{wick}) by the equation:

$$h_{wick} = \frac{m_{wick}}{\rho_l \times A_{cs} \times \phi_f} \tag{12}$$

Where A_{cs} and ϕ_f are the cross-sectional area and the porosity of the fibrous assembly, respectively. The porosity of the fibrous assembly was calculated using the total weight of liquid wicked in the fibrous assembly at steady state. From values of $h_{wick,}$ the authors determined permeabilities of fabrics by fitting the data to Washburn equation. The

authors found that reduction of the resin surface tension favors the wetting and wicking kinetics. Although lower fiber reinforcement porosity resulted in a higher capillary pressure, it reduced permeability. Thus there would be an optimum porosity at which the spontaneous impregnation rates are the highest.

Another important purpose wicking studies have been used for is to characterize the porosity, pore connectivity and pore size of the fabrics. Heish et. al. [6, 7] used wicking studies to determine the liquid absorption capacity, porosity, liquid uptake rate and mean or effective pore cross sectional area of cotton and polyester fabrics. The study was carried out using the force balance technique. Liquid absorption capacity (C_L) is the final weight recorded by the microbalance. Using known value of C_L , porosity (ϕ) values were then calculated by the authors using equation 13 [2],

$$\phi = \frac{C_L \times r}{1 + C_L \times r} \tag{13}$$

Where r is the ratio ρ_f , the density of fiber and ρ_l , the density of liquid.

The authors argue that vertically hung fabric method gives more appropriate values of porosity than the other methods such as mercury porosimeter, liquid porosimeter or direct determination of porosity (equation 14). The author states that mercury and liquid porosimeter gives somewhat wrong values as experiments are needed to be carried out under pressure which causes change in structure. Direct method also gives erroneous porosity values as the thickness of fabrics is measured under some standard pressure which changes the geometry of the pores.

$$\phi = 1 - \frac{\rho_b}{\rho_f} \tag{14}$$

where ρ_b is bulk density of fabric and ρ_f is density of fiber. Bulk density (ρ_b) can be calculated using the following formula.

$$\rho_b = \frac{Fabric.weight(g/cm^2)}{Fabric.thickness(cm)} \tag{15}$$

Liquid uptake rates for different fabrics were determined and compared by authors by plotting a graph of force vs. time, similar to that shown in Figure 4. Mean pore area (A_m) or effective pore cross sectional area (A_e), which are very good measures of porosity, pore connectivity and liquid transport in fabrics having different kinds of fibers, yarns, and configurations, were calculated by the authors using equations 16 and 17;

$$A_m = \frac{W_t}{l \times \rho_l} \tag{16}$$

where W_t is liquid retention amount in the fabrics at the end of liquid transport in the vertically hung fabrics. l is length of fabrics and ρ_l is density of liquid.

$$\frac{dw}{dt} = \left(\frac{\rho_l^{\,2} \times A_e^{\,5/2} \times \gamma \times \cos\theta}{4 \times \pi^{1/2} \times \eta} \right) \frac{1}{w} - \left(\frac{\rho_l^{\,2} \times A_e^{\,3/2}}{8 \times \pi^{1/2} \times \eta} \right) \times g^* \tag{17}$$

where w is mass uptake of liquid, A_e is effective pore cross sectional area, g^* is the effective gravity in the direction of liquid movement and η is viscosity of liquid. A_e and g^* are determined from the slope and interception of the plot (*dw/dt vs. 1/w*).

To acquire information about pore size and level of pore connectivity, the authors conducted liquid transport experiments on vertically hung fabrics of different lengths. Example of this has been shown below where experiments were conducted on fabrics whose lengths ranged from 10mm –140 mm. The decreasing trend in Figure 5 (below) indicates a reduction in saturation in the pores away from the liquid source. Slope of the curves gives the information about how fast the continuity in capillaries is decreasing.

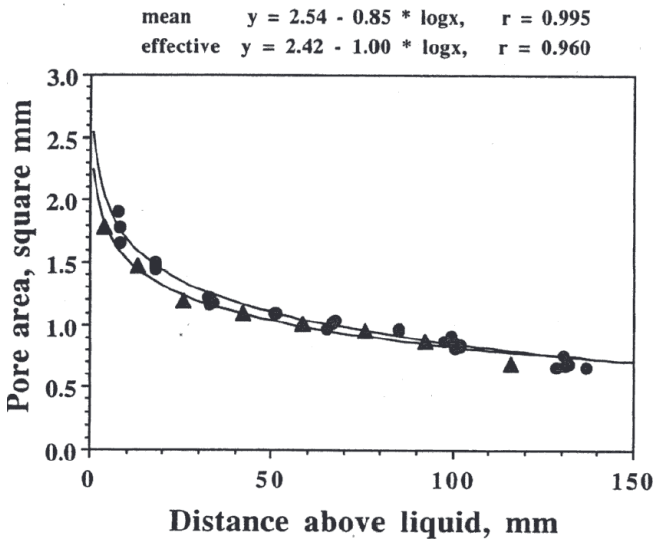

Figure 5: Mean (•) and effective (▲) pore areas in 100 % cotton fabrics at specific distance above liquid [2].

2.1.2 Sorption of a limited Quantity of Liquid

Studies on sorption of a limited quantity of liquid are often done by placing a small drop of a liquid on horizontally clamped yarn or fabrics. Some important studies which were performed on yarns and fabrics by different researchers using this method are reviewed below.

2.1.2 Drop Spreading on Yarns

Either the time required for a drop to completely penetrate inside the yarn sample or the distance travelled by a drop with time is measured in studies of this type. Capillary pressure at the liquid front is the dominant driving force for the wicking process.

Francis Manor and his coworkers performed such experiments on nylon and viscose yarns with different amounts of twist and with liquids of varying surface tension, viscosity and contact angle [18]. The size of droplets they used ranged from 3mm – 6mm in diameter. The size of yarn was much smaller; around 0.15 mm. The authors used the bigger sized drops so that they could observe for a longer time the wicking of droplets at various stages of drop depletion. Figure 6 shows the wicking of Ucon 50-HB-55 and polyethylene glycol in the loose nylon yarn. Graph shows that after a period of linear continuous region, wicking becomes nonlinear and progressively decelerated.

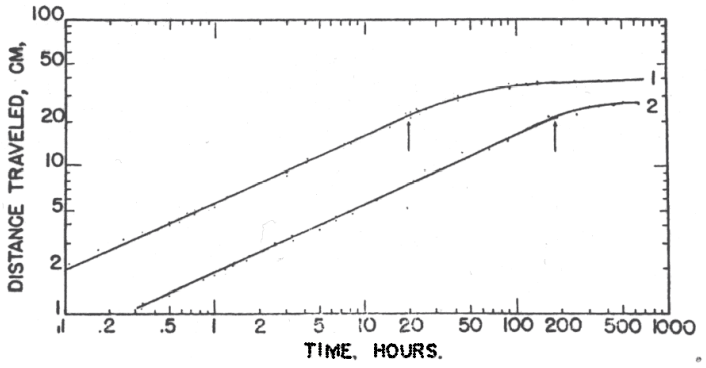

Figure 6: Wicking of Ucon 50-HB-55 (curve 1) and polyethylene glycol (curve 2) in loose nylon yarn [18].

Higher wicking rate for Ucon liquid was observed as it was a better wetting liquid than polyethylene glycol. The other important thing in the graph is that Ucon liquid

continued to wick even after the drop disappeared completely from yarn surface. Authors attribute this behavior to the difference in contact angle hysteresis among the various fiber-liquid systems. High contact angle hysteresis inhibits the wicking of liquid from bigger radius capillary to narrow radius capillary after the drop is completely absorbed into yarn. Their experiments on different yarns showed that for the period prior to the disappearance of the drop; Washburn's equation $h = K \times t^{0.5}$ was obeyed and the wicking rates were similar to those obtained from wicking studies which were carried out using unlimited reservoir. This showed that before the drop disappears, more liquid is always available for the yarn to take up, and as wicking proceeds, the reservoir becomes progressively depleted and Washburn's equation ceases to express correct wicking trend.

Further, the authors found that the rise of liquid is significantly higher in the case of open yarns (low twist). Authors observed very low level of wicking in the tightly packed viscose yarns compared to tight nylon yarns. They attributed this diminished wicking to the better packing efficiency of viscose fibers. Higher wicking rates than expected were observed in case of viscose filament yarns due to crenulations on the fiber surface, which also act as capillaries. The distribution of wicking liquid across the yarn segment was also measured by the authors. They found that the distribution pattern varies within yarn and also from liquid to liquid due to contact angle hysteresis.

In a more recent study, the wicking kinetics of liquid droplets into yams was studied by Chen and his coworkers [19] by a slightly different approach. They monitored droplet absorption using a computerized imaging system and analyzed the time needed for droplet disappearance as a function of droplet volume for various yams. The authors showed that for the liquids which can easily wet the yarns, the time of droplet absorption

T_w is a linear function of the square of initial droplet volume V_0^2. Authors state that the slope of this relationship provides important information about the porosity and capillary structure of yam. A mathematical model was also developed to describe the wicking kinetics. Their model predicts that droplet wicking can occur even if the advancing contact angle is slightly greater than 90°. However, for these liquids, the relationship between T_w and V_0^2 is nonlinear. Porosity and hydraulic radius values for different yarns were calculated by fitting the data to the model.

2.1.2 Drop Spreading on Fabrics

In drop spreading studies on fabrics, typically, a small drop is placed on fabric and the area covered by the drop with time is measured. A radial flow geometry allows the simultaneous study of more than one inflow direction. The shape and rate of a radially advancing fluid front can be used to determine the directional permeabilites in the plane. Thus drop-spreading studies can also be effectively used to compare structurally different fibrous networks.

Drop spreading study on textile fabrics is in use for many years, primarily to characterize the wettability of fabrics. In one study, Minor et. al. observed the spreading of organic liquids on textile fabrics [20]. They observed that some liquids may spread better on some fabrics than others (Figure 7). Patterns of drop spreading showed that in some samples, liquid can easily transfer from yarn to yarn while in some samples it is difficult.

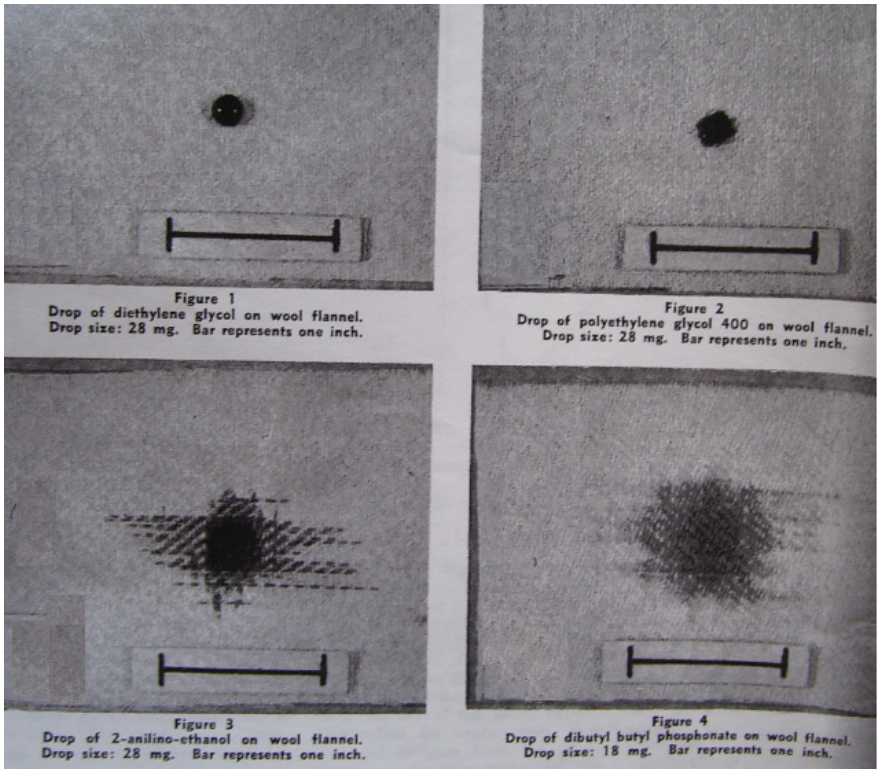

Figure 7: Drop spreading on textile fabrics observed by Minor et.al.[20].

They also observed that during drop spreading, liquid migrates or transfers from one yarn to the second yarn and they considered it as an important part of the drop spreading process. They examined this migration process using the experimental set up shown in Figure 8. Two yarns were hung in a criss-cross fashion with some contact in them. Some tension was applied to both the yarns. A big drop of liquid was placed on one of the yarns away from the intersection and the movement of liquid was observed. Distance traveled by the liquid in both the yarns in a given time or the time required for the liquid front to reach a specific distance can be measured and can be used to describe the migration process.

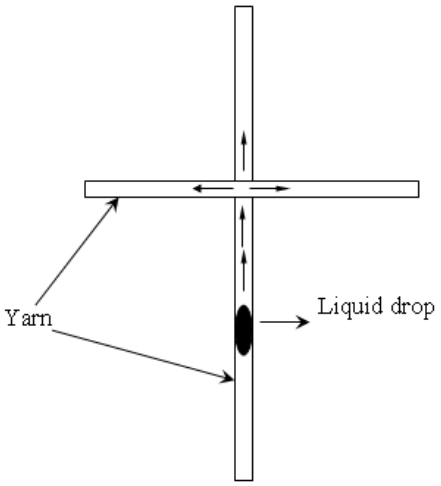

Figure 8: Experimental setup used by Minor et. al. to study the yarn to yarn liquid migration

The kinetics of the spreading of a drop is more complicated than the wicking of a liquid in fabric from an unlimited supply source. Mathematical analysis of the kinetics of drop spreading was first performed by Gillpesie [21]. According to his study, the spreading process needs to be viewed as occurring in two phases. In the first phase, the spreading occurs while the liquid drop is still present on the fabric, as shown in Figure 9. Phase 2 indicates the spreading process after the liquid drop placed on the fabric is completely absorbed in the fabric.

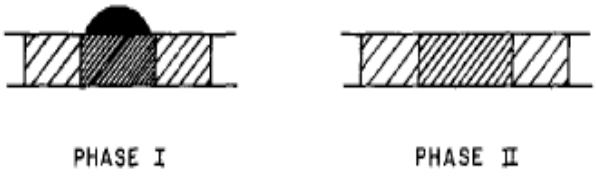

Figure 9: Spreading of a drop on a porous substrate: (a) phase I - liquid is sinking into the substrate and spreading, and (b) phase II - the spreading liquid is contained within the substrate [21].

Gillpesie studied the spreading of low vapor pressure liquid drops in various types of filter paper and in printflex card [21]. The diameter of the spreading liquid was measured as a function of time, using a microscope. For phase II spreading, Gillespie developed a rather complicated model for two-dimensional circular spreading as given in equation 18.

$$R^2[R^4 - R_0^4] = \frac{3\beta}{2}\left(\frac{3V}{2\pi h}\right)^2 t \tag{18}$$

Where R denotes the radius of the stain, R_0 is the radius of the stain at time zero, V is the volume of the liquid, h the thickness of the substrate, t is spreading time, and β is given by

$$\beta = \frac{bq_s\gamma \cos\theta}{c_s^3\eta} \tag{19}$$

Where b is a constant descriptive of the substrate, q_s is the permeability of the substrate, γ is the surface tension, η is the viscosity of the liquid, θ the advancing contact angle, and C_s the saturation concentration of the liquid in the substrate.

The Gillpesie's model was simplified by Kissa in his study on capillary sorption in fibrous assemblies [21]. Kissa's generalized model is shown in equation 20.

$$A = K(\gamma/\eta)^u V^m t^n \tag{20}$$

where K is a coefficient dependent on the advancing contact angle of the liquid on the fibers, the permeability and thickness of the fabric, t denotes the spreading time, γ the surface tension, η the viscosity, and V the volume of the liquid.

Kissa measured the spreading area of a liquid drop on fabric and paper as a function of time by simultaneously photographing the spreading liquid and a timer. The area depicting the spreading liquid was cut from the photograph and weighed. The method was calibrated by photographing a standard area. For liquid impermeable fibers (such as polyester), the exponents, u, m, and n were found to be 0.3, 0.7, and 0.3, respectively. For n-alkanes spreading on polyethylene terephthalate/cotton, polyethylene terephthalate, and cotton fabrics, Kissa found that the equation holds when the fibers are impermeable to the spreading liquid. However, when the liquid diffuses into the fibers, the exponent n was found to depend on the drop volume.

Drop spreading on textile fabrics was further studied by Kawase and his coworkers [22]. Kawase studied drop spreading dynamics on the fabrics containing liquid permeable cotton, rayon and nylon fibers. He found that during phase I, the capillary spreading can be reasonably approximated by sorption from an unlimited reservoir into porous substrate. As the external pressure driving the liquid is negligible compared to capillary pressure, spreading follows the generalized Washburn equation given below.

$$V_s = K(\gamma/\eta)^{0.5} t^{0.5} \tag{21}$$

For phase II, he found that values of n are much smaller than the theoretical value of 0.33 and also they vary with the volume of drop, increasing from 0.10 to 0.15 when the drop volume increases from 0.05 to 0.20. The author argues that this is because of diffusion of water inside cotton fibers at longer time periods. In the same research, Kawase also showed that, n is also affected by the atmospheric conditions and the hydrophilicity of the fabric surface. He also observed that for liquid water and rayon

fiber, the value of n remains constant at 0.14 for all drop volumes. Also, the water drop did not penetrate into nylon and PET fabrics owing to the larger apparent contact angle. He attributes the unusual behavior of rayon to its high water absorptivity, longer capillary lengths, and crenulated cross section. For phase II, for impermeable fibers, the exponents, u, m and n are 0.3, 0.7 and 0.3 respectively. For permeable fibers, Kawase found that the exponent n decreases, m increases and the exponent u remains almost constant. Thus the exponent n correlates with the hydrophobicity of the fibers.

In their next study, Kawase and his coworkers [23] investigated the effects of softening agents on the wetting of textiles by measuring the capillary spreading of liquid as a function of time. The values of the exponent n during phase II of the capillary spreading of softened fabrics increased in comparison with those of unsoftened fabrics, owing to the adsorption of the softening agent, which made the fiber surface more hydrophobic and produced a larger advancing contact angle of the fiber to the water (θ_A). Based on experiments with DTAC as a softening agent for nylon, the following quantitative relationship was found between the value of the exponent n and the advancing contact angle of water (θ_A): $n = (4.62 \times 10^{-3})\theta_A$, - 0.001. From this, reasonable advancing contact angles were also estimated for other fabrics.

Adams et. al. in their paper [24] have presented an in-plane flow technique that allows experimental quantification of directional in-plane permeabilities and flow anisotropies that can be used to characterize a wide range of fibrous networks. The authors determined the directional permeabilities using the models which were derived from mass and momentum balance equations. They showed that directional permeabilities depend upon only fabric structure and are independent of driving pressure,

fluid viscosity and fiber surface wettability properties. According to their analysis, two fabrics with identical structural features will have identical directional in-pane permeabilities, regardless of fiber type, because the experimental driving pressure is large enough to ignore capillary pressures in the systems.

In a more recent study by Arora et. al. [25], dynamics of drop spreading on fibrous porous substrates used in composite processing was investigated microscopically. They tracked the spreading front of silicon oil drops on borosilicate glass, quartz, and two different kinds of glass fiber mats: a woven fabric and an unidirectional mat. For the woven fabric, they found that spreading front progresses in steps of increasing and decreasing rate. For the unidirectional mat, spreading occurred primarily in the direction of fibers and the spreading front progressed with gradual decreasing rate. In order to compare results with other porous substrates, the authors fitted the experimental data to a power law model as shown in equation 22.

$$R(t) = R_0(1 + kt^n) \tag{22}$$

where $R(t)$, R_0, k, and n are spreading radius, initial spreading radius, spreading constant, and spreading exponent, respectively.

Their experimental data showed that for 3–15 μl drop sizes, two power exponents are required to describe the complete spreading, whereas for 27 μl drop, single power exponent is sufficient. Spreading behavior of 7 μl and 27 μl drop is shown in Figure 10. The transition between the two power law regimes has been indicated by a dashed line in the same figure.

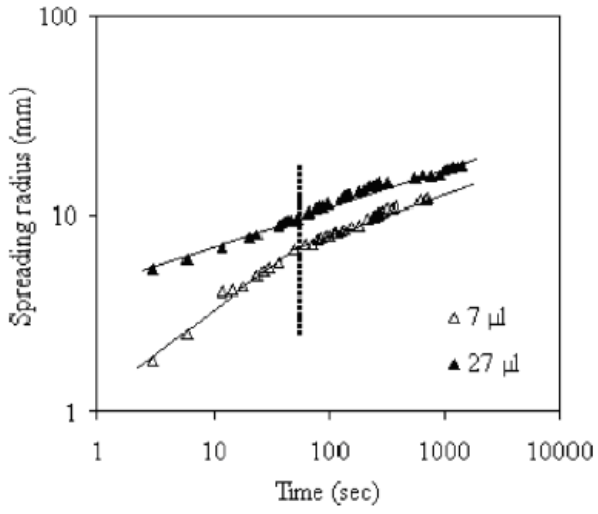

Figure 10: Variation of spreading radius with time for silicon oil on unidirectional mat [25].

The authors argue that this behavior originates from the interplay of inertial, capillary and gravity forces. Gravity plays a bigger role in the spreading of a 27 µl drop than in the spreading of a 7 µl drop. Gravity retards the spreading rate. The authors observed that the power law exponent applicable for the initial spreading of a 7-µl drop is higher than that for the later stage of spreading. This is due to the fact that mainly forces of inertia and capillarity act during the initial phase, whereas in the later stage of spreading, only the capillary forces contribute to the spreading.

In another similar study [26], wetting dynamics of silicon oil (SO) and polyvinyl-alcohol-water solution was investigated on a unidirectional mat (UDMAT) and woven fabric (WF). The drop-spreading behavior was examined by measuring the contact radius, height and contact angle. The authors observed that the height of the drop decreased monotonically. Spreading behavior for PVA and SO differed qualitatively and quantitatively. More spreading was observed for PVA before imbibition. PVA drops after

spreading to a large extent, imbibed extremely rapidly into the porous media. While, silicon oil drops spread and imbibed at equivalent rates. It was noted that the volume imbibed into the porous media varied linearly with time for PVA and varied as a square root function of time for SO.

2.2 Inkjet Printing on Textile Fabrics

Ink jet printing of textiles evolved at a rapid pace in the last few decades. It is now a well established technique but it is still being used mainly for special and short run printing purposes. Rapid technological advancements and increasing productivity and industrial acceptance rates are the signs of a bright future for ink jet printing of textiles. This technology can be expected to play a significant role in the bulk production of printed textiles in the near future. Moreover, ink jet printing technology is being used not only for conventional color printing of textiles but also for some smart applications such as printing of biological and electronic materials on textile fabrics for sensing applications [27, 28].

Canon, the global manufacturer of printers, demonstrated its first Bubble Jet textile printer in the mid-1990s, which could print up to 1.6 meters in width at a through put speed of 1 square meter per minute. However these printers did not get much industry attention due to the high price and low productivity. Some other models were demonstrated in subsequent years but they also did not get much attention. Dupont's Artistri 2020 printer developed in collaboration with Ichinose Toshin kogyo Company, however, won significant market adoption with about 160 printers installed by early

2006. As the technology is advancing, the Ink jet printing technology is proving to be a cost-effective solution for the short run production and just-in-time deliveries [29].

Ink jet printing system essentially involves the delivery of ink to a medium in the form of small droplets. The drops can be created and delivered to materials in various ways, which are explained in the following section.

2.2.1 Ink Jet Printing Technology

Ink jet technologies are typically classified in to two large classes namely, continuous Ink Jet (CIJ) and Drop-on-Demand Ink Jet (DOD). In CIJ technique, the jet of ink is continuously fired through the nozzle at constant speed and pressure. Instability breaks the continuous liquid jet into droplets. These droplets are either deflected by the application of electric field or allowed to fall on the material to be printed as shown in Figure 11[29]. Deflected drops are again transported to the ink reservoir. For the deflection of drops using electric field, the ink needs to be conductive, to be able to be charged.

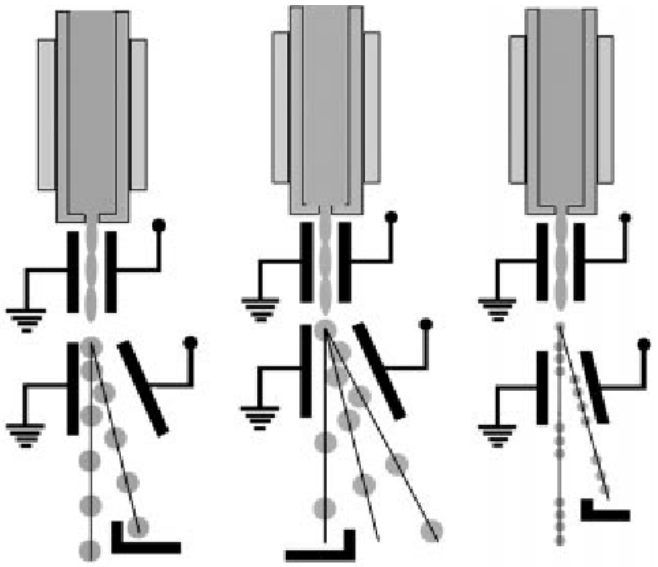

(left) Continuous ink jet – binary deflection.
(middle) Continuous ink jet – multiple deflection.
(right) Continuous ink jet – Hertz method.

Figure 11: Different methods of continuous ink jet printing [29].

In DOD technique, drops are not fired continuously as they are in the CIJ technique. Drops are created only when they are needed. There are mainly two techniques for the creation of drops: Piezoelectric Ink Jet (PIJ) and Thermal Ink Jet (TIJ). In PIJ system, the drop is created by quickly reducing the volume of the ink chamber inside the nozzle by means of piezoelectric actuators. The reduction of volume squeezes the ink droplet out of the nozzle. In the TIJ system, the temperature of a small heater located inside the chamber is raised to very high level to nucleate a bubble of ink inside the chamber. The explosive expansion of the vapor bubbles squeezes a drop of the ink out of nozzle. Piezoelectric actuators in PIJ system and thermal heaters in TIJ system can be placed in various forms inside chambers. One example of each system is shown in Figures 12 and 13[29].

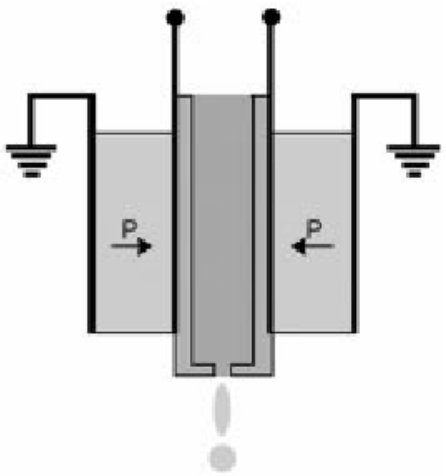

Figure 12: Drop-on-demand piezoelectric ink jet- squeeze mode [29].

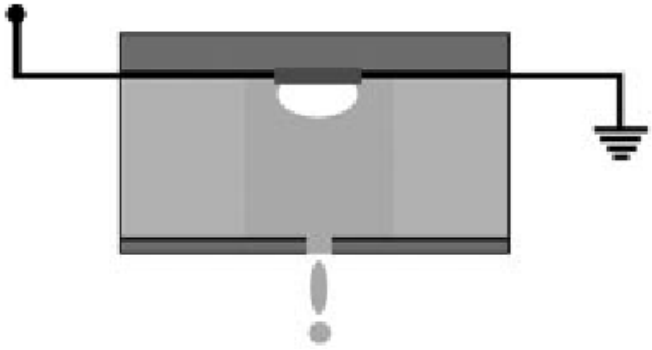

Figure 13: Drop-on-demand thermal ink jet- roof shooter [29].

Cost of the CIJ print heads are higher than the DOD print heads due the complexities associated with the CIJ system. However they are used in the industry quite often as operating frequency (number of drops per second) is much higher than that of the DOD systems [29].

Strength and weaknesses of the various technologies

Both PIJ and CIJ systems of drop creation have their own advantages and disadvantages. Reduction in volume that can be achieved using piezoelectric actuators is very small compared to what can be achieved by nucleation and expansion of the bubble. For this reason, packing density of nozzles in the PIJ system is very small, which limits the native resolution (number of nozzles per inch in the direction of the nozzle array). Another advantage of TIJ system is that the heaters required for drop nucleation can be simultaneously printed while electronic circuit is printed on the print head. Piezoelectric actuators however, need to be placed separately in the print heads. Therefore, TIJ print heads are less expensive and more compact than PIJ print heads. TIJ print heads are also considered good for printing quality as the possibility of dissolution of air in the ink and creation of small air bubbles in ink is small, compared to that of PIJ system. The presence of small air bubbles in ink lowers the image quality drastically.

A clear advantage of the PIJ system over TIJ system lies in the choice of ink type (latitude). Though some special inks have been developed for the TIJ system, only aqueous inks are commercially available for this system. Water is considered as the best medium for inks as it generates the necessary vapor pressure for bubble generation. Other solvents such as alcohols can not produce vapor pressure enough to eject a drop. Piezoelectric heads, on the other hand, can easily fire any fluid provided that the fluid is within a range of operating viscosity and surface tension. Another advantage of PIJ system is the possibility it offers for the creation of drops of different sizes, using pre-pulsing technique.

In TIJ system, some arrangement is necessary to take care of the excess heat produced by the heaters. The lifetime of PIJ system is therefore considered higher than that of TIJ print heads. Heaters in TIJ print heads get fouled by ink deposits and get corroded by the solvents.

All the current ink jet technologies can only print low viscosity inks. If low viscosity inks are used to print the fabrics, then the ink or dye drops are immediately absorbed or wicked inside the fabrics. This wicking inside the yarn or fabric does not render perfect color circles, which are important for good image quality. Pretreatment of fabrics is therefore necessary to avoid this rapid wicking of ink or dye. The following section focuses on the pretreatment of fabrics for ink jet printing.

2.2.2 Pretreatments, Dithering, Fixation and Washing

Pretreatment of fabrics before ink jet printing is an additional expense and it also creates more complexities in the process of ink-jet printing of textiles. Pretreatment generally involves coating of fabrics with pastes. These pastes consist of a thickening agent and a chemical, which help the fixation of dye on the fibers. The paste also prevents the wicking and penetration of dye inside fabric. This paste and unfixed dye need to be removed after printing which adds additional expense. The pretreatment is usually necessary while printing with reactive, acid or disperse dyes. However, pretreatment is not required for printing with pigment inks. Development of pigment inks for ink jet printing took some time as early pigment inks were used to give duller shades and also

tended to block the nozzles of print heads. However newly developed pigment based inks are much better and most of their drawbacks have been corrected to considerable extent.

Most common pretreatments given for cotton and polyester fabrics are given below [29]:

Cotton (for reactive dyes)

- 100 g/l medium viscosity sodium alginate
- 100 g/l Urea
- 20-30 g/l Sodium carbonates

Polyester (for disperse dyes)

- 100 g/l cibatey AR (Ciba)
- 100 g/l Sodium alginate

Dithering

In dithering process during printing, the placing of individual drops within pixels is carefully controlled or randomized to give smooth gradations to avoid any undesirable chevron or moiré effects in the prints [30]. Dithering algorithms vary from the original, simple Bayer system to the more sophisticated Stücki method, which uses error diffusion computation methods, and similar proprietary systems.

Fixation of dyes and washing of printed fabrics

Textile fabrics printed using reactive dyes are steamed under atmospheric pressure at just over 100°C. Polyester fabrics printed using disperse dyes require to be steamed at much

higher temperature at about 170-180°C. Pigment prints are cured using hot air. Some inks are cured by UV light. Printed fabrics subjected to pretreatment need to be washed. Cold wash followed by rinse by a hot wash is often employed. Some chemicals are added in wash bath to make the un-reacted dye inactive.

One of the objectives of this research is to understand how the micron sized drops spread, penetrate or wick inside the fabrics of different structures and how they affect the final printing quality. The following sections focus on the studies that have been done to understand the wicking of liquid and droplets inside the fabric and on the quality of printing obtained on fabrics of different weaves (plain, twill, and sateen) and with different treatments.

2.2.3 Studies on Ink Jet Printing of Fabrics

A limited number of studies have been undertaken in the past to investigate the effect of fabric structure and pretreatments on the ink jet printing quality. These studies mainly use the objective means for evaluating printing quality (PQ) which are developed by ISO (International Organization for standardization, PQ standards ISO/IEC 13660 200 / CE) [31]. These standards were originally developed for printing on paper; however, these are also widely used to evaluate the ink jet printing quality of textiles. Some important quality attributes that are often used are shown in

Table 1.

Table 1: Attributes used for printing quality assessment [32].

Image element	Quality attribute
Dot	• Dot location • Dot gain • Dot shape • Edge raggedness • Satellites
Line	• Line width • Edge sharpness • Edge raggedness • Optical density • Resolution (modulation)
Solid area	• Optical density (tone reproduction) • Color (lightness, chroma, hue, gamut) • Noise (graininess, mottle, background, ghosting)

Fan and Kim [32, 33] investigated the effect of weave of fabrics and pretreatment on the ink jet printing quality. They compared the width of lines that were printed on fabrics with width of lines printed on photo paper. They noticed that excessive wicking of ink in yarns renders wider lines, which hampers the printing quality. They found that plain weave fabrics have the highest line width gain followed by twill and sateen fabrics. Knitted fabric showed the lowest line width gain as shown in Figure 14. However no clear conclusion could be drawn about the effect of fabric structure on ink jet printing quality as the above fabrics had different types of finish on them. Depending upon finish,

characteristics of the fabrics varied from hydrophilic to hydrophobic as shown in Figure 15. As the inks were water based, higher water/alcohol wicking ratio (more hydrophilicity) promoted the wicking in yarns to render wider lines.

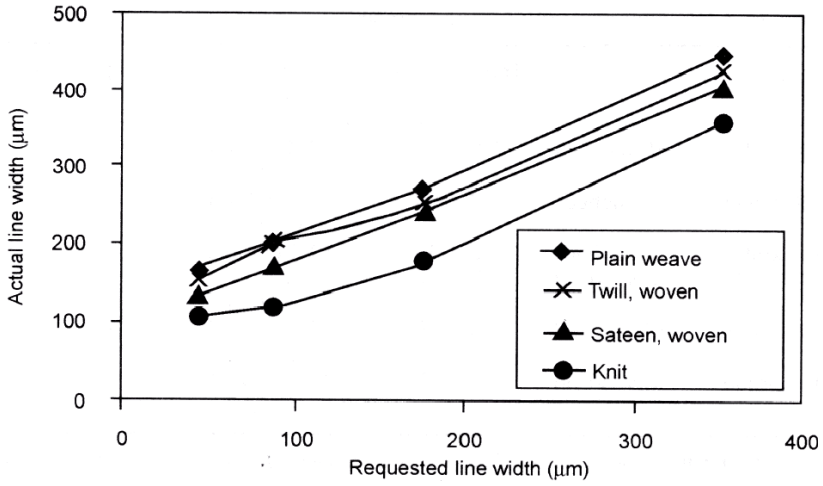

Figure 14: Effect of fabric weave and structures on line width gain [33].

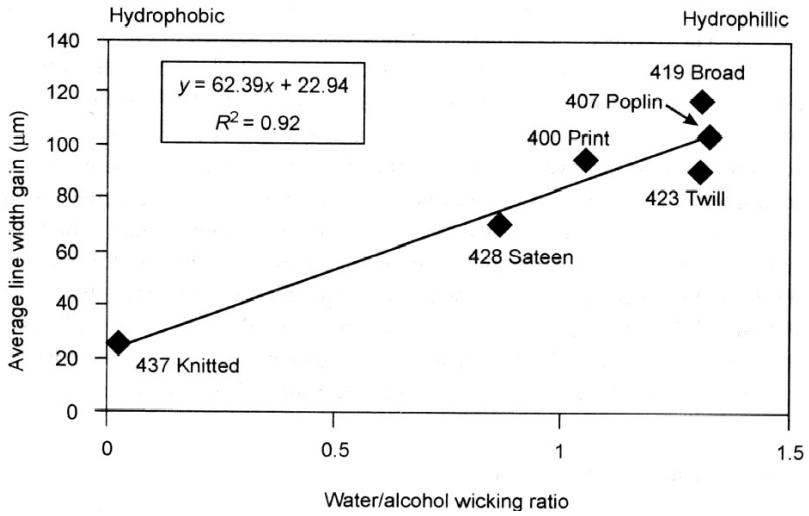

Figure 15: Correlation between average line width gain and water/alcohol wicking ratio [33].

The above authors also studied the effect of different treatments or coatings applied on the fabric. The treatment recipes they used comprised either alginate or silicon or nano-silica. The effects of pretreatments on line width gain are shown in Figure 16 and Figure 17. Results show that treatments improve the printing quality and quality was comparable to that on photo paper. Among different pretreatments, the nano-silica coating rendered higher quality. The authors observed that the effect of fabric structure on printing quality disappears when pretreatments are included.

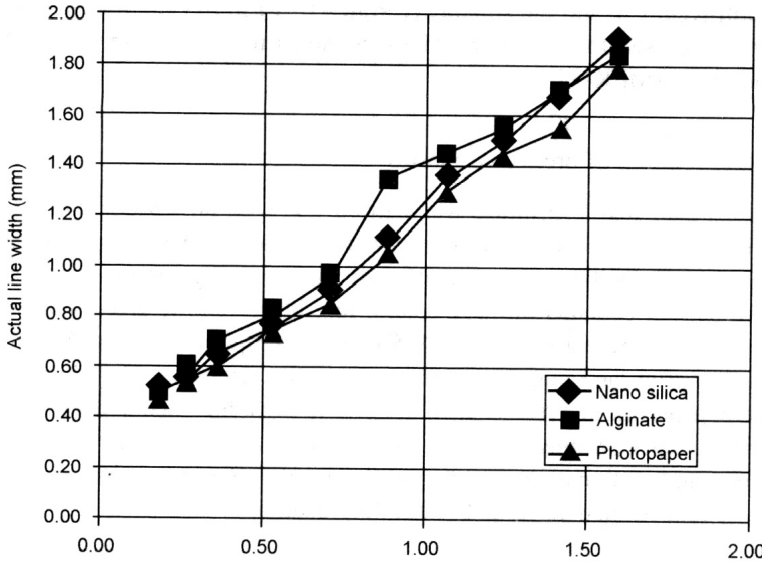

Figure 16: Effect of pretreatment on line quality (Woven Fabric) [33].

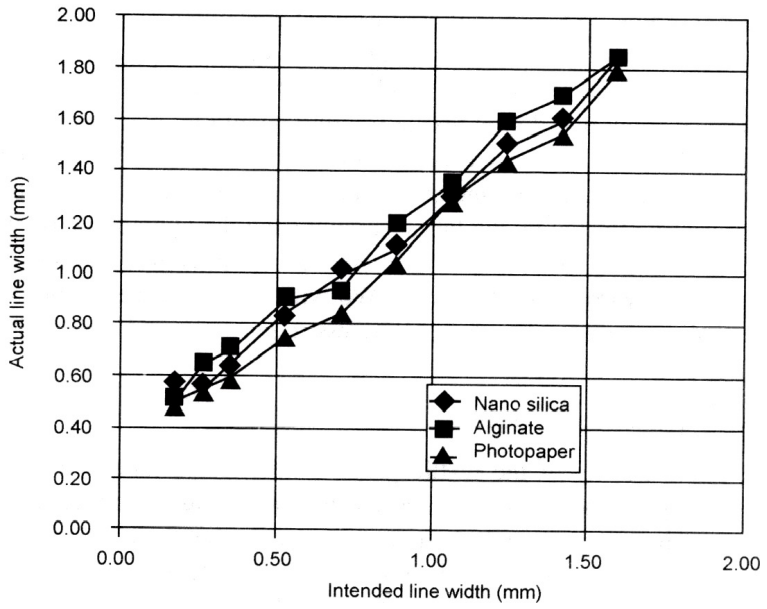

Figure 17: Effect of pretreatment on line quality (Knitted Fabric) [33].

Park and co-workers [34] conducted a similar study. They assessed mainly the effect of fabric structure (weave), pretreatments and ink type. They also found that image quality depends on fabric construction, especially for the untreated fabrics. Contrary to the study conducted by Fan, Park, et. al, they found that the line quality was better in the plain fabrics followed by twill and sateen fabrics. In twill and sateen fabrics, the authors explained, yarns float for longer distances due to less number of cross over points. Therefore ink wicks easily in those floated yarns. However in plain weave fabrics, wicking of ink is halted at cross over points which gives less line width gain and hence better printing quality. Authors also found that the printing quality could be considerably improved using certain types of coatings. Ink type was also found to be a very important factor. Alcohol based inks rendered images of good quality because alcohol evaporates faster, before significant wicking can occur.

In line with the above studies, other researchers [31] have also demonstrated the significance of fabric structure, yarn size and hydrophilic/hydrophobic nature of the fabric.

CHAPTER 3
SCOPE AND OBJECTIVES OF THE THESIS

3.1 Scope

3.1.1 Study of Liquid Migration

Literature review shows that liquid transport in textiles has been extensively studied. Different techniques such as direct observation, use of camera and image analysis techniques, use of liquid-sensitive sensors and use of force balance have been employed to quantitatively analyze liquid flow through yarns and fabrics. The application of multiple techniques to analyze liquid flow has helped to understand the influence of material and liquid properties on the wicking phenomenon. The wicking process has also been used to obtain structural information such as porosity, size and size distribution of pores, etc.

Although liquid transport studies have been used to compare different fabrics, the actual effect of fabric structure has not been investigated in a controlled manner. Further, almost all of the liquid transport studies that have been conducted on textiles consider textile assemblies as single capillaries, even though textile structures consist of capillaries that vary in diameter and length and are interconnected in a complex manner. Moreover, migration of liquid from one yarn to another yarn and from that yarn back to the first yarn is often overlooked despite the fact that it is an important part of the sorption process in fabrics.

When fabric is immersed in a liquid, the liquid first starts to wick through the longitudinal threads. When the traveling liquid front encounters transverse threads, some

of the liquid in longitudinal threads may move into transverse threads. The rate at which liquid transfers from one yarn to another depends upon the nature of capillaries and solid-liquid physiochemical parameters of the two yarns. The nature of contact and the actual area of contact also play important role. Transferred liquid remains in the segments of transverse threads and it may act as a new reservoir for the wicking process in the longitudinal threads. Due to these additional reservoirs, the rate of wicking of liquid in longitudinal threads can go up. Liquid may also get stored in the inter-yarn spaces, which can also act as additional reservoirs. This migration process from liquid reservoirs and its moderation by structural variations is mentioned [1, 20] but has rarely been studied. Full understanding of this process could enable the development of fabrics with superior wicking properties. In this research, the migration process is studied through direct visualization and also by the determination of the gain in wicking rate and the equilibrium wicking height of yarns, as a result of the yarns remaining an integrated part of the fabric. Influence of fabric structural parameters on the migration phenomenon and the wicking process has also been investigated.

3.1.2. Comparison of Wicking Results Obtained by Different Methods

Literature review shows that sorption in vertically hung fabrics from an unlimited reservoir can be studied by weight balance method as well as by the image analysis method, where weight or height of the liquid rise is measured as a function of time respectively. Researchers assume that one method can be substituted for the other or one can be used instead of the other. However the results obtained by these methods have never been compared for different types of fabrics. Therefore sorption of a liquid from an

unlimited reservoir is studied by weight balance and image analysis technique and the results obtained are compared.

Another mode of wetting of textile fabrics is sorption of a limited liquid quantity. Although dynamics of this kind of wetting has been deeply studied, the effect of fabric structure on spreading dynamics hasn't been sufficiently explored. This aspect is investigated by conducting drop spreading experiments on fabrics exhibiting systematic construction differences. An attempt has been made to understand the relationship that exists between yarn and fabric wicking rates from an unlimited reservoir and limited supply quantity of fluid.

3.1.3 Characterization of Ink Jet Drop Spreading and its Effect on Printing Quality

Literature review on textile ink jet printing shows that inks based on reactive, acid, disperse dyes and pigments are widely used. Several researchers have demonstrated the significance of fabric structure, ink type, yarn size, hydrophilic/hydrophobic character of the fabric and type of fabric pretreatment on the quality of printing achieved. Among different inks, pigment ink is becoming more popular because of its ability to give fuller and brighter shades without the need for any pretreatments. Because there is no pretreatment of the fabric involved, the printing quality of pigment inks can significantly depend on the fabric structure. Surface micro features of the fabrics which are influenced by the inter fiber and inter yarn spaces can affect the flow of ink drops. Printing quality is finally determined by how these drops flow and deposit on the surface of fabrics.

Therefore it is important to study the flow of ink jet drops on fabric surfaces and understand how the flow affects printing quality. As mentioned before, some biological

and electronic materials are being printed on textile fabrics for smart applications [27, 28]. Printing quality is extremely important for the desired performance of these applications. Therefore the spreading of ink jet drops on fabrics with different structures has been studied and the effect of spreading on printing quality has been defined.

3.1.4 Study of the Influence of Dithering on Printing Quality

Literature review shows that dithering is an important part of digital printing process to achieve homogenous images free of any chevron or moiré effects. Since the drop may spread in a random manner on textiles, it is interesting to find out if dithering process is essential while printing on textiles. This is investigated by printing dithered and undithered images on high quality ink jet paper and different textile fabrics.

3.1.5 Prediction of Ink Jet Printing Quality from Wicking and Millimeter Sized Drop Spreading Tests

In this research, the relationship between inkjet printing quality and wicking and spreading behavior of millimeter-sized ink drops is also investigated. A good understanding of this relationship would enable the prediction of the broad-based inkjet printing quality by just performing the wicking or drop test on textile structures. Establishment of appropriate correlations would help in the assessment of unknown fabrics for inkjet printing.

3.2 Goal and Objectives

The overall goal of this research is to understand the effect of fabric structure on liquid transport, ink jet drop spreading and printing quality.

The specific objectives are**:**

- Study the wicking of liquid in vertically hung fabrics from an unlimited reservoir by weight balance and image analysis methods.
- Understand the effect of fabric material, yarn type, thread density and yarn-to-yarn liquid migration on wicking of liquid in fabrics.
- Compare the wicking results obtained by the weight balance and image analysis methods.
- Characterize the spreading behavior of drops placed on horizontally positioned fabric samples using the highly evolved image analysis technique.
- Understand the effect of fabric material, thickness, yarn type and thread density on drop spreading behavior.
- Understand the relationship that exists between wicking and drop spreading behaviors.
- Print single dot, single line and solid figure patterns on fabrics with different structures, using Dimatix ink jet printer and pigment ink.
- Understand the factors that affect the ink jet drop spreading and final printing quality.
- Evaluate the relationship between wicking, drop spreading and ink jet printing quality.

CHAPTER 4
EXPERIMENTAL

4.1 Materials

Experiments were performed on a range of cotton and polyester fabrics which exhibited variations in fabric construction parameters. Description of the experimental fabrics is provided in Table 2. Plain woven cotton fabrics (Samples 1, 2, 3 and 4) were obtained from Cotton Incorporated, Raleigh, North Carolina, USA. Polyester fabrics (Samples 5, 6, 7 and 8) also with plain weave were obtained from Saraswati Polytex Ltd., India. Samples 9 and 10 were obtained from Mount Vernon Mills, Trion, GA and sample 11 was obtained from Testfabrics, Inc., NJ. The fabrics represented both natural and synthetic fibers and also staple fiber and continuous filament yarns.

Water based pigment ink (Fabric Fast Ultra ink) developed by Trident company (Brookfield, CT, USA) was used for printing. This ink is specially developed for textile fabrics and does not require any pretreatment of fabrics. Prints can be simply cured by subjecting the fabric to hot air. Viscosity and surface tension of the ink were measured by using Brookfield viscometer and Kruss bubble surface tension measurement equipment respectively. A VCA-Optima XE system (AST Products, Inc.) was used to measure the contact angles of ink on cleaned PET film.

High quality Epson ink jet paper (Product id S041111) was used for ink jet printing study.

Table 2: Description of experimental fabric samples.

No.	Fabric	Warp Yarn	Weft Yarn	EPI[a]	PPI[b]
1	Cotton 3508	280 Denier (19 Ne), Ring Yarn, Twisted (20 TPI[c]), Dia~270 µm	660 Denier (8 Ne), Ring Yarn, Twisted (10 TPI), Dia~500 µm	80	35
2	Cotton 4508	280 Denier (19 Ne), Ring Yarn, Twisted (20 TPI), Dia~270 µm	660 Denier (8 Ne), Ring Yarn, Twisted (10 TPI), Dia~500 µm	80	45
3	Cotton 6018	280 Denier (19 Ne), Ring Yarn, Twisted (20 TPI), Dia~270 µm	296 Denier (18 Ne), Ring Yarn, Twisted (13 TPI), Dia~300 µm	80	60
4	Cotton 7018	280 Denier (19 Ne), Ring Yarn, Twisted (20 TPI), Dia~270 µm	296 Denier (18 Ne), Ring Yarn, Twisted (13 TPI), Dia~300 µm	80	70
5	PET 4663	63 Denier (84 Ne), Filament Yarn, Twisted (25 TPI) , Dia~130 µm	63 Denier (84 Ne), Filament yarn, non-Twisted, Width~142 µm	112	46
6	PET 8863	63 Denier (84 Ne), Filament Yarn, Twisted (25 TPI) , Dia~130 µm	63 Denier (84 Ne), Filament yarn, non-Twisted, Width~142 µm	112	88
7	PET 4680	63 Denier (84 Ne), Filament Yarn, Twisted (25 TPI) , Dia~130 µm	80 Denier (66 Ne), Filament yarn, non-Twisted, Width~155 µm	112	46
8	PET 8880	63 Denier (84 Ne), Filament Yarn, Twisted (25 TPI) , Dia~130 µm	80 Denier (66 Ne), Filament yarn, non-Twisted, Width~155 µm	112	88
9	PET	490 Denier (11 Ne), Rotor Yarn, Twisted, Dia~340 µm	350 Denier (15 Ne), Filament yarn, non-Twisted, Width~350 µm	52	42
10	Sized PET	530 Denier, Rotor yarn, Twisted, Dia~300 µm	530 Denier, Rotor yarn, Twisted, Dia~300 µm	56	44
11	PET tape	280 Denier, Filament yarn, non-Twisted, Width~410 µm	310 Denier, Filament yarn, non-Twisted, Width~510 µm	60	40

Notes: a- Threads per inch in the warp direction of fabric, b-Threads per inch in the weft direction, c-Twists per inch of yarn

4.2 Desizing, Scouring and Washing of Fabrics

Fabric samples were taken at random from rolls but away from selvedges. Cotton fabrics were first desized and scoured. The following desizing and scouring procedures were used for cotton fabrics [35]:

Desizing recipe:

150 ml of 9.078 g/l solution of $Na_2H_2PO_4$

100 ml of a 9.472 g/l solution of Na_2HPO_4

2% owf Alpha-amylase (bacterial)

1% owf Nonionic surfactant (triton x-100)

1% owf Chelating Agent (EDTA, Na Salt)

25: 1 Liquor ratio

Desizing Procedure:

Fabric samples were placed in a large glass beaker and calculated amount of desizing solution (25:1 Liquor ratio) was added to the beaker. Solution was kept at 75 °C for 45 minutes. Finally, fabrics were removed from the bath and were rinsed using hot tap water.

Scouring recipe:

2.5 gram of sodium hydroxide

1.0 gram of sodium silicate, meta

1.0 gram of trisodium phosphate

0.5 gram of nonionic surfactant (Triton X-100)

0.5 gram of chelating agent (EDTA, Na Salt)

Dilute to 500 ml with water

25: 1 Liquor ratio

Scouring Procedure:

Fabric samples were placed in a large glass beaker and calculated amount of scouring solution (25:1 Liquor ratio) was added to the beaker. Solution was kept at boiling for 45 minutes with frequent stirring. Finally, fabrics were removed from the bath and were rinsed using hot top water. After rinsing, the samples were allowed to dry overnight at room temperature. All the samples were lightly ironed to remove the wrinkles and folds.

4.3 Determination of Fabric Structural Parameters

All the fabric samples were measured for their thickness using KAWABATA compression tester. The tester determines the thickness at different pressures. Thickness at a compressive pressure of 50 g/cm^2 (T_m) and thickness at zero compressive pressure (T_0) were determined for all the fabrics.

Samples were weighed as per ASTM D-3776 specification to determine their areal density (weight per unit area). Thread densities (warp threads or ends per inch (EPI) and weft threads or picks per inch (PPI)) were measured for each fabric. The threads were counted under a microscope.

Porosity values (ϕ_c) for all the fabrics for thickness T_0 and T_m were calculated from the knowledge of fabric density and fiber density (equation 23). Fabric density was calculated using equation 24.

$$\phi_c = 1 - \frac{\rho_{fabric}}{\rho_{fiber}} \tag{23}$$

$$\rho_{fabric} = \frac{Fabric.weight(g/cm^2)}{Fabric.thickenss(cm)} \tag{24}$$

4.4 Measurement of Water Transport in Vertically Hung Fabrics

4.4.1 Image Analysis Method

For measurement of the height of flow front, wicking process in the fabrics was recorded by a Canon camcorder. The recorded videos were converted into picture frames (1 frame per second) using video editing software. Each picture image was converted into grey scale image and wicking height (h) as a function time (t) was measured by analyzing the images, using codes written in Matlab (Appendix A and B). Wicking tests were performed on fabric strips of size 3 cm long and 1.5 cm wide. Fabric strips were dipped in the liquid just to touch the liquid surface. Wicking experiments were done on constituent yarns using the same method as above and 3 cm long yarn segments were used.

Ten samples for each fabric and yarn were tested and the average and standard deviation values were determined. Experiments were done warp way and weft way for each fabric. The data for the first sixty seconds was analyzed for all the fabrics and wicking coefficient or wicking rate (K) for that period was determined for all the yarns and fabrics by fitting the data to generalized Lucas-Washburn equation (equation 25).

$$h = K \times t^{0.5} \tag{25}$$

The gain in wicking rate of longitudinal yarn (ΔK) just because now it is an integrated part of the fabric was determined using equation 26.

$$\Delta K = \frac{\left(K_f - K_y\right)}{K_y} \times 100 \tag{26}$$

Where K_f is the wicking rate of fabric and K_y is the wicking rate of yarn.

4.4.2 Measurement of Equilibrium Wicking Height

The equilibrium wicking heights (L_{eq}) for yarns and fabrics were determined by dipping one end of the sample in an excess quantity of liquid for 12 hours. The % gain in equilibrium wicking height (ΔL_{eq}) was calculated as per equation 27, which is analogous to equation 26.

$$\Delta L_{eq} = \frac{\left(L_{eq\,f} - L_{eq\,y}\right)}{L_{eq\,y}} \times 100 \qquad (27)$$

4.4.3 Weight Balance Method

Experimental setup as shown in Figure 18 was used to investigate the water transport in vertically hung fabric. A dish containing copious amount of liquid (distilled water or ink) was kept on a digital weight balance, which was kept on a raisable platform. Fabric strip of size 3×1.5 cm was clamped to metal stand. Raisable platform was slowly raised until fabric just touched the liquid. Decrease in weight of liquid inside dish was recorded with time until it became steady. Platform was then slowly lowered and weight of the liquid retained by fabric was determined from the initial and final weight of liquid in the dish.

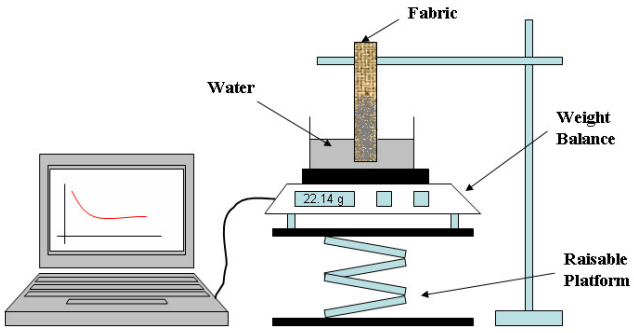

Figure 18: Experimental setup for studying the wicking of water in vertically hung fabrics.

During wicking test, weight shown by the weight balance first decreases sharply and then decreases gradually. The initial sharp decrease in weight is mainly caused by the instantaneous wetting of fabric by the liquid. After instantaneous wetting, gradual wicking of liquid inside the fabric causes a gradual decrease in the weight. When fabric is completely removed, absolute value of the weight shown by balance gives the weight of the liquid retained by fabric. If the weight values were converted into absolute numbers the trend appears as shown in Figure 19.

To determine the wicking rate K_w, wetting force value was subtracted from all the weight values. Data for the first sixty seconds was analyzed for all the fabrics and wicking rate for that period was determined for all the fabrics by fitting the data to power law model as shown in equation 28.

$$w = K_w \times t^{0.5} \tag{28}$$

Where w is weight of the liquid absorbed by fabric and t is time.

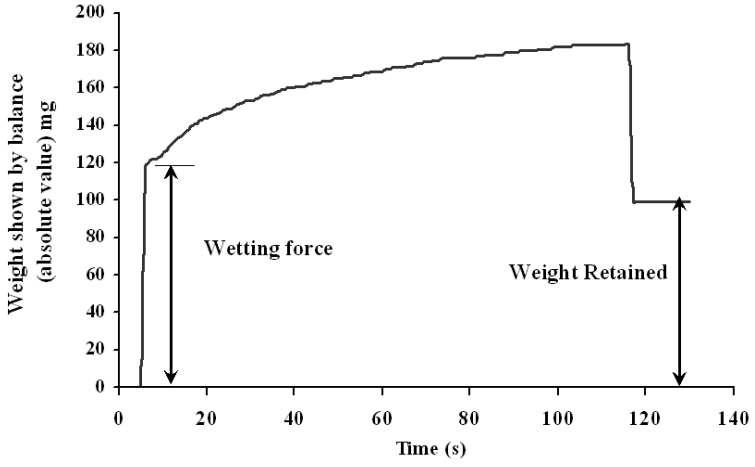

Figure 19: Analysis of wicking curve.

Ten tests for each fabric were done and the wicking rate and liquid retention values were computed for all the fabrics.

4.5 Measurement of Drop Spreading on Fabrics

Experiments on drop-spreading kinetics were performed using the set up shown in Figure 20. Drop is ejected from a syringe as syringe pump pushes the plunger of the clamped syringe through some finite distance. Instrument was calibrated to eject a single drop of volume 0.012 ml. At this setting, set up produced perfect single drop with no liquid remaining at the tip of needle. Reproducibility of drop ejection was very good and standard deviation was found be 0.00043 ml.

Fabric was clamped in such a way that drop ejected from the syringe falls in the centre of the sample. Drop spreading was recorded by the Canon camcorder from the underside of the fabric as shown in the figure. The recorded videos were converted into picture frames (1 frame per second) using video editing software. Each picture image was converted into grey scale image and drop spreading area (A_d) as a function time (t) was measured by analyzing the images using codes written in Matlab (Appendix C). Drop spreading area was measured by counting the number of pixels, which have grey scale value less than 40. Grey scale threshold of 40 was chosen after visually observing the magnified images of the Matlab image analysis tool. This tool gives the grey scale value of each pixel. For all the fabric samples where ink was present, the pixels had a grey scale value less than 40. This technique very precisely estimates the drop spreading area as it also includes any minute ink spikes that protrude the main drop spreading area.

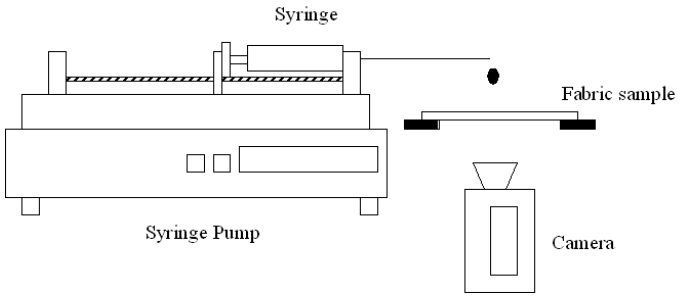

Figure 20: Experimental setup used for drop spreading studies

As described in the literature review, the drop spreading occurs in two phases. It has been shown by Kissa [21] that phase II drop spreading on fabrics for impermeable fibers follows the equation 20. Therefore drop spreading rates K_D for polyester fabrics were determined by fitting the data to this generalized equation.

$$A = K_D \times t^{0.3} \tag{29}$$

For permeable fibers, Kawase and his coworkers [22] showed that exponent n (exponent factor for time) is much smaller. For cotton fabrics they found that values of n are much smaller than theoretical value of 0.33 and they also vary with volume of drop, increasing from 0.10 to 0.15 when drop volume increases from 0.05 to 0.20. Assuming a linear relationship between drop volume and exponent n, this exponent n can be predicted. For drop volume of 0.012 ml. the exponent n was found to be 0.092. The value of K_D, the drop spreading rate of cotton fabrics was therefore determined by fitting the experimental data to the following generalized model.

$$A = K_D \times t^{0.092} \tag{30}$$

4.6 Ink Jet Printing on Fabrics

4.6.1 Printer and Ink

Ink jet printing on fabrics was done using Dimatix 2800 materials printer (Figure 21) [36]. This printer allows the deposition of fluidic materials on 8x11 inch or lower dimension substrates, utilizing a disposable piezoelectric ink jet cartridge. For optimum performance, the viscosity of the fluid is recommended to be around 10-12 centipoise and surface tension, around 28-33 dynes/cm. A variety of patterns can be created and printed using the pattern editor program. The printer has a vacuum platen system to secure the substrate in place and temperature of the platen can be adjusted up to 60°C. Additionally, a waveform editor and a drop-watch camera system allow manipulation of the electronic pulses to the piezoelectric jetting device for optimization of the drop characteristics as it is ejected from the nozzle. The printer is also equipped with a built-in cleaning station and choked up nozzles can be cleaned in a variety of ways [36].

Dimatix printer has unique print-head system, which is a MEMS-based cartridge-style print-head that allows users to fill their own fluids. Each cartridge has a capacity of 1.5 ml and has to be disposed once the ink is finished. Cartridges can be easily replaced to facilitate printing of a series of fluids. Each single-use cartridge has 16 nozzles linearly spaced at 254 microns with a typical drop size of 10 picoliters (50-60 μm drop diameter).

Figure 21: Dimatix ink jet printer [36].

Due to these sophisticated features the printer is ideal for printing various features such as single drops, line of single drops, solid lines and figures such as squares on the textile fabrics. Fabric Fast Ultra ink was used for all the printing experiments.

4.6.2 Printing of Single and Multiple Drops

Using the Dimatix printer, single and multiple ink drops (one, ten and twenty drops) were made to hit at the same location on the yarn. The spreading of drops was observed under microscope and spreading length in the direction of fiber was measured.

4.6.3 Printing of Lines

Lines were printed on all the experimental fabrics using the Dimatix printer. Ten lines having a width of 100 μm were printed in warp and weft directions of each fabric and also on high quality Epson inkjet printing paper. The distance between two successive drops was 21 μm. Lines were observed under microscope and the width of the line on longitudinal and transverse thread segments was measured at several locations. Five lines were printed for each fabric and direction and average line width was determined.

The relationship between wicking, drop spreading and ink jet printing quality was evaluated in this research. For this purpose the wicking tests were performed on each yarn used in the fabrics of this study. Wicking tests were performed on yarns with one end dipped in the excess quantity of ink. The distance traveled by ink after 2 minutes was measured. The drop-spreading test was performed by gently placing a 0.5 μL pigment ink drop (approximately1 mm in diameter) on fabrics. Drop was allowed to spread until the ink dried up completely. Fabrics were scanned and the drop spreading distance in warp

and weft directions and the spreading area were measured using image analysis techniques.

Drop spreading area was measured by counting the number of pixels, which have grey scale value less than 40. Grey scale threshold of 40 was set by visually observing the magnified images of the Matlab image analysis tool. This tool gives the grey scale value of each pixel. For all the fabric samples where ink was present, the pixels had a grey scale value less than 40.

The technique described above estimates the drop spreading area very precisely as it also includes any minute ink spikes that protrude the main drop spreading area. Ten drops were placed on each sample and the average values of spreading distance (d) and spreading area (A_d) were computed based on measurements made on all ten drops.

4.6.4 Printing of Solid Figures

To study the effect of fabric characteristics on ink coverage on fabrics, solid squares were printed on selected fabrics. Further, to investigate if there is need for a dithering process in ink jet printing of textile fabrics, squares were printed with and without dithering. Patterns were designed in such a way that they would cover around 25%, 50% and 75% area on high quality Epson ink jet paper. Single repeat units and some parts of the full patterns are shown in Figures 22 and 23. Figure 22 shows undithered patterns while Figure 23 shows dithered patterns.

The printed paper and fabrics were observed under microscope to see if the pattern is retained on the sample and qualitative remarks were made. Further, printed

samples were scanned and the average grey scale value of each sample was determined by using the Matlab code shown in the Appendix D.

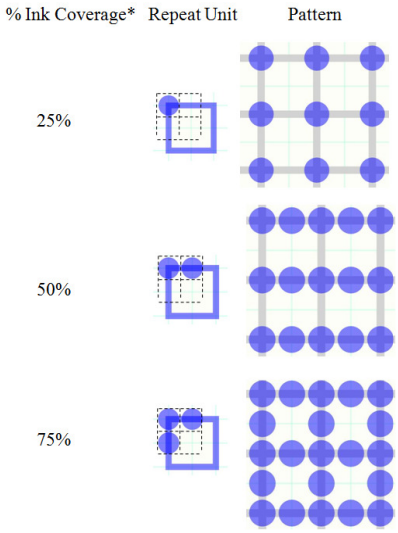

Figure 22: Undithered patterns used for ink jet printing on fabrics

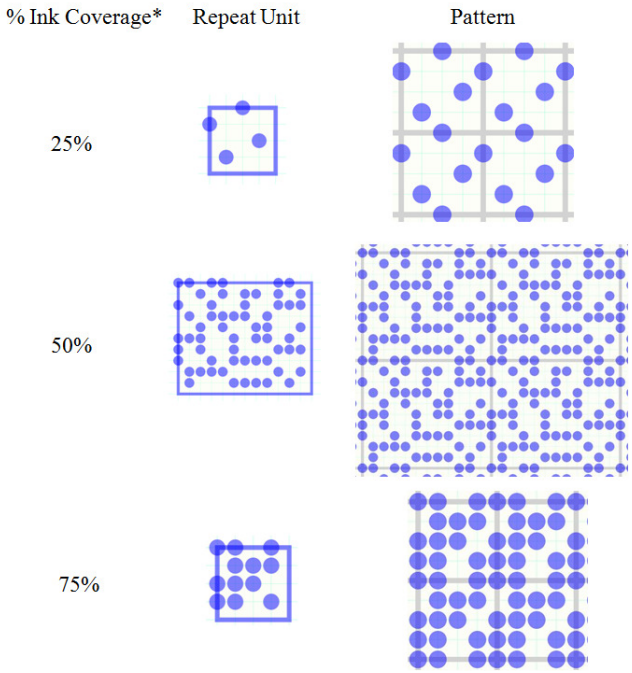

Figure 23: Dithered patterns used for ink jet printing on fabrics

CHAPTER 5
RESULTS AND DESCUSSION

5.1 Fabrics and their Characteristics

Thickness and aerial density values of all the fabrics are given in Table 3. In this table, T_0 is the thickness at zero pressure and T_m is the thickness at a pressure of 50 g/cm^2. Cotton fabrics were thicker than all other polyester fabrics. Bulk density values of fabrics at thickness T_0 and T_m are shown in the last two columns of Table 3.

Table 3: Thickness, aerial density and other characteristics of experimental fabrics.

No.	Fabric	Thickness T_0 (um)	Thickness T_m (um)	Areal Density (g/m^2)	Bulk Density @T_0 (g/cm^3)	Bulk Density @T_m (g/cm^3)
1	Cotton 3508	900	630	211	0.23	0.33
2	Cotton 4508	860	590	256	0.30	0.43
3	Cotton 6018	750	460	197	0.26	0.43
4	Cotton 7018	760	440	216	0.28	0.49
5	PET 4663	155	140	47	0.30	0.34
6	PET 8863	130	125	58	0.45	0.46
7	PET 4680	185	160	49	0.26	0.31
8	PET 8880	150	130	61	0.41	0.47
9	PET	650	390	205	0.32	0.53
10	Sized PET	550	500	250	0.45	0.50
11	PET tape	160	150	107	0.67	0.71

Surface images of some of the experimental fabrics are shown in Figure 24. Observation of microscopic images showed that cotton fabrics consist of spirally oriented discontinuous capillaries. PET Tape fabric consisted almost continuous capillaries in both warp and weft threads as continuous filament yarns were used for warp and weft threads.

Remaining polyester fabrics consisted discontinuous capillaries in warp threads (as twisted yarns were used) and quite continuous capillaries in weft threads.

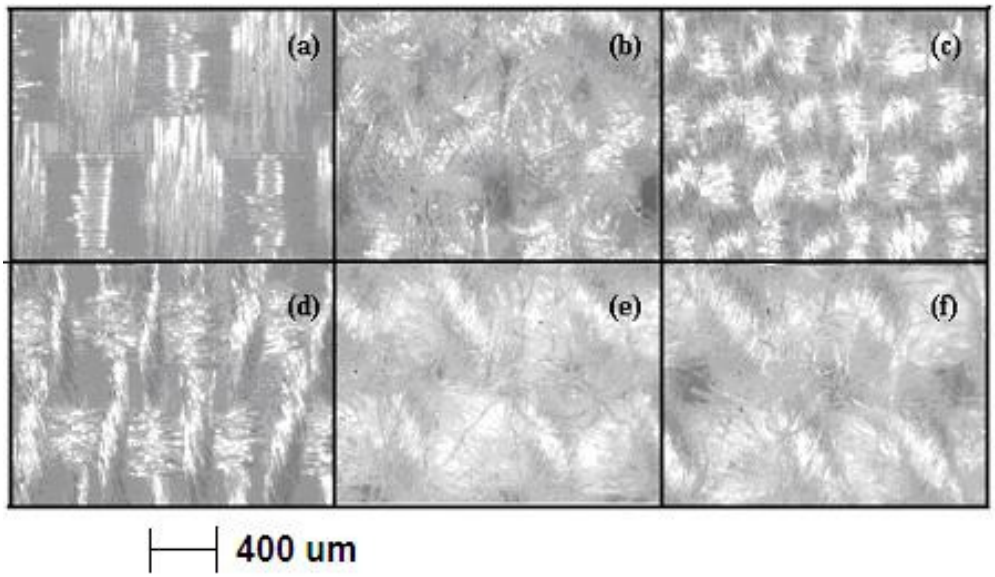

Figure 24: Microscopic images of fabric samples: (a)PET Tape, (b) Sized PET, (c) PET 8880, (d) PET 4680, (e) Cotton 4508, and (f) Cotton 3508.

5.2 Characteristics of Ink

Viscosity and surface tension of the Fabric Fast Ultra ink was found to be 3 cp and 36 dynes/cm, respectively. Contact angle of the ink on amorphous polyester film was found to be 54 degrees, which means that ink can wet both polyester and cotton fabrics. Contact angle of the ink on cotton fibers could not be determined due to the 8inadequate size of the cotton fibers.

The density of ink was found to be 1.23 g/cc. TGA analysis showed that the ink contained around 65% Water and 35% Solids. Amount of pigments in the ink is possibly 5 - 10%. Relevant graphs are shown in the Appendix E.

5.3 Effect of Fabric Structure on Wicking of Liquid from an Unlimited Reservoir

Experiments on wicking from an unlimited reservoir were done only on cotton, PET and Sized PET fabrics. Wicking experiments could not be carried out on PET 4663, PET 8863, PET 4680 and PET 8880 fabrics because these fabrics tend to curl during wicking experiments. As explained in the experimental section, wicking experiments were carried out using both weight balance and image analysis methods. Only pigment ink was used for image analysis experiments while distilled water and pigment ink were used for the weight balance experiments. Pigment ink renders very clear and sharp flow front as liquid wicks into fabric. Simple dye based water solutions give a sort of fuzzy flow front in fabrics, which is often difficult to detect, and the flow appears to change with the type and intensity of the surrounding light source, posing problems in the analysis of the images. Results of the wicking experiments are discussed below.

5.3.1 Image Analysis Method

5.3.1.1 Wicking rates of Fabrics and Yarns Removed From Fabrics

The average wicking rates of the warp and weft yarns used in the fabrics are shown in Table 4. Wicking rates of fabrics in the warp and weft direction and also the gain in wicking rates are shown in the same table. Standard deviations are shown in Table 5. Results are also presented in Figure 25.

Yarns of different counts were used in the cotton fabrics. However, as the warp threads used in all cotton fabrics were the same, they had the same wicking rates. In case of weft threads, thicker cotton yarns (higher denier yarns) showed higher wicking rates as

they had lower twist levels as shown in Table 2. Low twist levels keep the yarns more open and hence the effective capillary radius is more in case of open yarns. The path liquid has to take is also less tortuous. In highly twisted yarns, liquid has to take more tortuous path and since fibers are tightly packed, capillary radius is less; hence these yarns show low wicking rates. Overall, cotton yarns showed better wicking rates than polyester yarns as the cotton fibers are more wettable by water-based ink than polyester fibers. The highest wicking rate was observed in PET filament yarns of the PET fabric. Wicking rate was very high in these yarns because these were twist-less filament yarns with somewhat open structure. Although yarns in the PET Tape fabric were also twist-less filament yarns, low wicking rates were observed in these yarns as the filaments in these yarns were closely packed. Close packing reduced the capillary radius and hence the wicking rate. The sized warp yarns in the Sized PET fabric showed the lowest wicking rate. As most of the capillaries in sized yarns are filled by size coating formulation, wicking in these yarns is negligible and occurs very slowly. Also size coating formulations are not easy to wet as they contain hydrophobic wax in their composition.

The above observations show that Washburn's law is quite applicable in case of textile yarns. Yarns with lower capillary radius indeed showed low wicking rates and yarns with higher capillary radius showed high wicking rates.

Table 4: Yarn and fabric wicking rates.

	Wicking Rate *K* (cm/s$^{0.5}$)				% Gain in wicking rate	
Sample	**Yarn-warp**	**Yarn-weft**	**Fabric-warp**	**Fabric-weft**	**Warp**	**Weft**
Cotton 3508	0.18	0.34	0.36	0.38	100	12
Cotton 4508	0.18	0.34	0.31	0.34	72	0
Cotton 6018	0.18	0.20	0.30	0.30	67	50
Cotton 7018	0.18	0.20	0.28	0.27	56	35
PET	0.18	0.42	0.38	0.30	111	-32
PET Tape	0.15	0.19	0.11	0.11	-27	-42
Sized PET	0.03	0.19	0.09	0.12	200	-37

Table 5: Standard deviations of yarn and fabric wicking rates.

	Wicking Rate *SD* (cm/s$^{0.5}$)			
Sample	**Yarn-warp**	**Yarn-weft**	**Fabric-warp**	**Fabric-weft**
Cotton 3508	0.024	0.016	0.007	0.014
Cotton 4508	0.024	0.016	0.013	0.012
Cotton 6018	0.024	0.017	0.003	0.005
Cotton 7018	0.024	0.017	0.003	0.004
PET	0.019	0.044	0.003	0.004
PET Tape	0.012	0.014	0.008	0.007
Sized PET	0.009	0.011	0.004	0.008

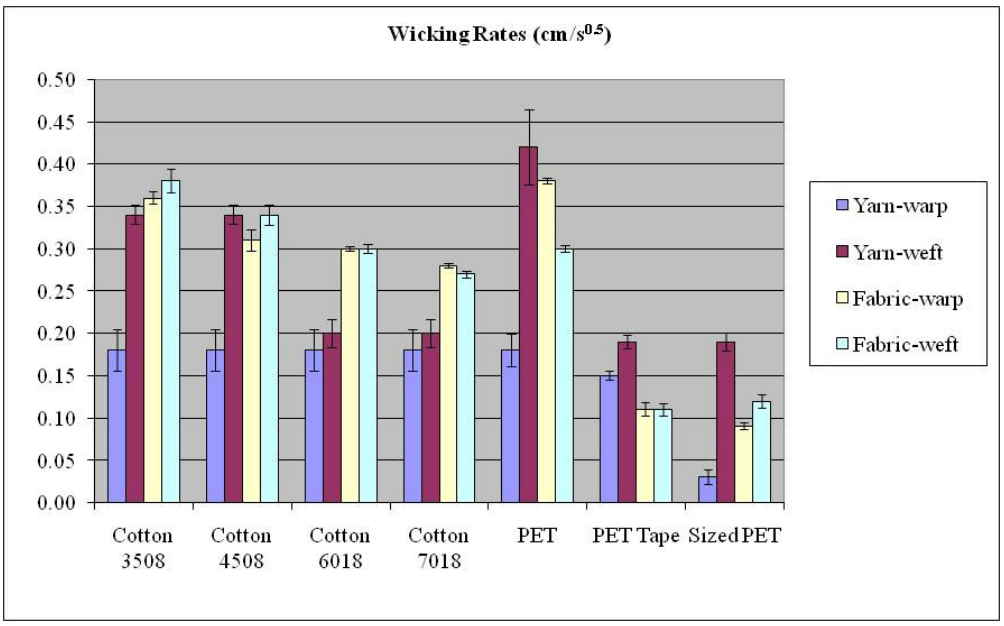

Figure 25: Yarn and fabric wicking rates.

As can be seen in Table 4 and Figure 25, most of the fabrics showed wicking rates higher than their constituent yarns. Higher fabric wicking rates were observed in 3508, 4508 and PET fabrics whose constituent yarns showed higher wicking rates. Also, as the thread density of the fabrics went up, wicking rates went down. The % gain in wicking rates of the corresponding yarns in fabrics is shown in the last two columns of Table 4. The highest gain was observed in the warp direction of Sized PET fabric, followed by the warp direction of PET and Cotton 3508 fabrics. Lowest wicking rates and negative gains were observed in the case of PET Tape and Sized PET fabrics and in the weft direction of PET fabric. Cotton fabrics containing 18 count (Ne) weft yarns showed lower wicking rates than cotton fabrics containing 8 count (Ne) weft yarns and this agrees with the lower wicking rate shown by the 18 count yarn compared to the 8 count yarn.

In addition to the quantitative study of wicking through yarns and fabrics, the nature of the liquid front was observed under the microscope as the liquid wicked through

the fabrics. It was noticed that the liquid front propagates through fabrics in one of three ways or patterns as shown in Figure 26. List of samples that exhibited the particular pattern is given below that pattern. In the first case, before liquid front can pass any transverse thread, all previous transverse thread segments were completely filled. This indicates very quick transfer of liquid from longitudinal threads to transverse threads. Liquid stored in those transverse threads is thus readily available for transfer from transverse threads back to longitudinal threads. Hence samples which exhibited this pattern showed highest gains in wicking rate. In the second type of liquid front pattern, few transverse threads (typically 2) remain unfilled because the rate of wicking in the longitudinal thread is quite high. This indicates somewhat inefficient migration process. The samples that exhibited this pattern showed very low wicking rate gains. In the third type, due to very poor migration of liquid between threads, many transverse thread segments (typically more than 4) remain unfilled. Longitudinal threads lose liquid to transverse threads and they fail to gain any liquid from transverse threads, thus explaining the negative gain in wicking rate observed in the case of PET Tape fabric.

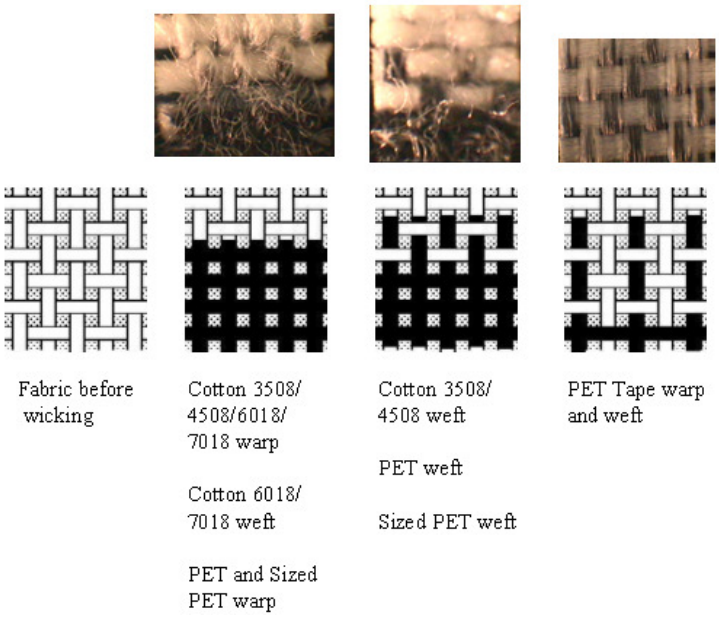

Figure 26: Typical patterns of the liquid front exhibited by different samples.

5.3.1.2 Equilibrium Wicking Heights

Trends similar to those seen in wicking rates were observed for equilibrium heights of the yarns and fabrics (Table 6). Standard deviations are shown in Table 7 and all the results are presented in Figure 27. Higher equilibrium lengths were observed in the case of cotton and PET fabrics. Contrary to the gain in wicking rates, the percent gain values for equilibrium wicking height were positive for all fabrics, except for the Sized PET fabric. This means that, at shorter times, the migration of liquid from longitudinal yarns to transverse yarns is not complete and hence in some cases the transverse threads do not act as reservoirs, thus producing negative gain in wicking rates. However at longer time periods, migration is complete and transverse threads act as reservoirs to give positive gains in equilibrium wicking heights in most of the cases.

Higher gains were observed once again in the warp direction of Sized PET fabric followed by the warp direction of PET and Cotton 3508 fabrics. Equilibrium wicking heights as well as gains decreased with increasing thread density. Sized PET fabric showed negative gain in the weft direction. This is because the flow of liquid is hindered as the liquid encounters difficult-to-wet sized warp threads as it is moving through the fabric.

Table 6: Equilibrium wicking heights of yarns and fabrics.

	Equilibrium Wicking height (cm)				% Gain in wicking height	
Sample	**Yarn-warp**	**Yarn-weft**	**Fabric-warp**	**Fabric-weft**	**Warp**	**Weft**
Cotton 3508	2.0	4.2	6.6	7.6	230	81
Cotton 4508	2.0	4.2	5.4	6.6	170	57
Cotton 6018	2.0	2.4	4.4	5.0	120	108
Cotton 7018	2.0	2.4	4.2	4.7	110	96
PET	1.9	3.8	6.4	5.8	237	53
PET Tape	1.3	1.0	1.6	1.5	23	50
Sized PET	0.2	2.0	0.7	1.4	250	-30

Table 7: Standard deviations of equilibrium wicking heights of yarns and fabrics.

	Equilibrium Wicking height SD (cm)			
Sample	**Yarn-warp**	**Yarn-weft**	**Fabric-warp**	**Fabric-weft**
Cotton 3508	0.24	0.41	0.17	0.30
Cotton 4508	0.24	0.41	0.20	0.09
Cotton 6018	0.24	0.20	0.14	0.15
Cotton 7018	0.24	0.20	0.27	0.14
PET	0.10	0.14	0.21	0.18
PET Tape	0.15	0.11	0.13	0.07
Sized PET	0.12	0.17	0.07	0.11

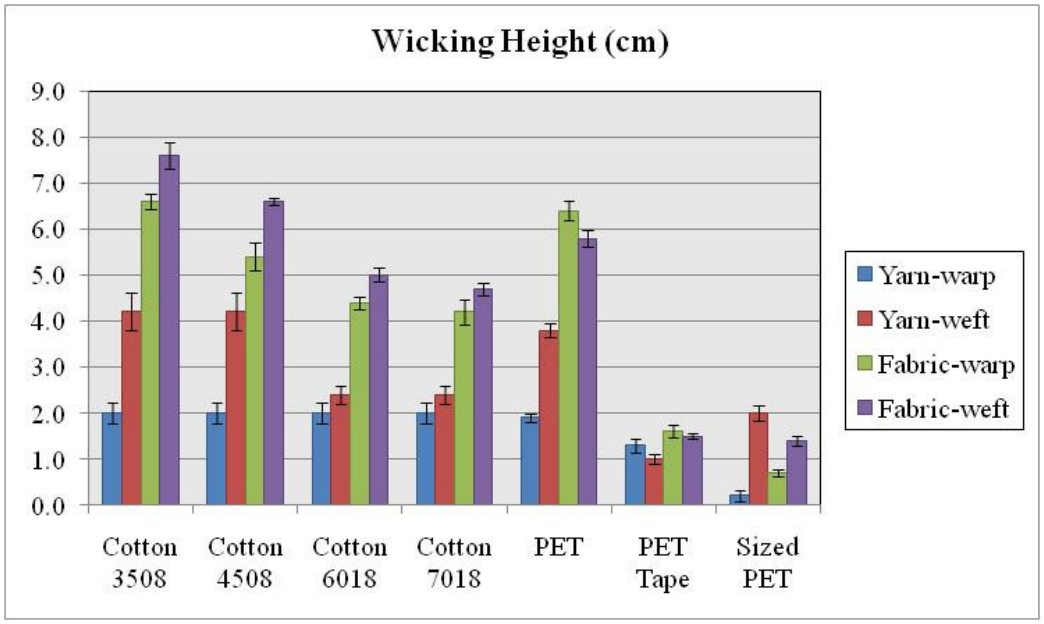

Figure 27: Equilibrium Wicking Heights of Yarns and Fabrics.

From the data it is thus clear that wicking in fabrics is determined by the wicking rates of the yarns, thread spacing and more importantly by the speed at which liquid migrates from the longitudinal to transverse threads and back from the transverse to the longitudinal threads. Results suggest that the migration process is affected by the wicking rates of the yarns, yarn or thread types, and the thread spacing.

If the wicking rate of the longitudinal threads is very high, these threads may end up only giving the liquid to transverse threads but may not gain the benefit of liquid migration from transverse threads back to them. This will lower the gain in wicking rate as well as the wicking rate. This phenomenon was observed in the weft direction wicking of the PET fabrics.

Further, migration from longitudinal yarns to transverse yarns occurs only when longitudinal yarns become sufficiently saturated, meaning that there is enough liquid

available on the surface of the longitudinal yarns. It was found that migration from longitudinal yarns to transverse yarns occurs more easily if the longitudinal yarns are twisted and occurs less easily when they are twist-less (twist-less filament yarns). The surface profile of the twisted yarns is rougher than that of the twistless yarns, which leaves more liquid on the surface of these yarns compared to filament yarns. Hence liquid migration from longitudinal yarns to transverse yarns is poor when filament yarns are present in the longitudinal direction. This is why negative wicking rate gain and very low gains in equilibrium heights were observed in the case of PET and PET Tape fabrics.

Migration from transverse yarn segments back to longitudinal threads seems to depend on the relative size of the capillaries present in these yarns. For a given liquid, yarns with higher wicking rate normally suggest higher capillary radius. Capillary pressure is higher for lower radius capillaries and vice versa (equation 1). Thus finer capillaries can easily pull the liquid from larger capillaries. Therefore, longitudinal yarns with finer capillaries can easily pull up the liquid from transverse threads that have bigger capillaries. This boosts wicking rate and wicking height in longitudinal direction. Cotton 3508 and PET fabrics therefore exhibited the highest gains in warp direction as the warp yarns had finer capillaries and weft yarns had larger capillaries.

Further, capillary pressure is less in the case of filament yarns than in the twisted yarns. Therefore more gain in the warp direction was observed in the case of the PET fabric (111 % in wicking rate and 237 in equilibrium wicking height) compared to that of Cotton 3008 fabric (100 % in wicking rate and 230 in equilibrium wicking height). This indicates that the presence of twisted yarn in longitudinal direction and filament yarn in

the transverse direction can establish the best contact for easier migration of liquid and can render the fabric with superior wicking properties.

Wicking rate, equilibrium wicking height, gain in wicking rate and wicking height were all affected by the thread spacing. Measured values for all these parameters decreased with the increase in thread density. This means that liquid stored in inter-yarn spaces also plays a major role. Liquid fills these inter-yarn spaces after all the surrounding yarns are saturated and enough liquid is available to fill up the inter-yarn space. Inter-yarn spaces are generally larger than inter-fiber spaces in the yarn. Hence liquid stored in inter-yarn spaces is governed by low capillary pressures and it is readily available for pick up. Thus inter-yarn spaces are more efficient reservoirs to boost the wicking rate and wicking height. Better wicking properties can be achieved by increasing thread spacing. However, if thread density is decreased too much, inter-yarn spaces may remain unfilled and improvement in wicking properties may not be achieved.

Correlation coefficients between fabric construction parameters and measured wicking properties were also computed. The related correlation table is shown in Appendix F. Very high correlation was observed between yarn wicking rate and fabrics wicking rate. A good inverse relation between bulk density of fabric and fabric wicking rate was also observed, which shows that as bulk density dropped, fabric wicking rates increase. This is primarily due to the fact that lower bulk density implies more open fabric and higher effective capillary radius for which the wicking rate is higher. This is in accordance with Washburn equation (equation 3).

It was observed that equilibrium wicking height values of the yarns and fabrics were not in accordance to those predicted by equation 2 and 3. Equation 3 suggests that wicking rate is proportional to the square root of capillary radius. Thus capillaries with larger radius should give higher wicking rates. Also, capillaries with higher radius should show lower equilibrium heights as equilibrium height is inversely proportional to capillary radius as described by equation 2. Therefore there should be an inverse relationship between the wicking rate and equilibrium wicking height. The relation between the wicking rates of fabrics and equilibrium wicking heights of the same fabrics is shown in Figure 29. Although inverse relationship is expected, mostly a direct relationship is observed between these two parameters. This clearly indicates that the classical capillary theories may not be applicable to textile assemblies. Anomaly in this case results from various factors. Twisted yarns for example show low wicking rates as well as low equilibrium wicking height due to the presence of discontinuous capillaries and tortuous liquid paths. As discussed before, storage of liquid in transverse yarn segments can boost both wicking rate and equilibrium wicking height. Decrease in thread density or increase in inter-yarn space results in storage of more liquid, which also boosts wicking rate and equilibrium wicking height. Migration process is thus a very important part of the wicking process in fabrics and the migration phenomenon requires further in depth investigation. Determination of the gain in wicking rate and wicking height is the best way to quantitatively describe the migration process.

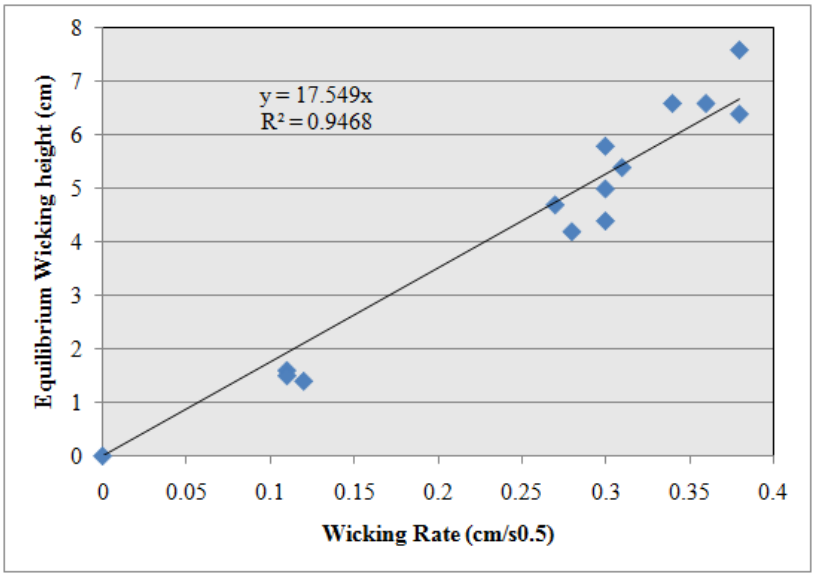

Figure 28: Wicking rate Vs. equilibrium wicking height.

5.3.2 Weight Balance Method

As stated before, both distilled water and pigment ink were used for the weight balance experiments. Weight balance method could not be used on PET Tape fabric because it absorbed very small amount of liquid, which could not be detected properly by the weight balance.

5.3.2.1 Wicking and Absorption of Water in Fabrics

The results of wicking tests carried out using distilled water are discussed in this section. Table 8 shows the wicking rates of fabrics in warp and weft direction. Wicking rates of the fabrics are also presented in Figure 29. Trends similar to those observed in the image analysis method are seen. However, no significant difference between warp and weft direction are observed despite the fact that wicking rates of warp yarn and weft yarns are completely different (Table 4). Cotton 3508 fabric showed the highest wicking rate while

PET sized fabric showed the least wicking rate. Data again proves that yarns with better wicking properties render better wicking properties in fabrics. Also as the thread density of fabrics went up, wicking rates went down. The effect of thread density was more pronounced in cotton fabrics having coarser count weft yarn (8 count as opposed to 18 count).

Table 8: Wicking rates of fabrics obtained by weight balance method using water as wicking agent

	Wicking Rate K_w (mg/s$^{0.5}$)			
Sample	**Warp**	**Weft**	**SD Warp**	**SD Weft**
Cotton 3508	28.94	28.46	0.65	0.81
Cotton 4508	21.31	21.57	0.79	0.49
Cotton 6018	17.63	17.60	0.55	0.84
Cotton 7018	17.40	17.89	0.50	0.80
PET	7.90	7.65	0.91	0.67
PET Sized	1.48	1.97	0.14	0.24

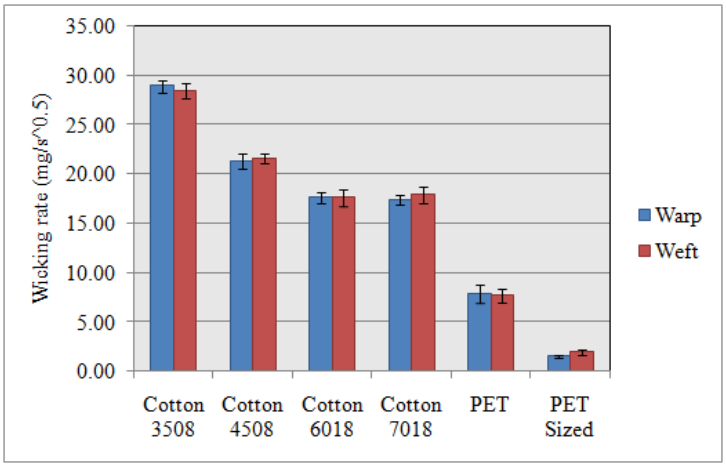

Figure 29: Wicking rates of fabrics obtained by weight balance method using water as wicking agent.

From the knowledge of the weight of liquid trapped in fabrics and thickness of fabrics, porosity and % absorption values were obtained for each fabric using the following equations:

$$Porosity(\phi) = \frac{Liquid.Volume}{Fabric.Volume} = \frac{W_L}{\rho_L \times (L_F \times W_F \times T_F)} \quad (31)$$

% Absorption = (Weight of liquid retained by fabric / Weight of fabric) * 100 (32)

Where,

W_L=weight of liquid retianed by fabric

ρ_L=density of liquid

L_F=length of fabric

W_F=width of fabric

T_F=thickness of fabric

From the two thickness values (T_0 and T_m) two porosity values were detemined. The data is shown in Table 9 and Figure 30. In Figure 30 the measured porosity values are compared with calculated porosity values which were caluculated using equation 24.

Table 9: Porosity and % absorption values of fabrics with water as wetting agent.

Sample	ϕ_{T_0}	ϕ_{Tm}	**% Absorption**	**SD** ϕ_{T_0}	**SD** ϕ_{Tm}	**SD % Absorption**
Cotton 3508	0.49	0.70	199.92	0.02	0.03	5.17
Cotton 4508	0.42	0.62	151.08	0.01	0.01	2.88
Cotton 6018	0.40	0.68	147.89	0.02	0.02	3.53
Cotton 7018	0.39	0.65	138.40	0.01	0.01	1.76
PET	0.37	0.61	115.23	0.01	0.02	3.02

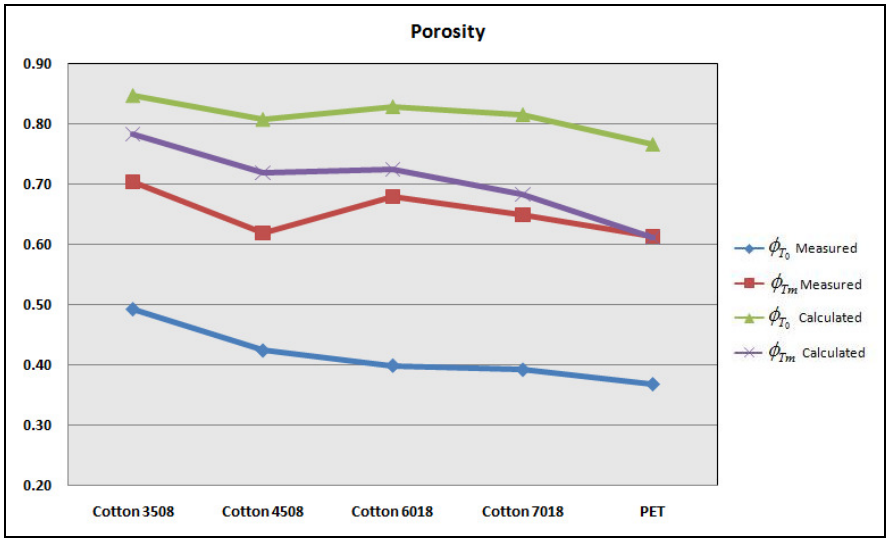

Figure 30: Measured and calcualted values of porosity of fabrics with water as wetting agent.

It can be noted that the measured porosity values corresponding to both fabric thicknesses were lower than the corresponding calulcualted porosity values. This means that not all the available pore volume in fabric is filled by liquid. This happnes because unlike closed cylinder capillary strucutre, capillaries in textile strucutres are open in nature and are only partially filled due to the physio-chemical properties of the liquid and the local fabric surface geometry as shown in Figure 31. The phenomena of capillary rise beween open cylinders has been studied by Liu and his coworkers in some detail [37].

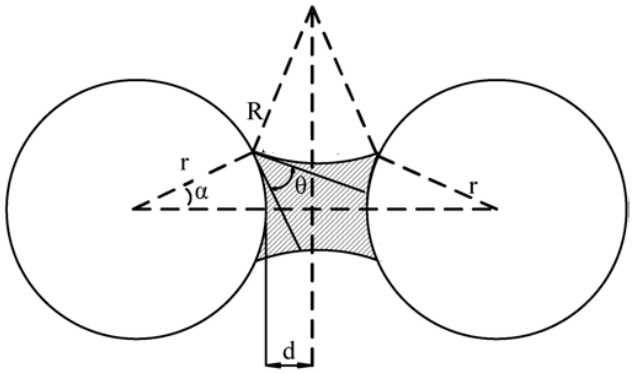

Figure 31: Capillary rise between two open capillaries [37].

Further it can be seen that there is a big diffrence between calculated ϕ_{To} and measured ϕ_{To}. Calculated ϕ_{Tm} and measured ϕ_{Tm} values were also different but diffrence was not as much as the diffrence between calculated ϕ_{To} and measured ϕ_{To}.This is because of the fact that for the same areial density, calculated ϕ_{To} is directly proportional to thickness (equation 33), while for the same abosorbed ink amount, measured porosity value is inversely proportional to fabric thickness (equation 31). Therfore for lower thcikness values, the diffrence between calculated and measured porosity values is also less. The diffrence between Calculated ϕ_{Tm} and measured ϕ_{Tm} values was not that big as T_m values are lower than T_0 values.

Percent absorption data (Figure 32) showed that Cotton 3508 fabric absorbed the highest amount of liquid. Percent absorption values were lower for 18 count weft yarn cotton fabrics compared to 8 count weft yarn cotton fabrics. Also % absorption values decreased as thread density increased, which again proves that inter-yarn spaces retain substantial amount of liquid which may act as secondary reservoirs. Percent absorption values could not be calculated for Sized PET fabric as liquid did not wick through the

whole sample length. PET fabric showed the least absorption as polyester fibers do not absorb water. Water is merely retained in inter-fiber and inter-yarn capillary spaces due to capillary forces.

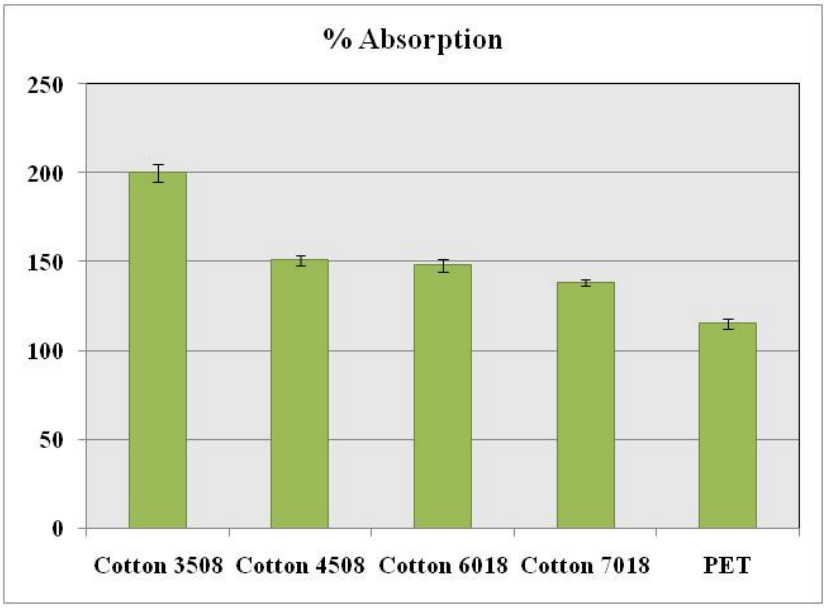

Figure 32: Percent absorption values of fabrics for water as wetting agent

5.3.2.2 Wicking and Absorption of Pigment Ink in Fabrics

Similar trends for wicking and absorption of pigment ink were observed as were observed for water. Results are shown in Tables 10 and 11 and Figures 33, 34 and 35. No significant difference was observed in warp and weft direction wicking rates for the experimental fabrics despite the fact that wicking rates of warp and weft yarns were different (Table 4). Cotton 3508 fabric once again showed the highest wicking rate while PET sized fabric showed the least wicking rate. Data again proves that yarns with better wicking properties render better wicking properties in fabrics. Also as thread density of

fabrics went up, wicking rates went down and the effect of thread density was more pronounced in cotton fabrics having 8 count weft yarn as opposed to 18 count weft yarn.

The characteristics of ink and water are completely different. The surface tension of water is 72 dynes/cm while it is 36 dynes/cm for pigment ink. Viscosity of water is 1 cP and for pigment ink it is 3 cP. It is interesting to see how the wicking behavior of these two liquids is different. The comparison is presented in the next section.

Table 10: Wicking rates of fabrics obtained by weight balance method using pigment ink as wicking fluid.

	Wicking Rate (mg/s $^{0.5}$)			
Sample	**Warp**	**Weft**	**SD Warp**	**SD Weft**
Cotton 3508	15.95	15.50	0.23	0.46
Cotton 4508	13.23	12.84	0.57	0.12
Cotton 6018	10.85	10.65	0.19	0.04
Cotton 7018	10.50	10.69	0.49	0.97
PET	7.00	6.93	0.51	0.04
PET Sized	1.24	1.08	0.15	0.42

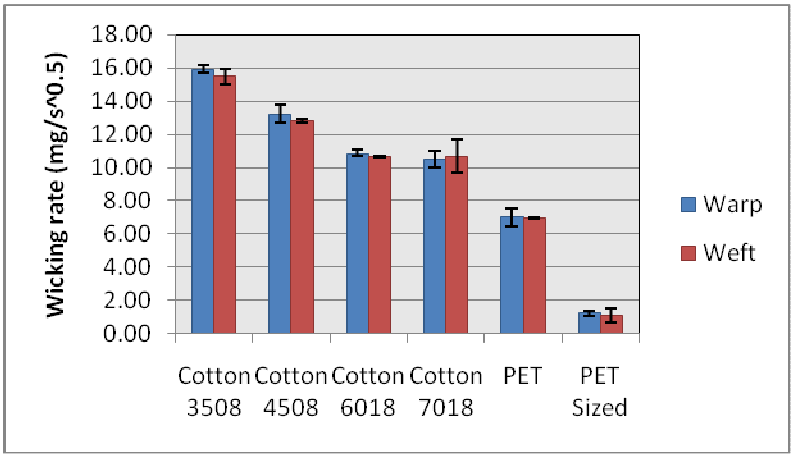

Figure 33: Wicking rates of fabrics obtained by weight balance method using pigment ink as wicking medium.

Table 11: Porosity and % absorption values of fabrics for pigment ink as wciking medium.

Sample	ϕ_{T_0}	ϕ_{Tm}	**% Absorption**	**SD** ϕ_{T_0}	**SD** ϕ_{Tm}	**SD % Absorption**
Cotton 3508	0.39	0.55	196.22	0.01	0.02	7.57
Cotton 4508	0.33	0.49	147.15	0.01	0.02	5.93
Cotton 6018	0.32	0.51	146.20	0.02	0.03	6.92
Cotton 7018	0.28	0.49	126.81	0.02	0.03	7.07
PET	0.28	0.47	105.20	0.00	0.01	3.76

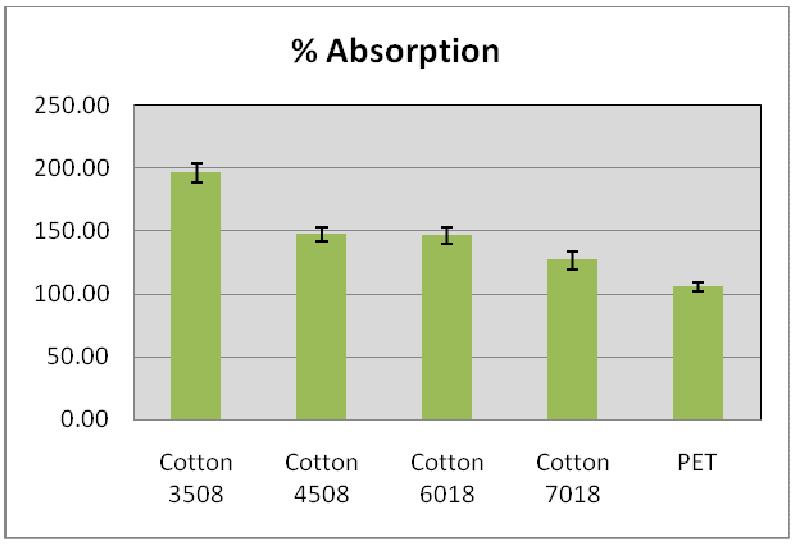

Figure 34: Percent absorption values of fabrics for pigment ink as wicking medium.

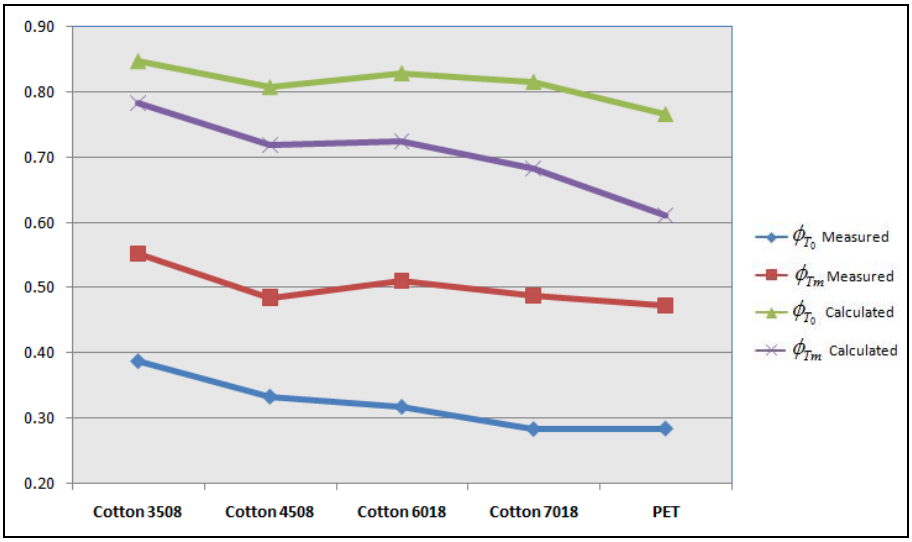

Figure 35: Measured and calcualted values of porosity of fabrics for pigment ink as wicking medium.

5.3.2.3 Comparison of Wicking and Absorption of Water and Pigment Ink in Fabrics

Wicking rates of pigment ink and water are compared in Figure 36. It can be seen that wicking rates of water were substantially higher than those of pigment ink. Washburn's equation (equation 3) predicts that wicking rate should be proportional to factor $\gamma.cos\theta/\eta$. Since contact angle of water and pigment ink with polyester film are known this factor can be calculated. Using the data from section 5.2, this factor for water was found to be 1512 and for pigment ink it is 708. Considering these numbers the wicking rate for water should be about twice the wicking rate of pigment ink. The ratio of wicking rate of water and that of ink is given in Table 12. This table also shows the ratio which is normalized by liquid density which indicates ratio of volumetric wicking rates. Average volumetric ratio is indeed close to 2. This shows that wicking rates are indeed proportional to factor $\gamma.cos\theta/\eta$ as was proposed by Lucas and Washburn. This ratio however was low for polyester fabrics (average 1.6) compared to that for cotton fabrics (average 2.08). This may be because of the difference in the contact angle hysteresis.

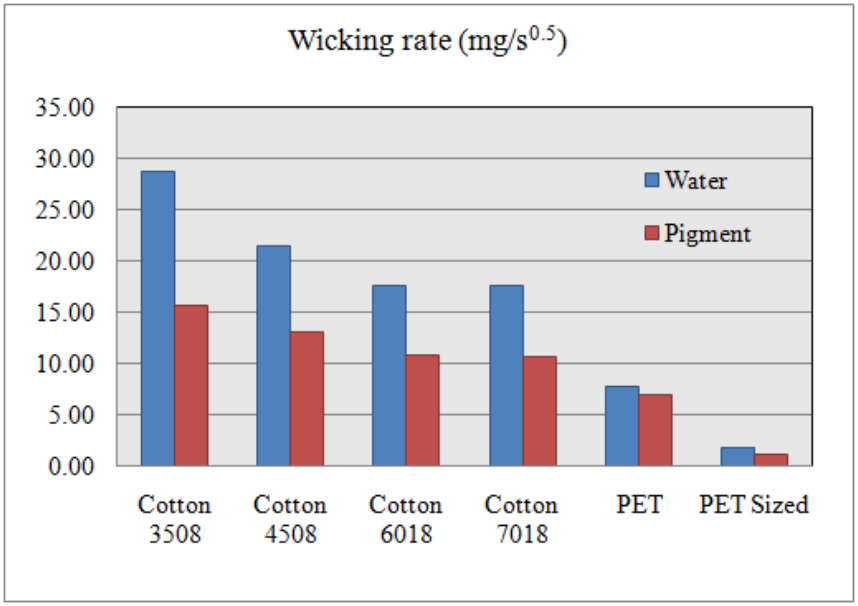

Figure 36: Comparison of wicking rates of water and pigment ink.

Table 12: Ratio of wicking rate of water to wicking rate of ink.

Sample	K_W/K_I	K_W/K_I*
Cotton 3508	1.83	2.24
Cotton 4508	1.64	2.02
Cotton 6018	1.64	2.02
Cotton 7018	1.66	2.05
PET	1.12	1.37
PET Sized	1.49	1.83
Average	**1.56**	**1.92**

*-ratio normalized by density of liquid

Only a small difference was observed between % absorption values of pigment ink and water for all the fabrics (Figure 37). Fabrics absorbed slightly less ink than water. However when weight absorption values are normalized by the density of liquid, larger difference is noted as shown in Figure 38. Thus volumetrically, fabrics absorb more

water than ink. Since fabrics absorbed more water, they showed higher porosity values as can be seen in Figure 39.

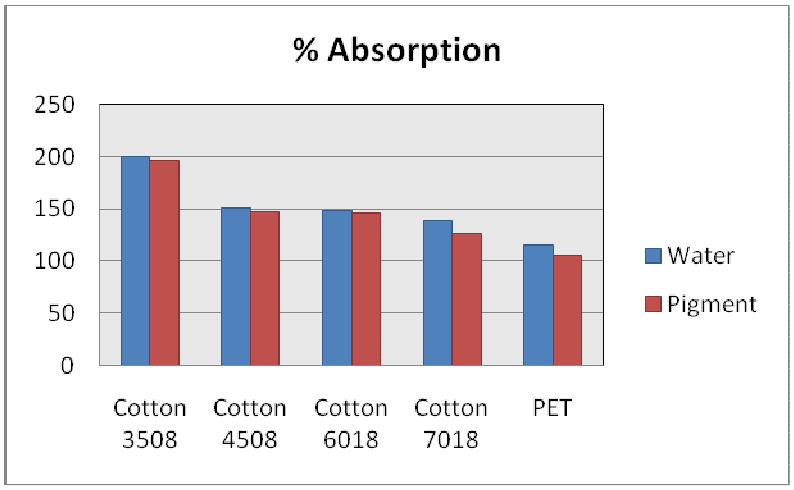

Figure 37: Comparison of % absorption of water and pigment ink in fabrics.

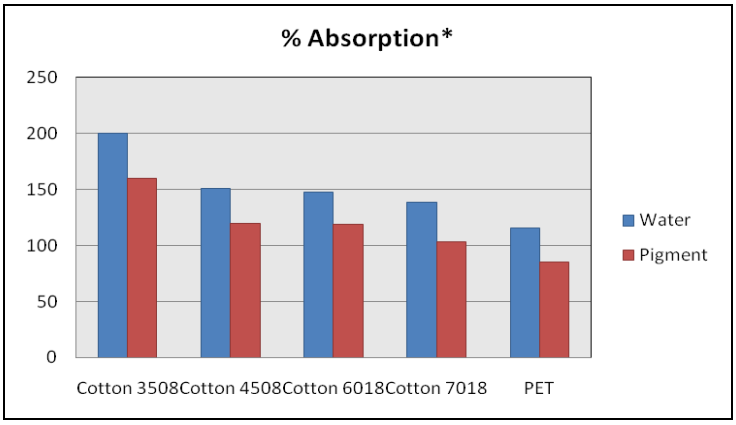

Figure 38: Percent absorption of water and pigment ink - values normalized by density of liquid.

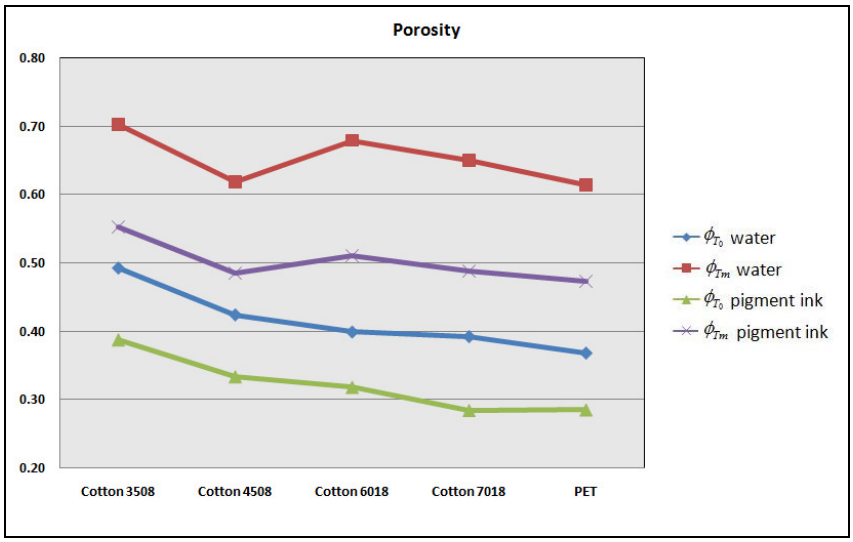

Figure 39: Comparison of measured porosity values for water and pigment ink as wicking media

5.3.3 Comparison of Wicking Results Obtained by Weight Balance and Image Analysis Methods

Literature review showed that sorption in vertically hung fabrics from an unlimited reservoir has been studied by weight balance method as well as by image analysis method, where weight or height of the liquid rise in fabrics is measured respectively as a function of time. Researchers assume that these two methods are complementary to each other i.e. one can be used in place of the other [2, 17]. However the results of these methods have never been compared for different types of fabrics. Since the wicking of pigment ink was studied using both image analysis and weight balance methods, results of the two methods are compared below.

Weight wicking rate values obtained by weight balance method were converted to height wicking rate values and compared to those obtained by the image analysis method. The method of converting weight data to height data has been shown by Patel and Lee

[17]. The authors converted the weight data to height data using equation 12. The porosity values were calculated by measuring the amount of liquid retained by fabrics after wicking experiments. Similar technique was used and wicking rates in $cm/s^{0.5}$ were calculated from weight wicking rates ($mg/s^{0.5}$). The data is shown in Table 13 and also presented in Figure 40. ϕ_{To} and T_0 values were used for conversion. But ϕ_{Tm} and T_m values also give same wicking rate numbers.

It was expected that the converted and measured wicking rate values will match. But surprisingly they did not match except for Cotton 7018 fabric as can be seen in Figure 40. Both image analysis and weight balance methods showed that as thread density goes up wicking rate goes down. This trend was not observed in converted data. To find the causes of deviations, the wicking of liquid in yarns and fabrics was microscopically observed.

Table 13: Conversion of weight wicking rates of fabrics to height wicking rates.

				Wicking rate ($cm/s^{0.5}$)	
Sample	ϕ_{T_0}	**T_0**	**Wicking rate ($mg/s^{0.5}$)**	**Weight balance method**	**Image analysis method**
Cotton 3508	0.39	0.90	15.72	0.25	0.37
Cotton 4508	0.33	0.86	13.03	0.25	0.33
Cotton 6018	0.32	0.75	10.75	0.25	0.30
Cotton 7018	0.28	0.76	10.60	0.27	0.28
PET	0.28	0.65	6.96	0.20	0.34

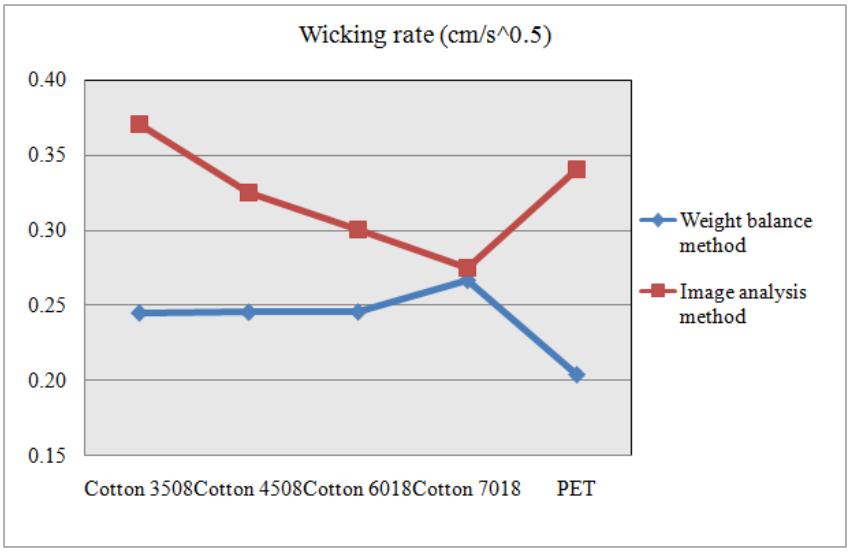

Figure 40: Converted height wicking rates and actual height wicking rates of fabrics.

The experiments on yarn were done on PET tape filament yarns as very good cross-sections of threads could be obtained and also liquid wicked into these threads very slowly, permitting easy monitoring of liquid flow in different capillaries. Snapshots of wicking process are shown in Figure 41. According to Washburn equation, liquid flows faster in bigger radii capillaries than small radii capillaries. However images show that smaller capillaries filled first and when sufficient liquid was available, bigger capillaries were filled. Thus during initial part of wicking, only some part of available pore volume is used. At longer times, larger capillaries get filled and this implies more available pore volume is occupied with the passage of time.

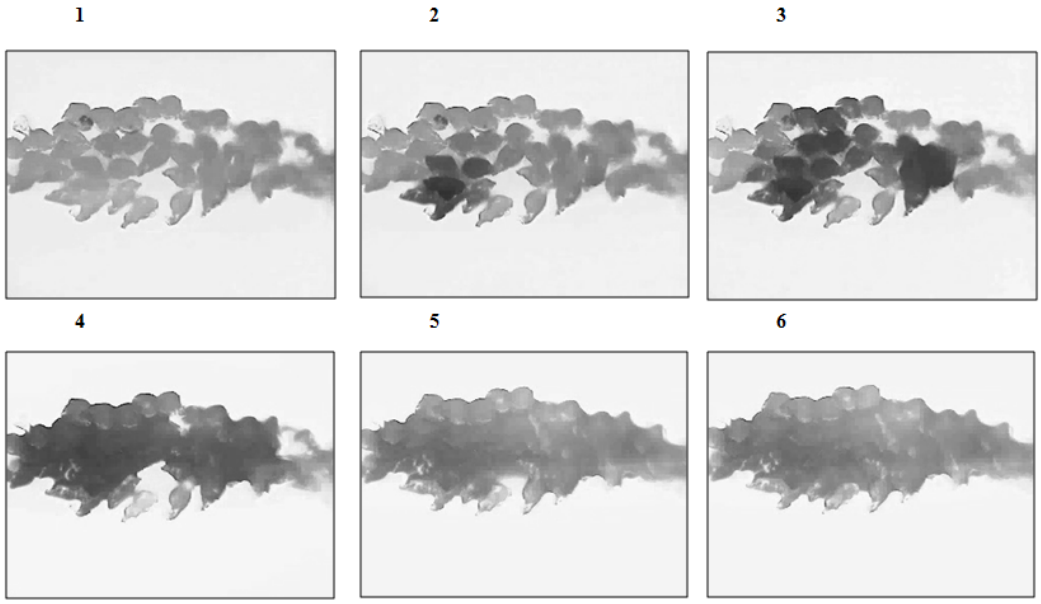

Figure 41: Snapshots of wicking of liquid in filament yarn.

Microscopic images of wicking in fabrics show that inter-yarn spaces are filled after the inter-fiber spaces around the vicinity of inter-yarn space is completely filled as shown in Figure 42.

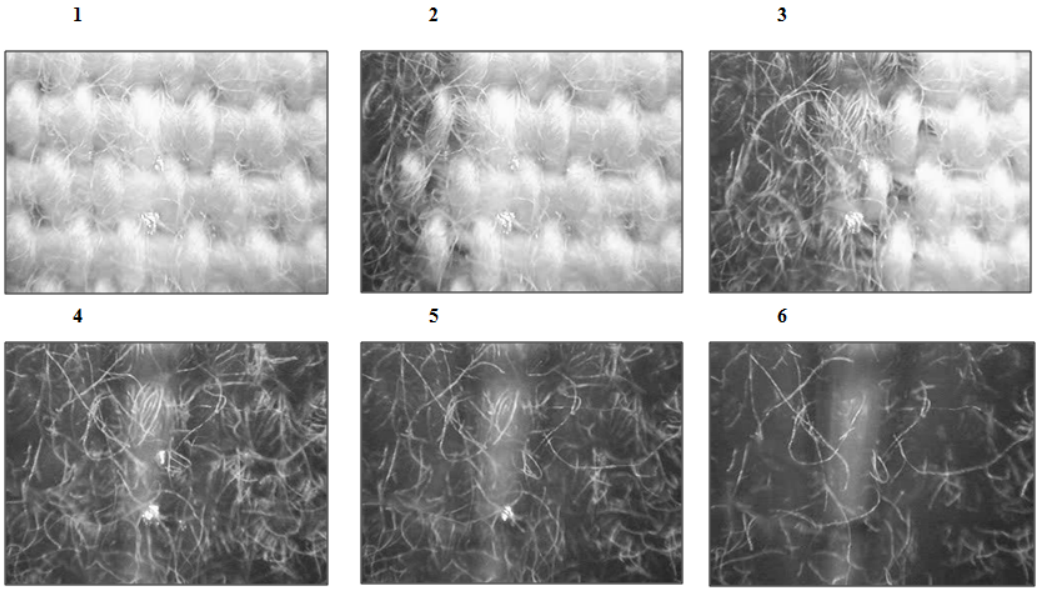

Figure 42: Snapshots of wicking of liquid in Cotton 3508 fabric.

The porosity value which was used for conversion of weight to height wicking rate was determined from the weight of liquid retained by fabrics, which was measured at the end of wicking experiment. This gives higher values of measured porosities. According to equation 12, higher value of porosity gives lower value of wicking rate. That is why weight balance method gave lower height wicking rates compared to those obtained by image analysis method. Further, the equation shows that calculated height is inversely proportional to the measured porosity. The height wicking rate of Cotton 3508 fabric had higher porosity than Cotton 4508 fabric. Converted wicking rate of Cotton 4508 fabric was higher as it had lower ϕ_{To} value. Therefore the wicking trend shows a deviation. The difference between converted wicking rates and actual wicking rates was higher in case of more open fabrics and was lower for compact fabrics. For the most compact fabric, Cotton 7018, the converted wicking rate and actual wicking rate were same. Diffrence between converted and actual wicking rate for PET fabric was also large. This may be due to the fact that weight wicking rate of PET fabrics was very low as PET fibers do not absorb any water. It may also be due to the fact that PET fabric was an open and rough fabric.

Results show that weight balance method cannot be considered a substitute for image analysis method, especially if the method is to be used for more open fabrics. Results also show that weight balance method and image analysis method give different results for fabrics having different fiber materials such as cotton and polyester.

5.4 Effect of Fabric Structure on Drop Spreading

Drop spreading experiments were done on all the experimental fabrics. Since fabrics were clamped on a plastic frame with the help of cellophane tape, PET 4663, PET 8863, PET 4680 and PET 8880 fabrics did not curl during drop spreading experiments. When a drop is placed on the fabric, it immediately starts spreading radially outwards. It was found that for a drop volume of 0.012 ml, the drop spreading process completed within two minutes for all the fabrics. The images of drops on fabrics at time, t=0 and final drop spreading images for all the fabrics are shown in Figure 43, 44 and 45. Images show that the shape of a drop on fabric at t=0 is near circular for all fabrics. Initial and final drop sizes are given in Table 14 and Figure 46. The initial size of drop was found to be slightly smaller for rough fabrics such as Cotton 3508, PET 4663 and PET Sized fabric. Rough surface obstructs the flow of liquid after the impaction of a drop. Wetting characteristics of fabrics may also affect this phenomenon. Sized PET fabric showed smallest initial area, possibly because it was least wettable. Final drop spreading area seemed to depend upon thickness of fabric. Final drop spreading area correlated well with thickness data as can be seen in Figure 47. The shape and size of final drop spreading area were completely different for all the fabrics. Final drop spreading areas for some fabrics were near circular and hence symmetrical, while for other fabrics they were unsymmetrical or anisotropic and approached elliptical shape. Anisotropy of drop spreading is discussed in section 5.4.2.

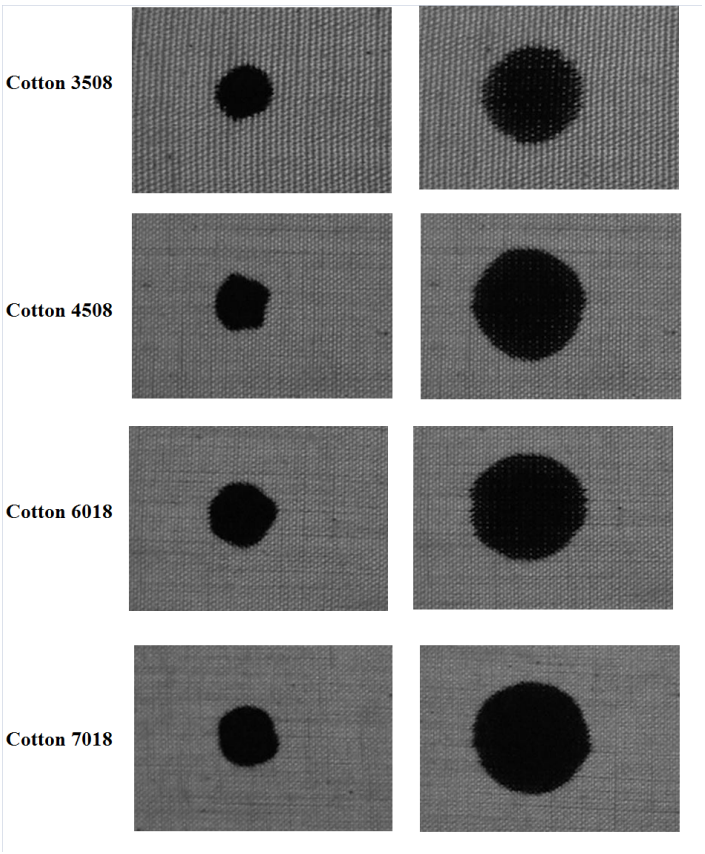

Figure 43: Spreading of drop on cotton fabrics.

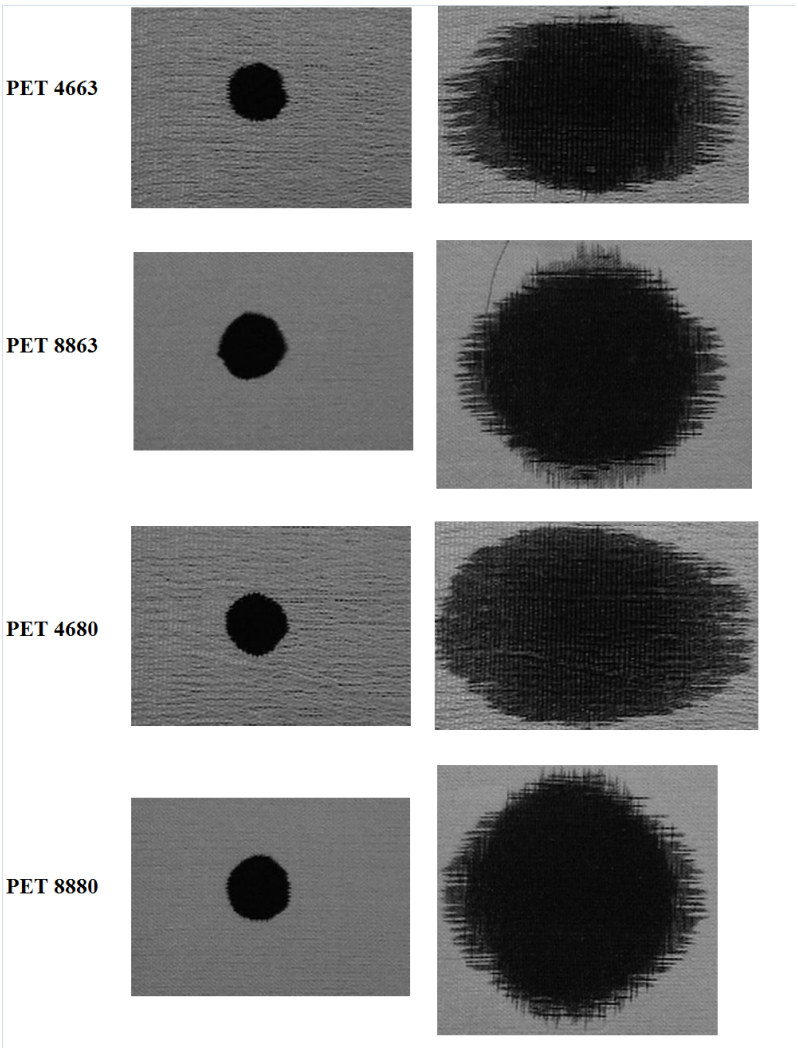

Figure 44: Spreading of drop on polyester fabrics.

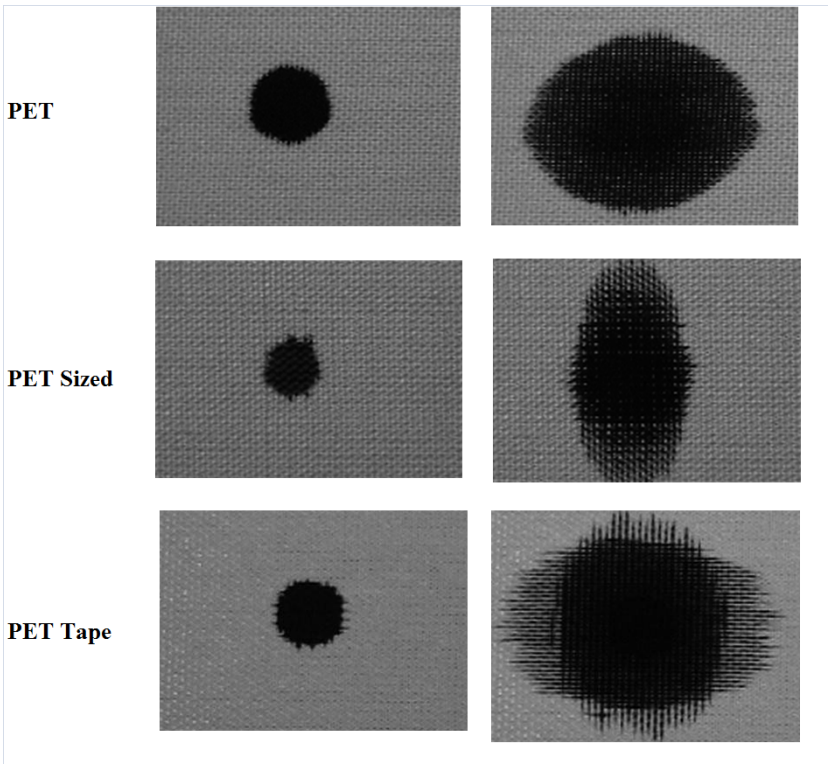

Figure 45: Spreading of drop on polyester fabrics.

Table 14: Spreading of pigment ink on fabrics - initial and final drop spreading areas.

Sample	Initial Area (cm2)	SD	Final Area (cm2)	SD
Cotton 3508	0.31	0.07	0.83	0.12
Cotton 4508	0.32	0.13	0.96	0.05
Cotton 6018	0.32	0.07	1.22	0.09
Cotton 7018	0.33	0.08	1.39	0.08
PET 4663	0.30	0.05	3.89	0.18
PET 8863	0.36	0.07	4.69	0.26
PET 4680	0.32	0.04	4.40	0.38
PET 8880	0.38	0.02	4.92	0.22
PET	0.26	0.06	2.49	0.07
Sized PET	0.23	0.03	1.40	0.14
PET tape	0.36	0.07	3.49	0.42

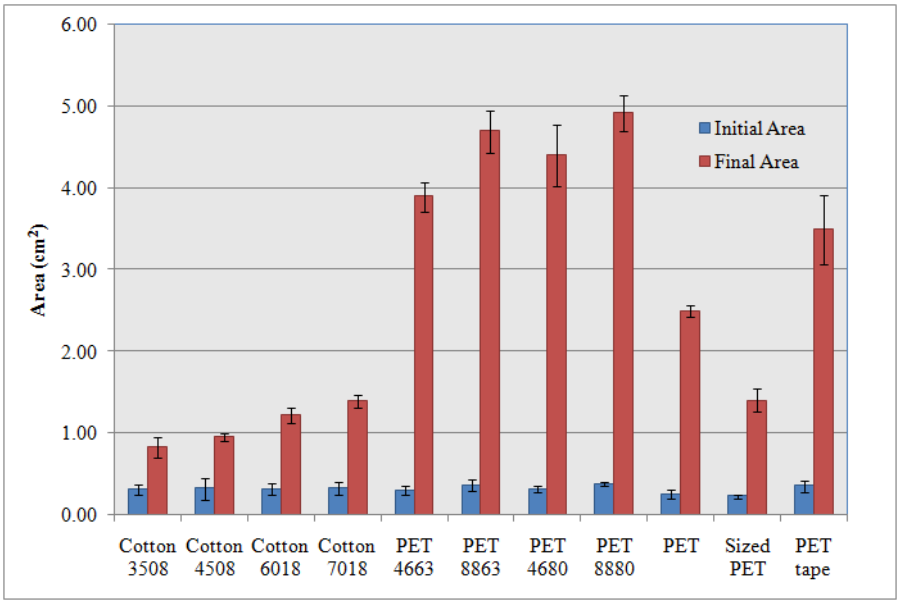

Figure 46: Spreading of pigment ink on fabrics - initial and final drop spreading areas.

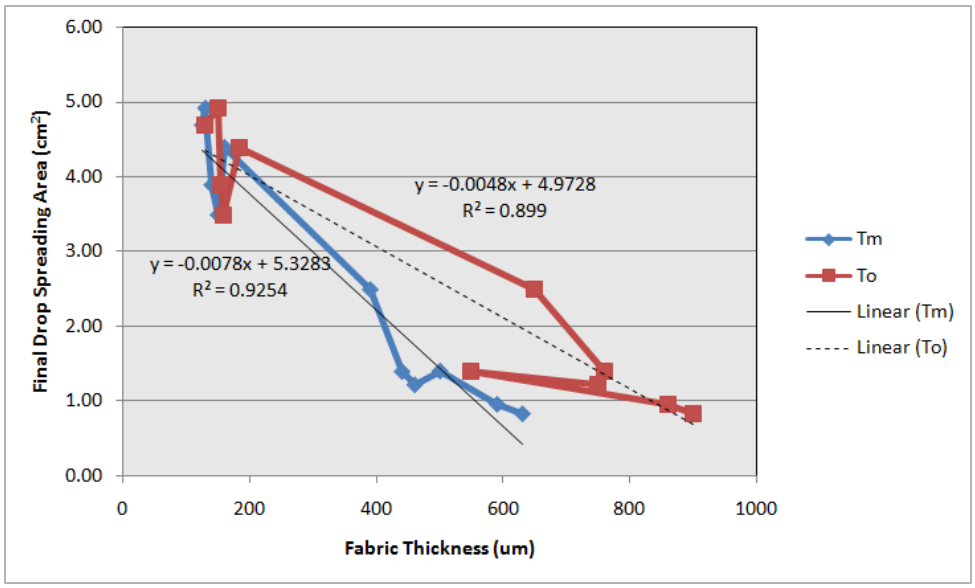

Figure 47: Relation between thickness of fabric and final drop spreading area.

5.4.1 Spreading Rates of Fabrics

The calculated drop spreading rates are presented in Table 15 and Figure 48. Cotton 7018 and PET 4680 fabrics showed the highest drop spreading rates, while the sized PET fabric, as expected, showed the least drop spreading rate. In general, thinner and more compact cotton fabrics showed higher drop spreading rates. Higher drop spreading rates were also observed in the case of PET fabrics, PET 4663, PET 8863, PET 4680.

Data shows that drop spreading rates were different for different fabrics, which means fabric structure definitely affects the drop spreading rates. Kissa and Kawase assert that the factor K_D is fabric thickness dependent but they did not give any specific relation between them [21, 22]. Figure 49 shows the correlation between drop spreading rates and the two thickness values, T_0 and T_m. R^2 values suggest that no strong association exists between fabric thickness and drop spreading rate. Between T_0 and T_m, T_m shows a slightly better association but the strength of association remains weak even between T_m and rate of drop spreading. It is possible that drop spreading rate is influenced by several structural parameters namely, thickness, thread spacing, yarn count, yarn type etc. Effect of fabric structural parameters on drop spreading rate is discussed again in section 5.5.

Table 15: Rates of spreading of pigment ink drop on fabrics.

Sample	K	SD
Cotton 3508	0.74	0.07
Cotton 4508	1.37	0.15
Cotton 6018	1.91	0.27
Cotton 7018	2.90	0.44
PET 4663	1.81	0.04
PET 8863	2.21	0.25
PET 4680	2.78	0.40
PET 8880	1.76	0.03
PET	0.96	0.05
Sized PET	0.52	0.02
PET tape	0.94	0.03

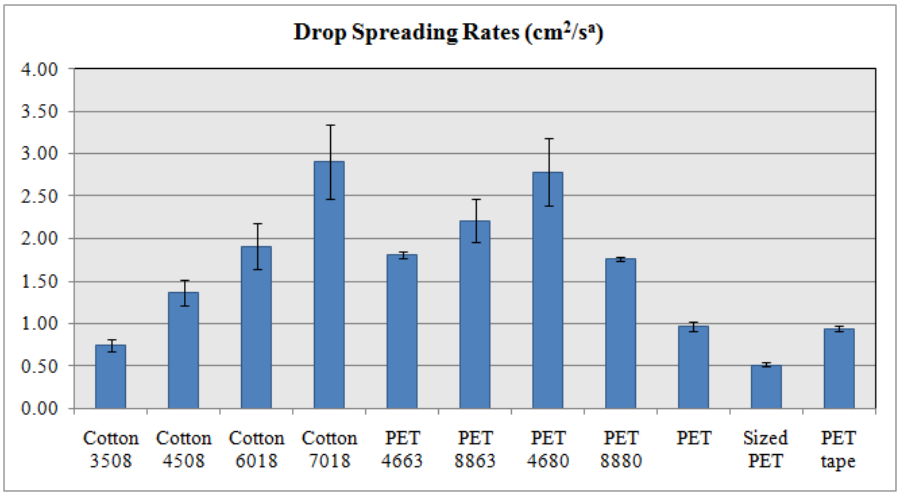

Figure 48: Rates of spreading of pigment ink drop on fabrics.

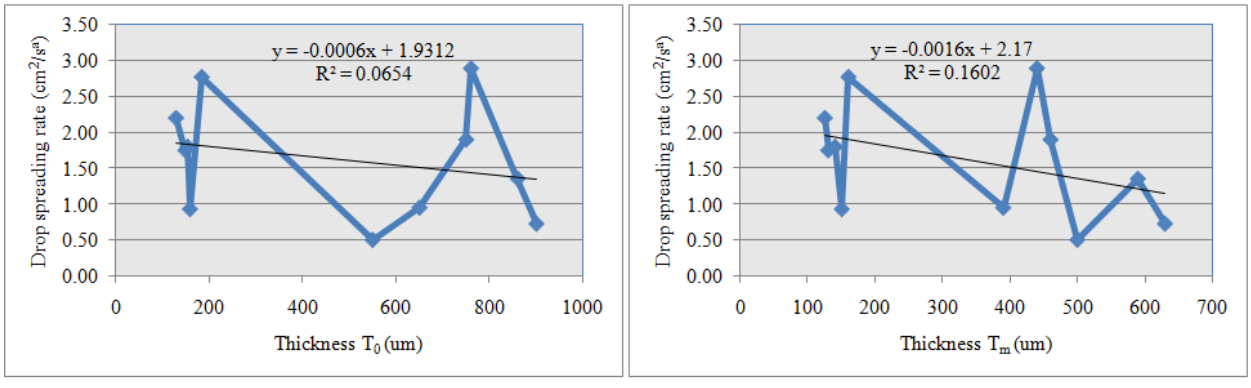

Figure 49: Relationship between drop spreading rate and fabric thickness.

5.4.2 Anisotropy in Drop Spreading

As discussed before, drop spreading was anisotropic in many fabrics. Anisotropy of drop spreading was studied by Adams and coworkers [24]. They believed that anisotropy originates from the differential permeability of fabrics in different directions and concluded that drop spreading study is the best way to simultaneously find the directional permeabilites of porous structures such as textile fabrics.

Anisotropy in simple terms, can be defined as the difference between drop spreading distances in two mutually perpendicular directions. Larger the absolute difference, larger the anisotropy. Anisotropy was determined by subtracting drop spreading distance in weft direction from drop spreading distance in warp direction or vice versa. The absolute numbers are given for all the fabrics in Table 16 and are also presented in Figure 50. It is observed that cotton fabrics showed least amount of anisotropy while almost all the polyester fabrics showed high amount of anisotropy. Several other things were also observed. As thread density went up, anisotropy decreased. This is probably due to the fact that the fabric structure becomes more balanced. In other words, the absolute difference in thread density between warp and weft directions approaches zero.

Anisotropy can be considered to originate due to the difference in the wicking rates of warp and weft yarns. For example PET, Sized PET and PET Tape fabrics showed very high anisotropy and the difference between their warp and weft yarn wicking rates (Table 4) was also very high. However despite the fact that there was very high

difference in warp and weft yarn wicking rates, Cotton 3508 and Cotton 4508 fabrics showed least anisotropy.

Table 16: Anisotropy in drop spreading.

	Final Drop Spreading Distance in Direction		Anisotropy
Sample	**Warp (a)**	**Weft (b)**	**absolute(a-b)**
Cotton 3508	1.24	1.16	0.08
Cotton 4508	1.18	1.21	0.03
Cotton 6018	1.69	1.56	0.13
Cotton 7018	1.40	1.34	0.06
PET 4663	3.30	1.94	1.36
PET 8863	3.01	2.41	0.60
PET 4680	2.87	2.01	0.86
PET 8880	2.90	2.72	0.18
PET	2.39	1.82	0.57
Sized PET	1.27	2.18	0.91
PET tape	2.85	2.41	0.44

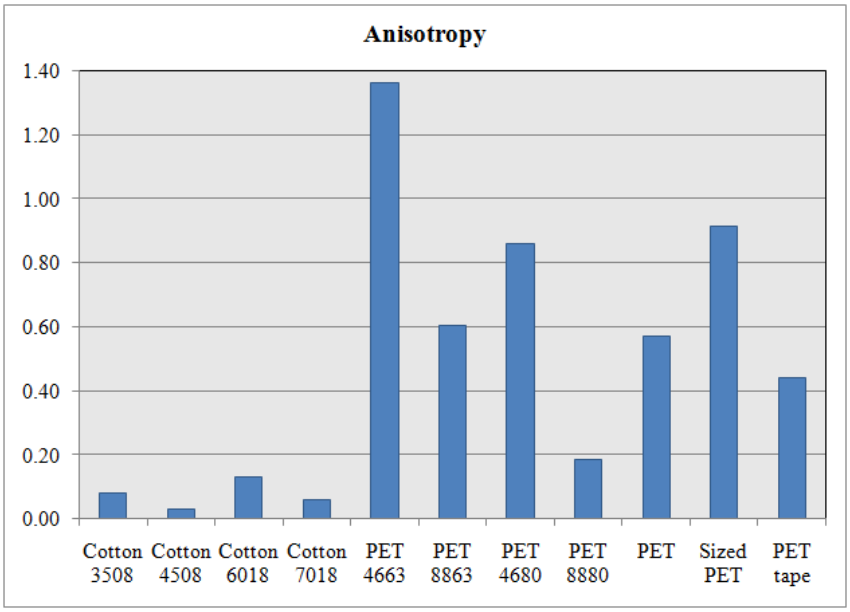

Figure 50: Anisotropy in drop spreading.

This implies that anisotropy is not entirely dictated by the difference in the wicking rates of warp and weft yarns or by the difference in thread densities. It may also be influenced by the way liquid migrates from one yarn to another. To study the yarn-to-yarn liquid migration phenomenon, and its effect on anisotropy, some novel but simple experiments were carried out.

As shown in Figure 51, fabric strips were cut in such a way that only one yarn end sufficiently protrudes from the fabric. The open yarn end is immersed in a large reservoir of pigment ink. Wicking process in the fabric was recorded by a Canon camcorder. Liquid starts to wick in a dipped thread and starts to migrate from one thread to another. The migration process gives a characteristic shape to the advancing liquid front. The images of the fabrics which were taken after one minute of migration are shown in Figure 52. Wicking experiments could not be carried out on PET 4663, PET 8863, PET 4680 and PET 8880 fabrics because these fabrics tended to curl during the experiments.

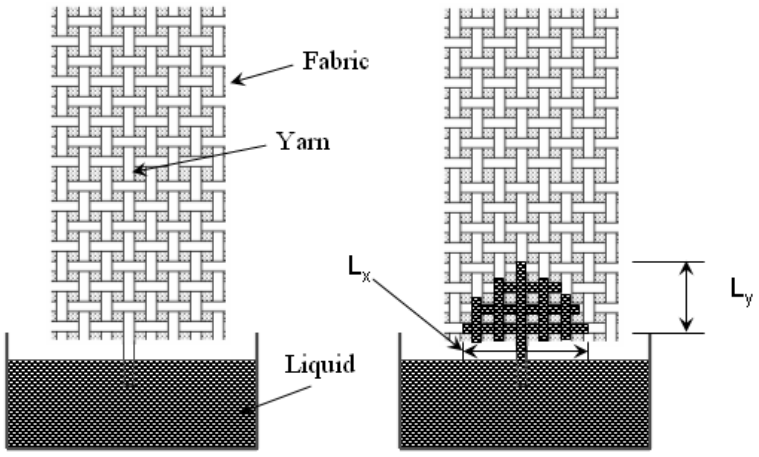

Figure 51: Schematic of experimental setup to study yarn-to-yarn liquid migration.

Images (Figure 52) show that for cotton fabrics the shape of liquid front was slightly elliptical and the shape was similar for warp and weft direction. This shows that migration from warp yarn-to-weft yarn and weft yarn-to-warp yarn is similar and the transfer of liquid occurs at the same rate. However for all other polyester fabrics there was a tremendous difference in the shape of liquid front when experiments were carried out in warp and weft direction. Images of PET fabrics show that migration of liquid from weft yarn to warp yarn occurs at a faster rate than the migration from warp to weft yarn. This implies that liquid prefers to move in warp direction than in the weft direction. This observation also matches with the observations made in the image analysis of wicking experiments. Warp threads in these fabrics are twisted yarns for which capillary forces are very high. Weft threads in these fabrics are filament PET yarns which have low capillary pressure. Therefore twisted warp threads of polyester fabrics drew liquid from weft threads more rapidly and efficiently, giving higher spreading distances in the warp direction than in the weft direction. A similar phenomenon can be observed in PET Tape fabric. In PET sized fabric, since the sized warp yarns absorb less amount of liquid, very little migration was observed. The above experiment suggests that yarn-to-yarn liquid migration is a major factor governing the anisotropy of drop spreading.

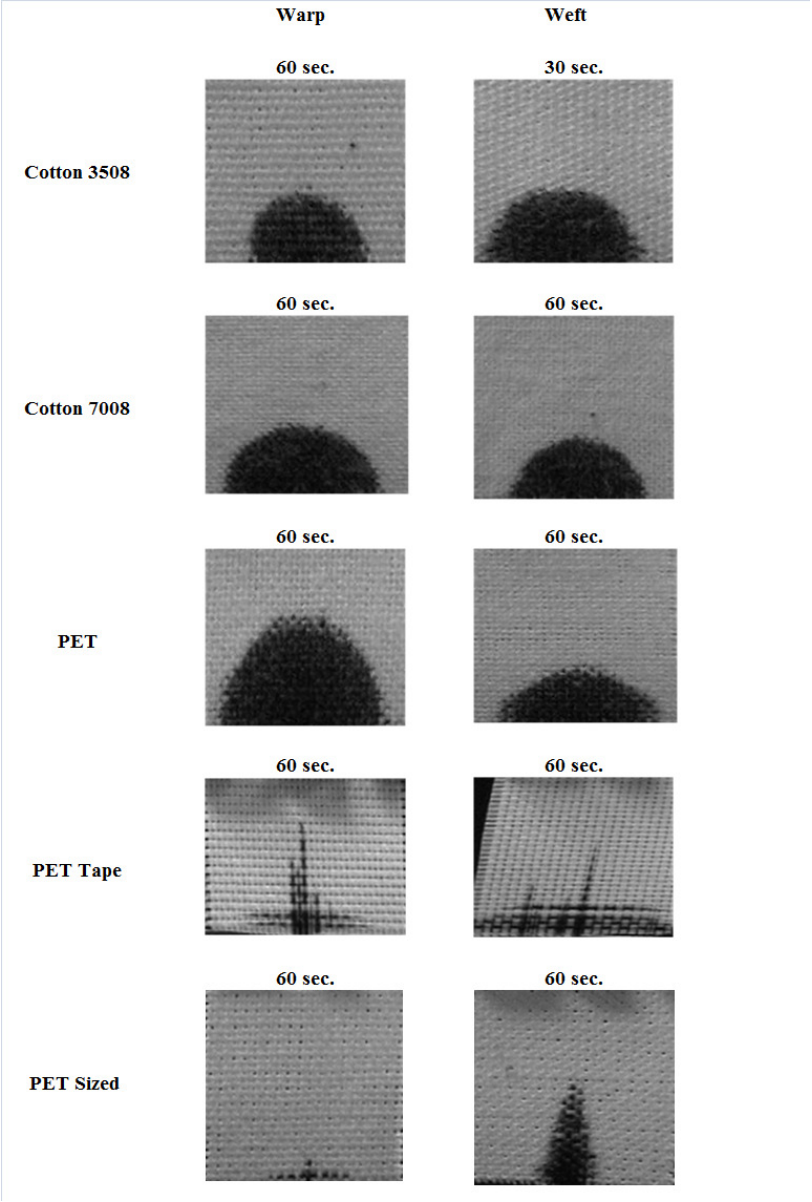

Figure 52: Yarn-to-yarn liquid migration in fabrics.

5.5 Comparison of the Wicking Behavior of Unlimited and Limited Supply Sources

Drop spreading rates and wicking rates of fabrics are compared in Figure 53. It is observed that these rates are completely different. Very poor correlation between these

two rates (R^2=0.06) can be seen in Figure 54. For cotton fabrics the trend, in fact, is opposite. Wicking rate decreased with increase in thread density while drop spreading rate increased with increase in thread density. This implies that inter-yarn spaces that boost wicking rate do not influence drop spreading rate. This may be because of the fact that the drop volume used in experiments was very small and it depletes very fast. Depletion time was just 4 seconds for cotton fabrics, around 25 seconds for all the polyester fabrics, except the PET Tape fabric for which it was around 120 seconds. There may not be enough liquid available to fill up the inter-yarn spaces. Microscopic investigation has showed that inter-yarn spaces only fill when surrounding inter-fiber spaces saturate fully with liquid. Inter-yarn spaces may get filled during early period of drop spreading when there is enough quantity of liquid available and they may not find enough ink to continue filling in the later stages of drop spreading.

Drop spreading rate in the case of cotton fabrics increases with the increase in thread density, possibly because of the closer proximity of the neighboring threads. Excellent wettability of cotton possibly favors the migration process. As soon as liquid encounters an un-wetted thread, it immediately tries to wet it which results in higher drop spreading rate. However, if liquid continues to travel in the same thread, instead of migrating to others, liquid propagation rate decreases with time as capillary pressure is reduced and as the equilibrium wicking height or length is reached, the capillary pressure becomes zero. For these reasons possibly, drop spreading rates of cotton fabrics show an increase with increase in thread density.

Further, low drop spreading rates were observed in 8 count cotton fabrics compared to 18 count cotton fabrics. This possibly happens because 8 count cotton yarns

are thicker than 18 count cotton yarns. Penetration time required for liquid after migration from warp yarn to the 8 count weft yarn is going to be more than the penetration time required for liquid after migration from warp yarn to the 18 count weft yarn. This is why possibly 8 count cotton fabrics show lower drop spreading rates compared to 18 count weft yarn fabrics.

PET 4663, PET 8863, PET 4680 and PET 8880 showed completely opposite trend compared to that of the cotton fabrics. PET 4663 fabric showed lower drop spreading rate compared to the other fabrics in that group as it was extremely open and loose. The inter-filament spacing for the texturized weft yarn was more resulting in lower capillary pressure in the yarn. Final drop spreading area was also lower for this fabric (Figure 46). The drop spreading rates of the polyester fabrics showed somewhat unusual trend with respect to thread density. Polyester is difficult to wet by ink than cotton. When fabrics are difficult to wet by ink there is a brief period of slog time before liquid starts to wick in threads or fabric. Decreased drop spreading rate in the 88 denier PET fabric with increase in thread density was observed possibly because of this reason.

The PET fabric showed low drop spreading rate although it showed very high wicking rate, possibly because of the longer time it takes for the ink to penetrate through thicker yarns. Lower drop spreading rate might also be because of wettability issues. As inter-yarn spaces and thread segments do not enhance drop spreading rate due to very limited drop volume, high drop spreading rate was not observed.

As expected, sized PET fabric showed low drop spreading rate as well as low wicking rate. PET Tape fabric showed good drop spreading rate compared to other fabrics, possibly because of the very low thickness filament yarns it contained.

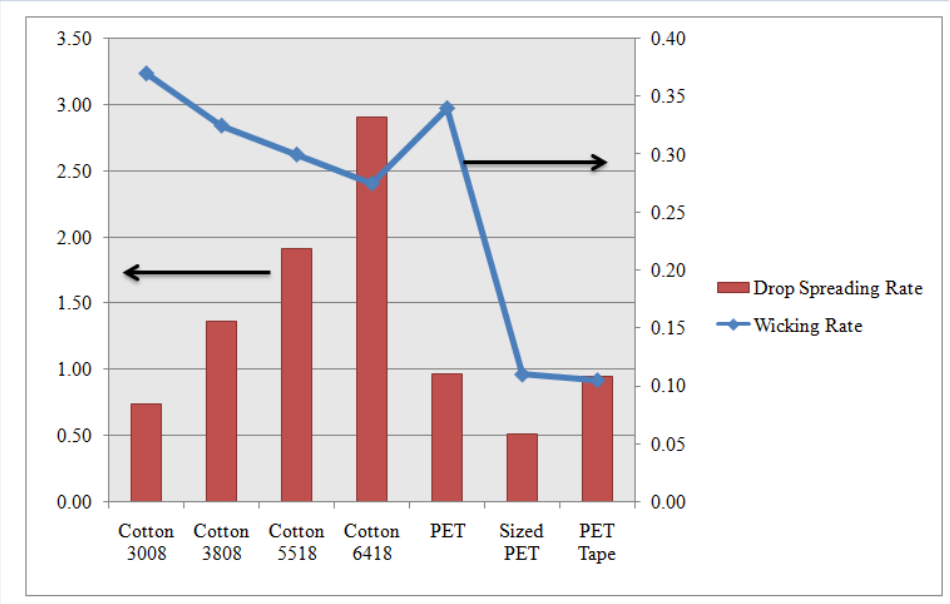

Figure 53: Comparison of drop spreading and wicking rates.

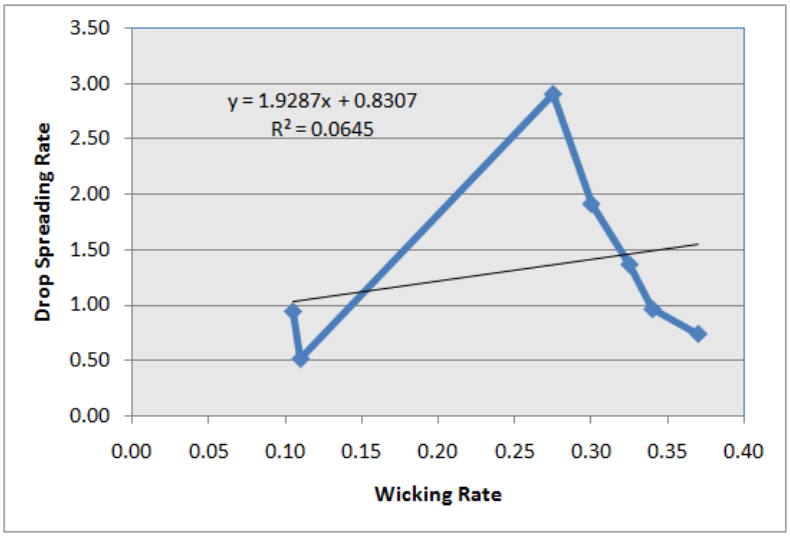

Figure 54: Relation between drop spreading and wicking rates.

5.6 Effect of Fabric Structure on Ink Jet Printing Quality

As explained in the Experimental section, ink jet printing experiments were done using Dimatix printer and Fabric Fast Ultra ink which was received from Trident Company. Optimum firing voltage and firing frequency for perfect, circular, satellite free drops were found to be 11 V and 20 KHz, respectively. Results of different experiments which were carried out to understand the effect of fabric structure on printing quality are discussed in this section.

5.6.1 Spreading Behavior of Ink-Jet Drops on Textile Yarns

Typical spreading behavior of the ink jet drops on various yarns is shown in Figure 55. The wicking phenomenon was observed mainly in polyester filament yarns. Drop spreading behavior on cotton yarns was substantially different from that observed on filament polyester yarns. It was observed that water in the ink tends to diffuse in single cotton fibers instead of wicking in the channels formed between fibers (Figure 55 (c)), whereas a combination phenomena appeared to exist in the case of polyester yarns. Drops sometimes wicked; sometimes spread along the surface of filaments and in few cases, formed near circular dots on the surface of filaments. Spreading on single filament occurred, when the drop hit single filament that is separated from the bulk of yarn. Drops on these separated filaments appeared almost circular. However when drop fell in the closely packed region, it wicked in narrow channels between the filaments. Sometimes single drop was found to split and liquid wicked in more than one capillary. This happened because the diameter of the drop (40-50 μm) is larger than the diameter of a

single fiber or filament (~15 μm in most of the fabrics). While drops can land on several capillaries, they wicked more in smaller capillaries, as capillary pressure is substantially higher in narrow capillaries. Spreading in multiple capillaries or pores was mainly observed in the twisted polyester filament yarn. Twisted polyester filament had closely packed small and narrow capillaries which allowed the drop to spread in several capillaries. Wicking was not observed in cotton yarns. This may be due to the fact that water in the ink quickly diffuses inside the fiber, leaving behind the pigments on the surface. The diffusion rate in cotton dominates the wicking rate and then ink jet drops being very small, enough liquid is not available to wick through the inter-fiber channels.

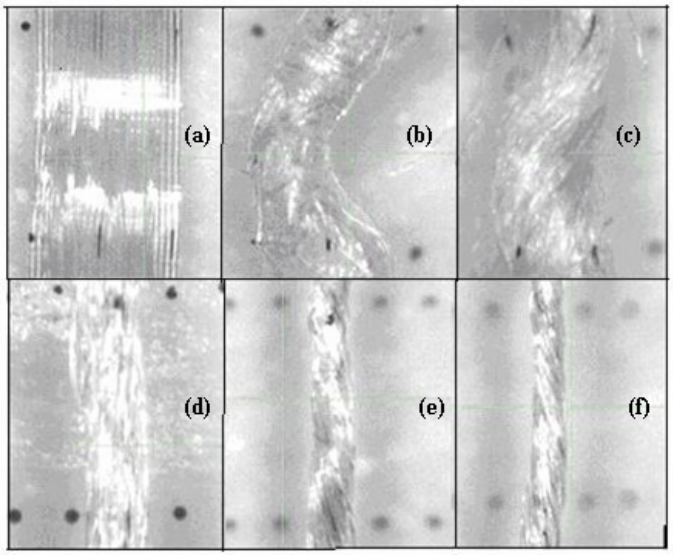

Figure 55. Drop spreading on yarns (a) PET Tape yarn (b) Sized PET rotor yarn(c) Cotton yarn 3508 weft (d) PET 8880 non twisted filament yarn (e) PET 8880 twisted yarn (f) PET 8880 twisted yarn.

It was also found that ink jet drops spread only in the fiber or filament length direction. Spreading was not noticed in the direction perpendicular to the fibers.

Spreading along the fiber or filament direction was measured using the microscope provided in the Dimatix printer. Figure 56 shows the average spreading of pigment ink in microns along the fiber or filament length. Spreading in twisted filaments could not be determined because drops spread in many small pores and traces of the ink were difficult to locate. PET Tape yarns showed the maximum spreading. Continuous and narrow capillaries that were formed between filaments promoted the wicking of ink and drop spreading was higher in these yarns.

Sized PET and cotton yarns gave the lowest drop spreading measurements almost comparable to the high quality Epson ink jet printing paper.

Single and multiple ink drops (one, ten and twenty drops) were made to hit at the same location on the yarn. Results obtained (Figure 56) show that the spreading distance does not increase significantly when ten or twenty drops hit the same location. This may be because of the low firing frequency of the ink jet printing process. The ink drop hitting the surface of the fabric possibly evaporates before successive drops hit the same location again. Therefore pigments in the ink drops simply deposit on each other and further spreading is restricted. The very nature of the pigment ink and its special properties may also be responsible for this. Very high loading of pigments, around 10%, presence of binder molecule on the surface of pigments and also the presence of polymer dispersant molecules in the medium [38-40], possibly restrict the flow of successive drops due to high molecular frictional drag. This feature can be helpful where higher color depths are required. Darker color shades can be achieved without hampering printing quality. This feature can also prove to be important for smart applications where higher quantity of the material being applied is required on the surface of the fabrics for appropriate

enhancement of functional performance. Impaction of ten and twenty drops at the same location improved the color depth of the dots. Ten and twenty drops gave the darker drop compared to that of a single drop.

Very high variability was observed in the data. This originates from variable nature of the capillaries present in the yarns. Capillaries vary in their diameter from place to place and may be narrower or broader. Narrower capillaries give higher drop spreading distance compared to broader capillaries. If drop falls on separated fiber or filament it spreads to very short distance. Epson ink jet paper showed the least variability due to the absence of capillaries.

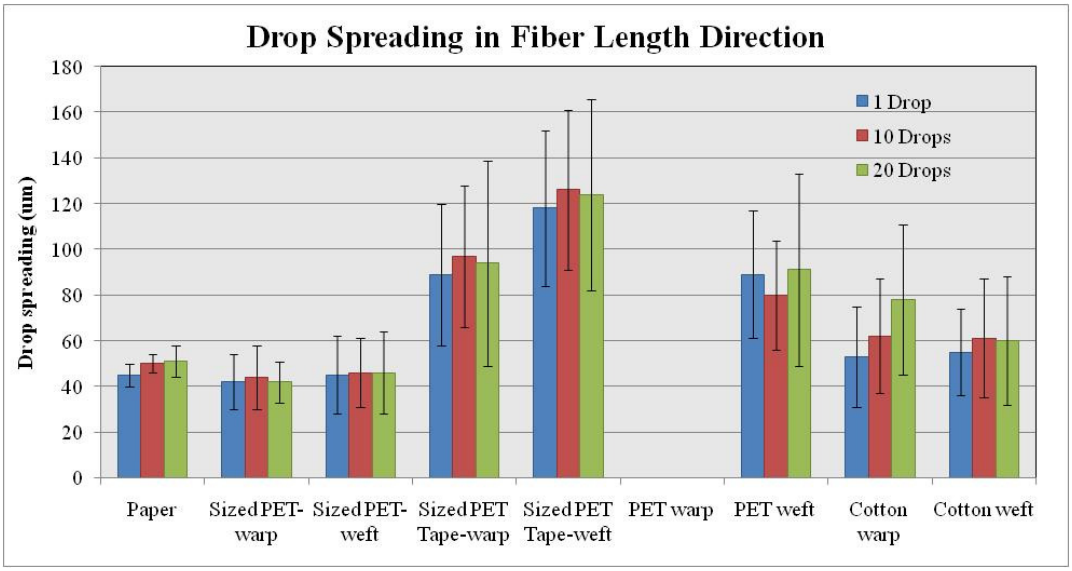

Figure 56. Drop spreading in Epson paper and experimental yarns.

Excessive wicking of yarns results in poor quality of printing while less wicking gives more regular and circular drops, reflecting better quality of printing. Printing quality on all the fabrics was evaluated by printing lines on fabrics. The drop-spreading results suggest that the cotton and the sized PET fabrics should give very high line

quality. Results and observations of line printing on textile fabrics are discussed in the next section.

5.6.2 Effect of Fabric Structure on Ink Jet Line Printing Quality

As explained in experimental section, lines having width of 100 μm were printed in warp and weft direction of each fabric. The lines were also printed on the high quality Epson ink jet printing paper. The lines were observed under microscope and width of the line was measured at several locations. Images of the lines on various fabrics are shown in Figures 57-60. The width of line was found to be affected by several factors which are discussed below.

Effect of Orientation of the Fibers or Filaments

The width of the printed line on transverse threads was always higher than that on longitudinal threads. This can be observed clearly in the images b, c, d & e of Figure 57, which represent the four woven fabrics while the image 'a' represents the printing paper. Threads parallel to the printed line are longitudinal threads and those perpendicular to the line are Transverse threads Width of the line on transverse threads was more due to the fact that fibers in the transverse yarn are oriented in the widthwise (transverse) direction, making it easy for the ink to flow in the fiber channels formed in this direction.

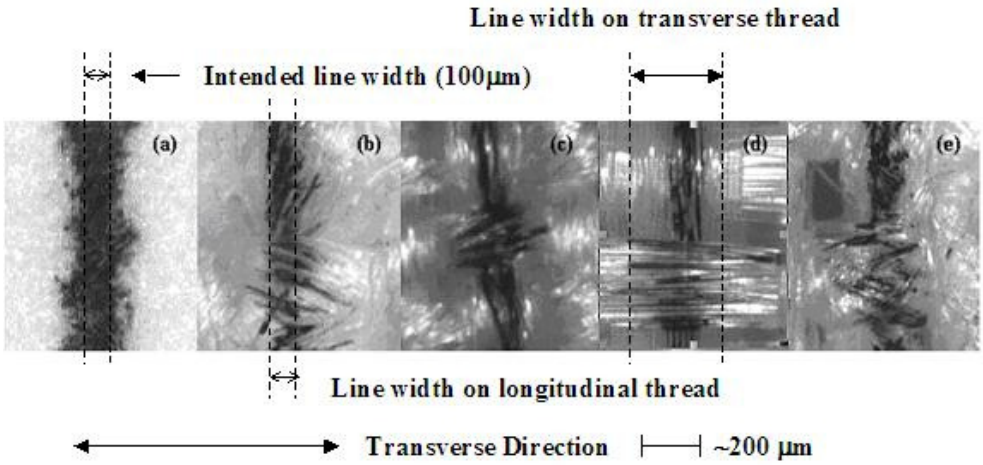

Figure 57. Microscopic images of lines on (a) Paper (b) Cotton 3508 fabric (c) PET 8880 fabric (d)PET Tape fabric (e) Sized PET fabric.

Table 17 shows the average width on longitudinal and transverse threads and also shows the total average width of the line printed in warp and weft direction of each fabric. Standard deviation values are shown in the parentheses. Table 17 shows that for cotton and sized PET fabrics, the average length of spread of line in the longitudinal threads is higher than that for PET Tape, PET 8880 and 4680 fabrics (weft direction), even though the drop spreading distance is less in these yarns. This is because the yarns are twisted in these fabrics and ink spreads or wicks in the helical direction to give higher line widths. This is schematically shown in Figure 58.

Table 17. Average width of the line in Epson paper and fabrics

Line width (um) (SD)				
	Longitudinal Threads	Transverse Threads	Average	Category Average
Paper			160 (7)	160
Sized PET-warp*	138 (17)	225 (34)	182	173
Sized PET-weft	153 (28)	176 (22)	165	
PET Tape-warp	124 (17)	364 (46)	244	215
PET Tape-weft	111 (13)	261 (41)	186	
PET 8880-warp	111 (14)	205 (11)	158	154
PET 8880-weft	105 (11)	205 (24)	155	
PET4680-warp	112 (5)	193 (17)	153	
PET4680-weft	106 (14)	194 (10)	150	
Cotton 4508-warp	144 (20)	169 (26)	157	160
Cotton 4508-weft	140 (20)	184 (12)	162	
Cotton 3508-warp	136 (13)	191 (15)	164	
Cotton 3508-weft	138 (15)	177 (19)	158	

* indicates the direction of length of line in fabric (warp way or weft way)

Effect of fiber material

It was found that pigment inks work better in hydrophilic fibers (cotton) compared to hydrophobic fibers (polyester). Overall cotton fabrics gave better line quality than polyester fabrics. Although average line width for polyester fabrics was slightly less, it was very high on transverse threads of polyester fabrics. This gives very ragged lines. As mentioned before, the cotton fabrics show lower line widths probably because of water

quickly diffusing inside the fibers, leaving behind the pigment on the surface of the fibers. However, as polyester fibers do not absorb water, the ink wicks through the capillaries formed by the fibers or filaments which gives wider line widths.

Greater non-uniformity of yarn diameter and hairy nature of the cotton fabric, however, gives somewhat irregular, inhomogeneous printing. Use of cellulosic filaments such as viscose rayon may overcome these problems and can give excellent printing quality due to their hydrophilic nature, where water in the ink can diffuse before ink can wick.

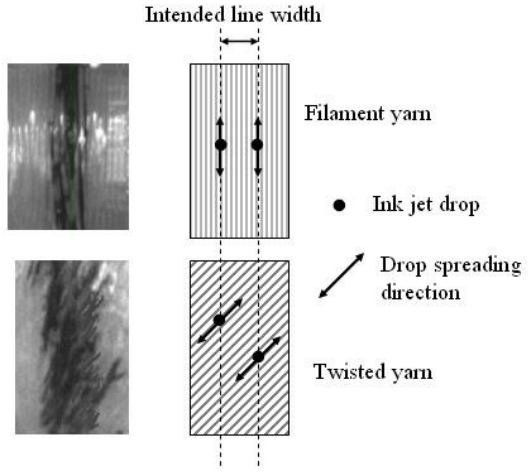

Figure 58. Effect of twist on drop spreading and line width - wicking or spreading in helically oriented fibers or filaments in twisted yarns gives higher line widths

Effect of Surface Topography and Size Coating

Based on the drop spreading results it was expected that cotton and the sized PET fabrics would give the best line quality. As expected, lower line widths were observed in cotton fabrics but not in sized PET fabrics. This is because several narrow capillaries were present especially on the surface of weft yarns of the sized PET fabrics. Ink wicked

through these capillaries to give higher line widths. Wicking of ink drops in these yarns was not observed in drop spreading experiments as drops hit the separated fibers most of the time. Warp yarns of these fabrics however were sized. As size coating fills up the capillaries on the surface, no wicking occurred, which gave improved line quality. As only the warp yarns are sized, wicking or spreading was found to be on average 25 % less in warp yarns compared to that in weft yarns. Size coating thus was found to work as an anti-wicking medium and rendered higher print quality of lines (Figure 59).

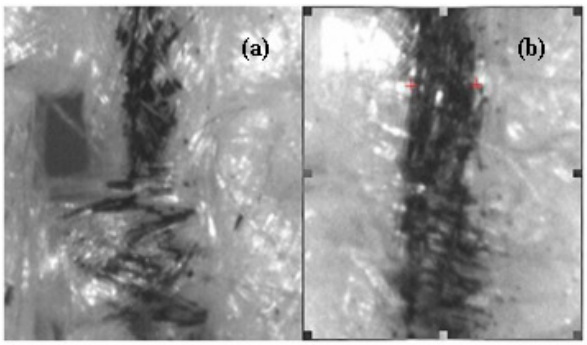

Figure 59. Effect of size coating on line width.

Effect of Thread Spacing

In PET 8880 and PET 4680 fabrics, the warp yarns were twisted yarns and the filling yarn was textured and untwisted continuous filament yarn. PET 8880 fabric had 88 picks in the filling direction while PET 4680 fabric had only 46 picks in the filling direction. Therefore PET 8880 fabric was much more compact than PET 4680 fabric. The un-twisted filament filling yarn in PET 4680 fabric were therefore much more open and hence had more capillary radius. The equilibrium wicking height is less for larger capillaries. Therefore when filling yarns were in transverse direction to printing, the width of the line was found to be less in PET 4680 fabric (193 um) compared to that for

PET 8880 fabric (205 um) as shown in Figure 60. Thus open filaments may give the higher quality of line due to less wicking than compact filaments. However if the filament is too open, drops may simply pass through the fabric. This phenomenon was observed only for PET 8880 and 4680 fabrics where warp yarn is twisted yarn and weft yarn is a textured multi-filament yarn. The influence of thread spacing was not evident in cotton fabrics.

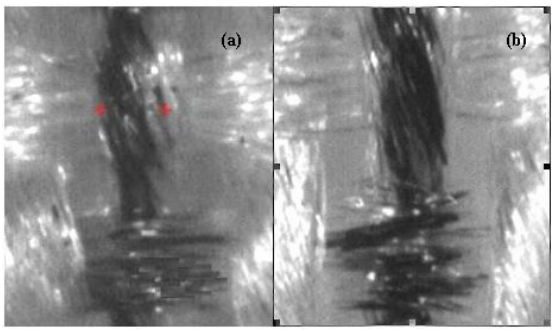

Figure 60. Effect of thread spacing on line width.

5.6.3 Solid Printing on Textile Fabrics

The undithered and dithered patterns as illustrated in the Experimental section were printed on Epson paper, Cotton 4508, PET Tape, PET Sized and PET 8880 fabrics. Scanned images of printed paper and fabrics with 50 % ink coverage are shown in Figure 61. Other images are shown in Appendix G. From the figures, it can be seen that printed patterns of ink drops are perfectly retained on Epson paper. Undithered patterns on paper show some distinctive features such as streaks which is undesirable in printing. Dithered patterns give somewhat randomized appearance and do not show any distinctive pattern as the undithered patterns. Images thus show that dithering is indeed important for printing on paper to get homogenous images. Scanned images of fabrics show that

although streaks are slightly visible on fabrics, the drop pattern is mostly lost on fabrics due to the spreading and wicking of ink on the yarn surfaces.

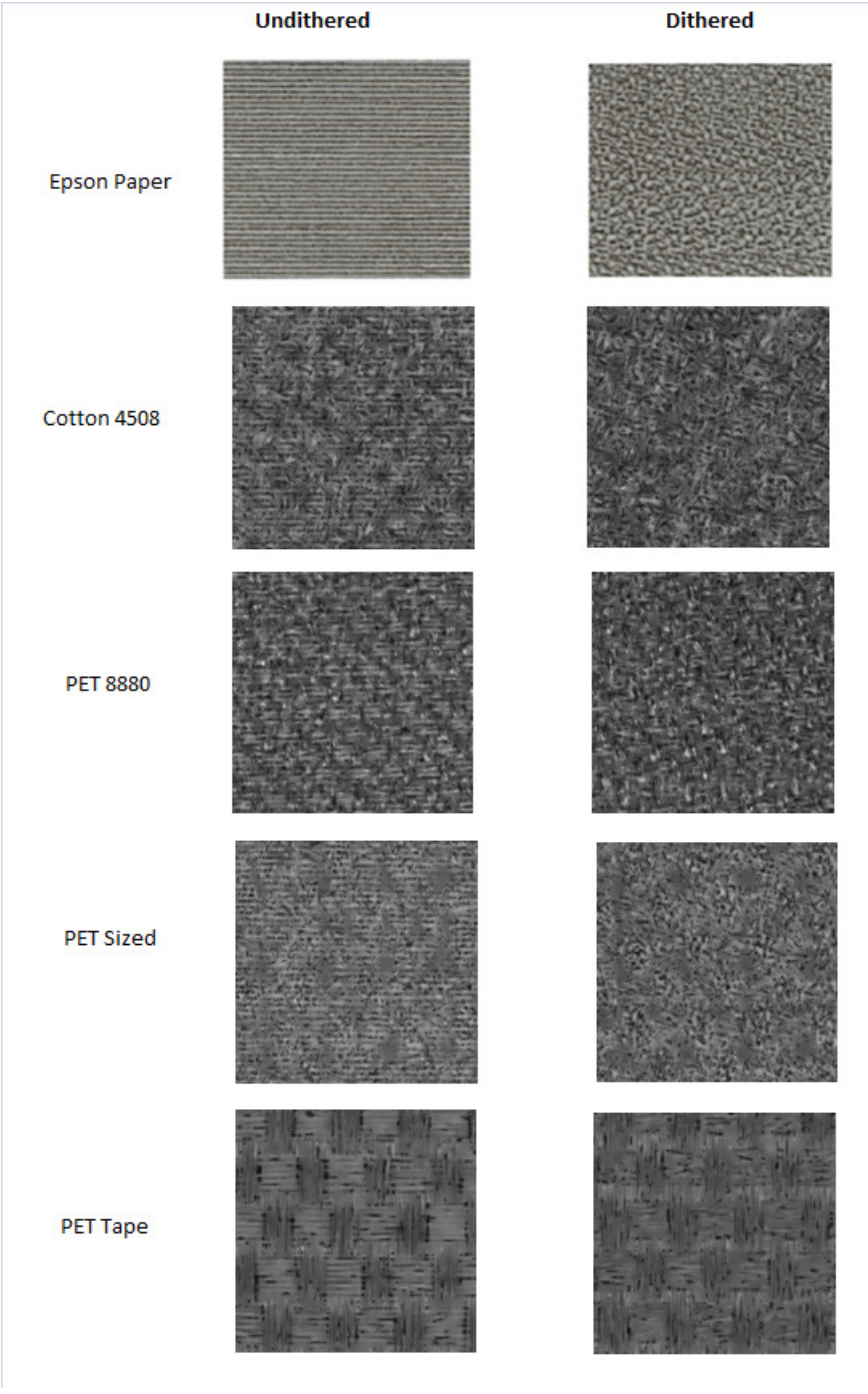

Figure 61: Undithered and dithered images on paper and fabrics with 50% ink coverage (scanned images).

Microscopic images of the printed patterns on paper and fabrics with 50 % ink coverage are shown in Figure 62. Other images are shown in Appendix G.

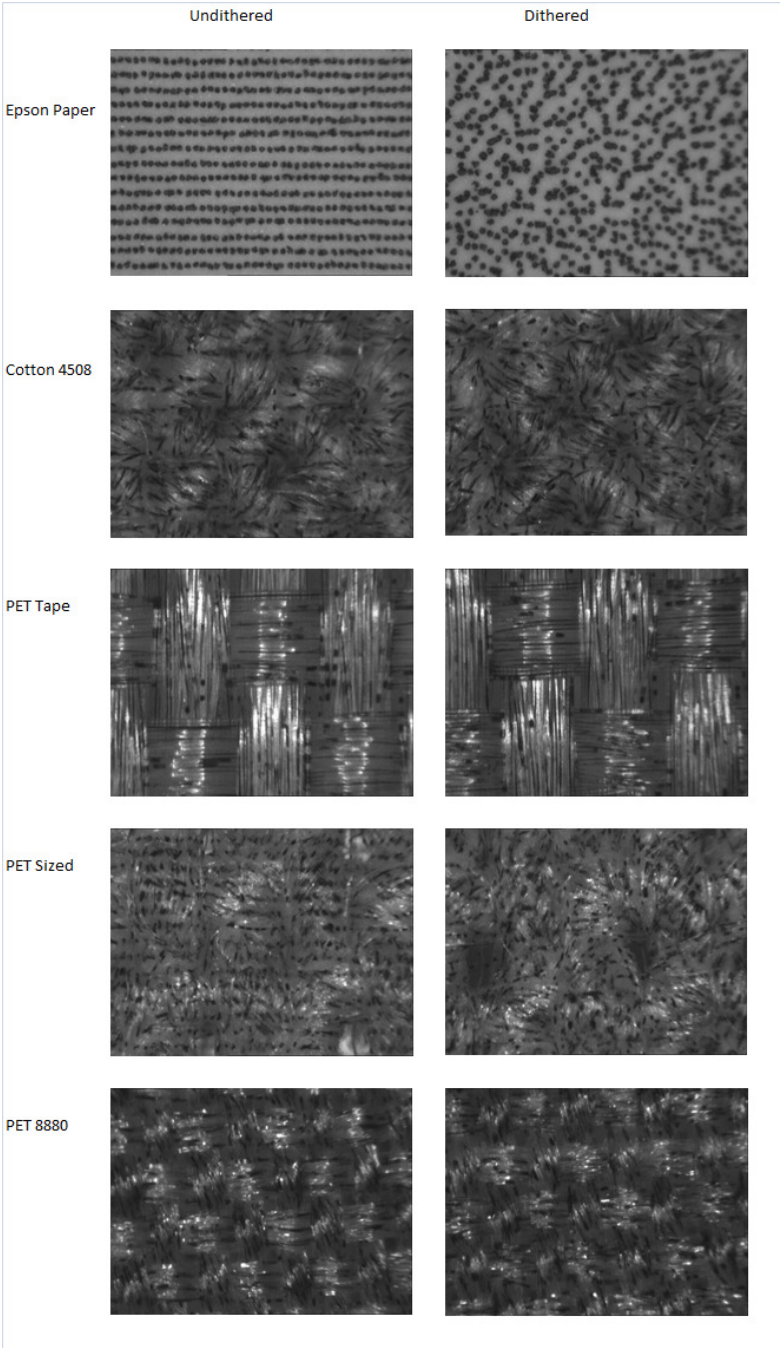

Figure 62: Microscopic images of solid prints on paper and fabrics with 50% ink coverage.

Using Matlab code the average grey scale values of all the scanned images were determined. The data is shown in Table 18. For better comparison all the grey scale values were normalized by the average grey scale value of blank paper. The normalized data is shown in Table 19 and is also shown in Figure 63. As expected, grey scale value decreased as ink coverage increased from 25% to 75%. However interestingly, dithered patterns showed in general less grey scale values than similar undithered patterns which means that dithered images were darker than undithered images. Percent decrease in grey scale value due to ditheration is shown in Table 20. Overall, dithered images were 4% darker than undithered images and the difference in darkness between dithered and undithered images is visible to the naked eye also. Dithered images were darker as the light reflected from the images is more diffused due to more randomized drop-spreading.

Analysis of solid prints thus shows that ditheration is also important in case of textile fabrics not only to avoid any undesirable moiré effects but also to obtain darker images with the same amount of ink.

Table 18: Average grey scale values of undithered and dithered scanned images of Epson paper and fabrics.

	Average Grey Scale Value (SD)						
		Undithered			**Dithered**		
	Blank	**25%**	**50%**	**75%**	**25%**	**50%**	**75%**
Paper	199 (10)	152 (16)	117 (14)	79 (14)	141 (14)	107 (14)	79 (12)
Cotton 4508	204 (16)	122 (22)	89 (19)	70 (18)	123 (22)	86 (17)	62(17)
PET 8880	195 (14)	125 (18)	90 (17)	71 (17)	116 (16)	86 (17)	67 (14)
PET Sized	216 (13)	138 (18)	104 (17)	77 (16)	145(19)	98 (18)	76 (15)
PET Tape	211 (18)	122 (27)	91 (25)	74 (23)	116 (27)	87 (23)	68 (20)

Table 19: Normalized average grey scale values of undithered and dithered scanned images of Epson paper and fabrics.

	Normalized Average Grey Scale Value						
		Undithered			Dithered		
	Blank	25%	50%	75%	25%	50%	75%
Paper	199	152	117	79	141	107	79
Cotton 4508	199	118	84	65	118	82	57
PET 8880	199	129	94	75	121	90	72
PET Sized	199	120	87	60	128	81	59
PET Tape	199	110	79	62	104	75	56

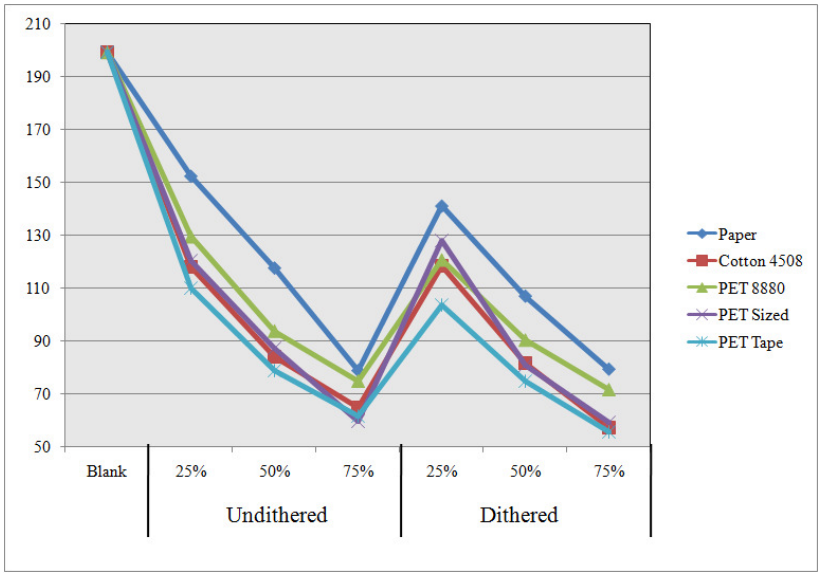

Figure 63: Normalized average grey scale values of undithered and dithered scanned images of Epson paper and fabrics

Table 20: % Decrease in grey scale value due to ditheration.

	% Decrease in Grey Scale Value due to Ditheration		
	25%	50%	75%
Paper	7	9	-1
Cotton 4508	0	3	12
PET 8880	7	4	4
PET Sized	-6	7	0
PET Tape	6	5	10
Average	3	6	5
Total Average	4		

5.7 Relation between Wicking, Drop Spreading and Ink Jet Printing Quality

As mentioned before, wicking tests and drop spreading tests were done on constituent yarns and assembled fabrics respectively and an attempt is made to find the correlation between the spreading behaviors and printing quality. If any correlation exists, the ink jet printing quality of fabrics can be predicted by just performing wicking test or drop test on the respective textile structures.

Width of the line in longitudinal direction of printing was almost similar in all the cases and was comparable to the width of the line on paper. Width of the line in this direction was found to be affected only by twist in the yarns. Twisted yarns showed higher line width compared to un-twisted or twistless filament yarns. Line width in the transverse direction however depends on many factors such as fiber material, yarn structure, capillary structure and any coating that is applied. Further, the excessive spreading/wicking in the transverse threads not only increases the overall line width but also makes the lines more ragged or uneven. Thus line width on transverse threads in textile fabrics is a good indicator of printing quality. Therefore line width in the transverse threads was compared to the wicking and drop spreading distances.

Average wicking distances in warp and weft yarns of the fabrics are given in Table 21. Poor correlation ($R=0.34$ and $R^2=0.11$) was found between wicking distance and line width in transverse threads. This suggests that perhaps wicking in yarns from an unlimited liquid source is governed by the bulk structure of the yarn, whereas spreading or wicking of ink jet drops is affected by the surface structure or nature of the capillaries present on the surface of the yarn.

Table 21: Wicking distances in yarns and their relation to line width on transverse threads.

Sample	Wicking Distance (mm)	Line width on transverse threads (um)
Sized PET-warp	1.5	176
Sized PET-weft	12	225
PET Tape-warp	5.5	261
PET Tape-weft	10	364
PET 8880 warp	6	205
PET 8880 weft	29.2	205
PET 4680 warp	6	194
PET 4680 weft	29.2	185
Cotton 4508 warp	13.5	184
Cotton 4508 weft	41	169
Cotton 3508 warp	13.5	177
Cotton 3508 weft	41	180

Drop spreading on fabrics

As explained in the experimental section, the drop-spreading study was performed by placing a small ink drop (0.5 μL) on the surface of the fabric. It was observed that the ink immediately penetrates inside the fabric through the inter-yarn spaces and then starts spreading in the outward direction from the place where the drop was placed. After the spreading was over and ink was fully dried, the fabrics were scanned. Typical drop spreading images of different fabrics are shown in Figure 64. The drop spreading behavior of the two cotton fabrics used in this study was very similar. Therefore the spreading behavior of only one of the cotton fabrics is shown.

The drop spreading distance in the warp and weft directions of different fabrics was measured using image analysis software. Drop spreading distances are given in Table 22. Drop spreading distance was the largest for the PET Tape fabric. For a given

drop volume, drop spreading depends on factors such as wetting characteristics, areal density (weight per unit area), porosity, absorbency and surface characteristics of the substrate. Lower areal density and lower porosity can give rise to higher drop spreading area provided that the substrate is wettable. If the surface characteristics of the substrate promote wicking, then drop spreading area can be expected to be higher. Non-absorbent fabrics such as a polyester fabric will not absorb any liquid and hence liquid spreads over more area. PET Tape fabric was non-absorbent, less porous, had less areal density and more importantly, had continuous narrow capillaries on its surface, all of which favored drop spreading; as a result, PET Tape fabric showed the largest drop spreading area. Cotton fabrics which were absorbent, more porous and had high areal density showed the least drop spreading. Although the sized PET fabric had a very high areal density, it showed significant spreading only in the weft direction as narrow continuous capillaries existed on the weft yarns. The sized warp yarns of this fabric showed very little spreading in the warp direction.

In all the above cases, ink penetrated fully throughout the thickness of all the fabrics. The effective porosity (ϕ^*) used by ink drop to spread on the fabric can be calculated using the following volume balance equation.

$$V_d = A_d \times T_f \times \phi^* \text{ hence } \phi^* = \frac{V_d}{A_d \times T_f} \tag{33}$$

Where A_d is area of drop spreading in cm^2, V_d is drop volume in cm^3 and T_f is fabric thickness in cm. As A_d, V_d and T_f are known ϕ^* can be calculated. ϕ^* here is not just the porosity of the fabrics. It is a combined measure of porosity, wettability, distribution and

continuity of capillaries present in the fabric. For example, in the case of fabrics with poor wettability, the drop spreading area will be less and this will give higher value of ϕ^* for these fabrics. For fabrics representing narrow and continuous capillaries, the drop spreading area will be more and this will give lower value of ϕ^* for these fabrics. Drop spreading area, fabric thickness and calculated ϕ^* values for all the experimental fabrics are given in Table 22. The ϕ^* value for paper could not be calculated because the drop did not penetrate fully inside paper. Drop was not at all visible at the back side of the paper.

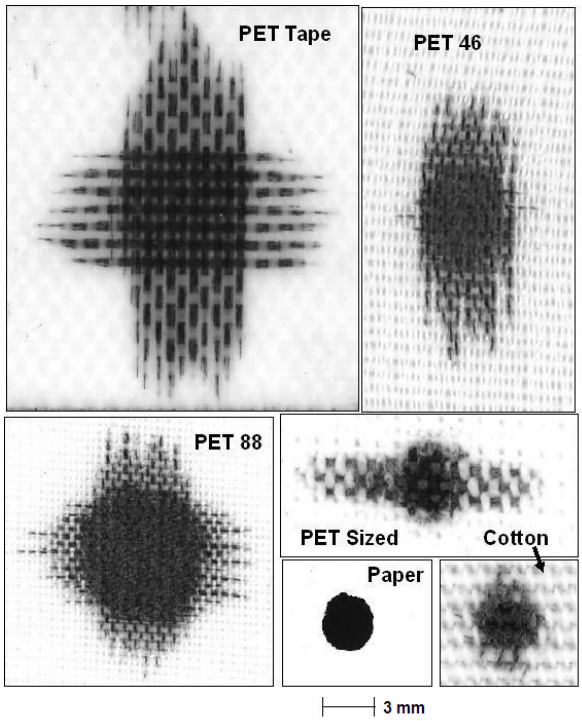

Figure 64: Drop spreading behavior of experimental fabrics.

Table 22: Drop spreading distance, fabric thickness, drop spreading area and calculated ϕ^* values for all the fabrics.

Sample	Drop Spreading Distance d (mm)	Fabric Thickness T_f (cm)	Drop Spreading Area A_d (cm2)	ϕ^* (%)
Paper	2.00			
Sized PET-warp	2.50	0.051	0.189	5.19
Sized PET-weft	7.00	0.051	0.189	5.19
PET Tape-warp	7.80	0.017	0.500	5.88
PET Tape-weft	11.80	0.017	0.500	5.88
PET 8880 warp	7.50	0.013	0.320	12.02
PET 8880 weft	8.20	0.013	0.320	12.02
PET 4680 warp	8.80	0.013	0.220	17.48
PET 4680 weft	4.00	0.013	0.220	17.48
Cotton 4508 warp	2.90	0.062	0.038	21.22
Cotton 4508 weft	2.50	0.062	0.038	21.22
Cotton 3508 warp	2.20	0.062	0.040	20.16
Cotton 3508 weft	1.90	0.062	0.040	20.16

Table 22 shows that ϕ^* values indeed were very low for the fabrics where narrow and continuous capillaries existed in the fabrics. ϕ^* value was the highest for the PET Tape fabrics and were the lowest for the cotton fabrics. In reality, ϕ^* values should be different for warp threads and weft threads. For example in Sized PET fabric as warp threads were sized, they would have higher value of ϕ^*; but weft threads would have lower value of ϕ^*. Separate determination of these values is difficult as the volume of liquid absorbed by each set of threads is unknown. Thus ϕ^* is a bulk fabric property which is a rather complex function of porosity, wettability and the nature of capillaries present in yarns

and fabrics. Total drop spreading distance *d* and the porosity parameter, ϕ^* are both influenced by the nature of capillaries present in the fabrics. Since the width of the printed line is also affected by the nature of capillaries present in the fabric, good correlation between drop spreading parameters (d and ϕ^*) and line width in ink jet printing can be expected. Results of the correlation studies are explained in the next section.

Correlation studies

The excess line widths on transverse threads were determined by subtracting intended line width (100 μm) from actual line widths. For the correlation studies, only excess line widths on the transverse threads were considered because, as explained before, wicking and spreading in the transverse threads is the main cause of poor printing quality. As mentioned before, excessive spreading/wicking in the transverse threads not only increased the overall line width but also made the lines more ragged or uneven. Width of the line in longitudinal threads (Table 17 column 2) in all the fabrics was comparable or somewhat less than that on the high quality inkjet paper. Thus width of the longitudinal lines is not a factor in the determination of printing quality. Printing quality is affected mainly by the width of the transverse lines. For further discussion, excess line width on transverse threads will be referred as E_{lw}.

The relationship between E_{lw} and the distance *d* is shown in Figure 65 (a). For a linear fit, the measured correlation coefficient value between E_{lw} and *d* was 0.8 (R^2=0.63). The correlation coefficient improves to 0.92 (R^2=0.85) when d/ϕ^*, as opposed to d is regressed against and E_{lw} (Figure 65 (b)). The better correlation is due to the fact

that the term d/ϕ^* represents the drop spreading distance that is normalized by the effective porosity ϕ^*, which is known to influence the spreading of liquid in fabrics. A close examination of the d/ϕ^* Vs E_{lw} plot reveals that the relationship between the variables is not linear. The plot also reveals that E_{lw} increases more rapidly than d/ϕ^*, thus suggesting a greater dependency of E_{lw} on d than on ϕ^*. Correlation coefficient of 0.98 (R^2=0.97) was observed when the term, d^2/ϕ^*, was used in the regression instead of d/ϕ^*. Considering very high R^2 values, it is clear that regression models can predict the excess line widths fairly well from the drop spreading distance and effective porosity values.

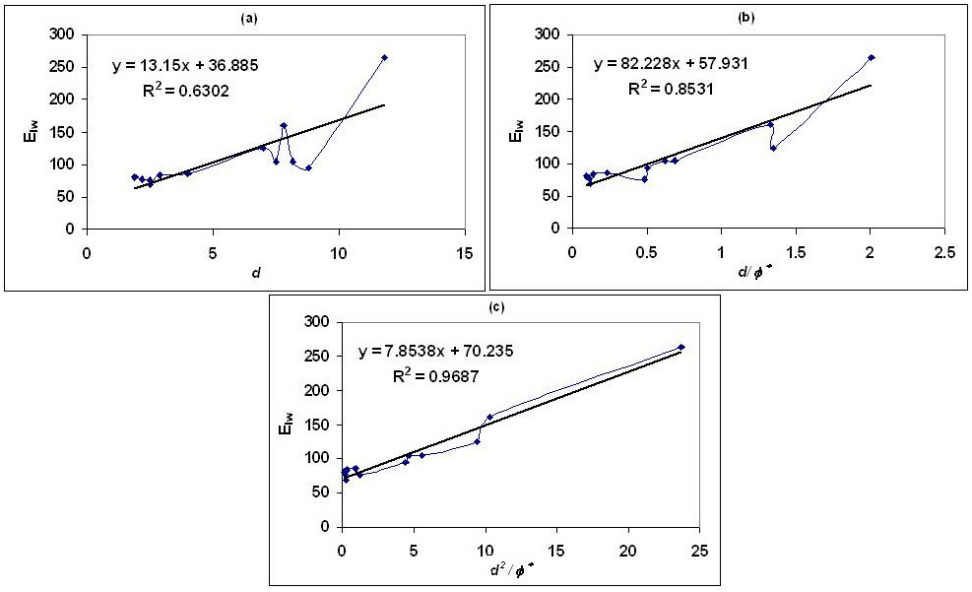

Figure 65: Correlation graphs: (a) Linear fit between drop spreading distance d and excess line width in inkjet printing, E_{lw} (b) between d/ϕ^* and E_{lw} (c) between d^2/ϕ^* and E_{lw}.

In order to verify the relationships, all three correlations were tested on unknown fabrics; high quality mercerized cotton fabric, desized PET fabric (same fabric as the second fabric in Table 2 but desized) and another desized 100% polyester fabric having twisted yarn in the warp direction and twist-less filament yarn in the weft direction. Lines

having a width of 100 μm were printed on these fabrics in warp and weft directions, following the procedure described in the experimental section. The actual excess width of the lines on transverse threads and the estimated excess line width using the above equations are given in Table 24. Percentage error value in each case is indicated in the adjacent column. It can be observed that the equation connecting d/ϕ^* and E_{lw} gave the least % error. Despite very high correlation between d^2/ϕ^* and E_{lw}, the percentage error values for this regression equation were high, due to the fact that the test fabrics gave data that corresponded to only the initial part of the regression plot. The error values for this equation could have been different, had the measured values of d^2/ϕ^* and E_{lw} of the test fabrics spanned the entire range used in the regression equation.

Table 23: Fabric thickness, drop spreading area, calculated ϕ^* and drop spreading distances for unknown fabrics.

Sample	**Fabric Thickness T_f (cm)**	**Drop Spreading Area A_d (cm2)**	**ϕ^* (%)**	**Drop Spreading Distance d (mm)**
Mercerized cotton-warp	0.019	0.188	13.92	4.70
Mercerized cotton-weft	0.019	0.188	13.92	6.50
Desized PET-warp	0.050	0.113	8.77	4.20
Desized PET-weft	0.050	0.113	8.77	5.00
PET-warp	0.039	0.188	6.74	7.00
PET-weft	0.039	0.188	6.74	5.70

Table 24: Actual and estimated excess line width on transverse threads using different correlations.

Sample	E_{lw} (μm)	Estimated E_{lw} using correlation between E_{lw} and					
		d	% Error	d/ϕ^*	% Error	d^2/ϕ^*	% Error
Mercerized cotton-warp	77	98.69	28.17	85.69	11.28	82.69	7.40
Mercerized cotton-weft	115	122.36	6.40	96.32	16.25	94.07	18.20
Desized PET-warp	106	92.12	13.10	97.33	8.18	86.04	18.83
Desized PET-weft	97	102.64	5.81	104.83	8.07	92.63	4.50
PET-warp	150	128.94	14.04	143.36	4.43	127.35	15.10
PET-weft	125	111.84	10.53	127.50	2.00	108.11	13.51
		Avg.	**13.01**	**Avg.**	**8.37**	**Avg.**	**12.92**

Correlation studies thus show that millimeter sized drop spreading studies can be effectively used to predict the ink jet printing quality performance for unknown fabrics. Similar approach can possibly be used to predict the quality performance of unknown ink. For a given fabric, the ink that gives a higher drop spreading distance will produce poorer ink jet print quality compared to an ink that gives lower drop spreading distance. Correlation models can be setup using different fabrics for a given ink and the models can be used to predict the printing quality of an unknown textile fabric for the same ink.

CHAPTER 6
CONCLUSIONS

Based on the results of various liquid transport and ink jet printing experiments conducted on fabrics, the following conclusions can be made. Conclusions are categorized under different objectives set for this research.

- Effect of fabric structure on liquid transport in vertically hung fabrics – transport from an unlimited reservoir
  - Results showed that the wicking in fabrics is determined by the wicking rates of the yarns, thread spacing and more importantly by the rate at which liquid migrates from longitudinal to transverse threads and again from transverse threads back to longitudinal threads.
  - Yarns with better wicking rates produced better wicking fabrics. Decrease in thread density resulted in increase in wicking rates. Larger inter-yarn spaces trapped more liquid which was readily available for migration. However beyond a certain level, larger inter-yarn spaces may remain unfilled, thus failing to further increase the wicking rate.
  - Migration process can be effectively quantified by measuring the gain in wicking rate and equilibrium wicking height. The gain in wicking rate describes the migration process at smaller times and the gain in equilibrium wicking height describes the migration process at longer times and hence the two are totally different.

- Yarn type, effective capillary size of the yarns, and thread spacing affect the migration process and hence they affect the wicking properties of fabrics. It was found that twisted yarns in the longitudinal direction and filament yarns or very low twisted yarns in the transverse direction of the fabric can maximize the migration process and hence can render very superior wicking properties.

- Comparison of wicking results obtained by weight balance method and image analysis method showed that weight balance method cannot be considered as a replaceable method for image analysis method, especially if the weight balance method is used for more open fabrics. Specially targeted experiments show that weight balance method and image analysis method give different results for fabrics having different fiber materials and yarns.

- Effect of fabric structure on drop spreading

  - Initial drop spreading area after impaction of drop on fabric was found to depend on wetting properties and roughness of fabrics. Final drop spreading area primarily depended on fabric thickness and on fabric structure to some extent.

  - Drop spreading rates were determined by fabric structure. However the relation between drop spreading rate and fabric structure appears to be very complex. In general, compact and thinner cotton fabrics showed highest drop spreading rates. However higher drop spreading rates were

also observed in thin polyester fabrics. Drop spreading rates are primarily affected by the manner and the rate at which liquid migrates from yarn to yarn.

- Very poor relationship was observed between drop spreading rates and thickness of fabrics containing cotton and polyester fibers. However, for the same kind of fiber material and yarn structure, drop spreading rate showed a decrease with fabric thickness. For fabrics with thicker yarns, yarn-to-yarn liquid migration rate was lower as the time required for penetration of liquid in the yarn is more. Fabrics with thicker yarns, therefore, showed lower drop spreading rates.

- If fabrics are easily wettable by liquid, drop spreading rate increased with increase in thread density. If fabrics are poorly wettable by liquid, drop spreading rate decreased with increase in thread density.

- Anisotropy in spreading of drop on fabrics arises from the difference between the rate at which liquid migrates from warp yarn-to-weft yarn and vice versa and not due to the differences in warp and weft wicking rates or thread densities in warp and weft direction.

- Relation between wicking from an unlimited reservoir and drop spreading

  - Very poor relation was observed between drop spreading rate and the rate at which liquid wicks from an unlimited reservoir. This shows that these two phenomena are entirely different and give totally different information regarding kinetics of absorption.

- Effect of fabric structure on ink jet drop spreading and line printing quality
  - Analysis of the results of ink jet printing of pigment ink on textile fabrics showed that excessive drop spreading and higher line widths were observed where continuous and narrow capillaries prevail on the surface of yarns. Yarn surface characteristics are more important than fabric construction parameters. Ink jet drop spreading or wicking occurs along the direction of fibers. For given pigment ink, number of drops impacted on the same location did not result in any significant increase in drop spreading.
  - In general cotton fabrics gave the best printing quality. This comes from the fact that water in the pigment ink diffuses inside the fibers before substantial wicking or spreading of the ink can occur.
- Relation between Wicking, Drop Spreading and Ink Jet Printing Quality
  - Very poor correlation was found between wicking distance and line width in transverse threads. This is due to the fact that vertical wicking in yarns is governed by the bulk structure of the yarn, whereas spreading or wicking of ink jet drops is affected by the surface structure or by the nature of capillaries present on the surface of the yarn. Good correlation was observed between drop spreading distance and line width on transverse threads which is a very good indicator of printing quality. Drop spreading study was found to simulate the spreading of ink jet drops fairly well. While the spreading distance by itself is a good predictor of printing

quality, the spreading distance normalized by the effective porosity can be a better predictor when predicting the printing quality of fabrics exhibiting major differences in structural parameters.

CHAPTER 7
RECOMMENDATIONS

It was observed in this research that the inter-yarn spaces in fabrics can absorb and store liquid and the stored liquid can boost or enhance the wicking rate. However, if the inter-yarn spaces are too large, the spaces may remain unfilled and the wicking enhancement may not be fully realized. It would be interesting to find out the optimum thread spacing at which the wicking enhancement ceases or fails to materialize. For this, it is important to find out how exactly the liquid moves through the gap between two yarns. This is analogues to the study of movement of liquid between cylinders; at what speed and until what height liquid moves and how it is different from movement of liquid in a single closed capillary. Such study has been done on glass cylinders by Liu and his coworkers. The authors controlled the distance between two cylinders using a differential micrometer and a telescope as shown in the Figure below and observed the effect of cylinder diameters and separation distance on equilibrium wicking height. Such a study can be done on textile yarns also. However, this study can only be done on somewhat stiff yarns which would remain straight during the experiments. The dynamics of liquid movement can be studied by using a telescopic camera.

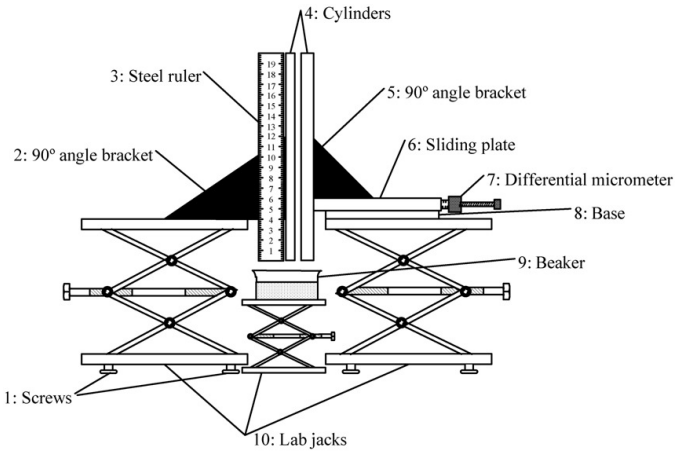

Figure 66: Setup used by Liu et al. to study the capillary rise between cylinders.

Due to time and resource constraints, the effect of fabric weave on liquid transport was not analyzed in this research. This is another aspect which can be studied in future.

It was understood in this research that yarn-to-yarn liquid migration is a very important part of wicking from an unlimited reservoir as well as a limited supply source such as a single drop. We suggested a new method to study this migration phenomenon (Section 5.4.2) where only one yarn end from a piece of fabric was dipped in a liquid and migration of liquid from yarn-to-yarn was observed. Only qualitative findings of these experiments are reported. The dynamics of liquid migration (increase in area, height and width of liquid front with respect to time) was also studied but it was found to be highly variable as the length of yarn dipped in the liquid could not be controlled. Within and between variability in yarn structure also contributed to the variability in the results of the experiments. Immersion depth of yarn can be controlled by using a platform which is raised or lowered by an electronically controlled motor. This arrangement can eliminate errors in the experiments and the dynamics of migration for different fabric structures can be studied.

APPENDIX A

MATLAB CODE FOR IMAGE ANALYSIS OF WICKING IN YARN

```
%%% Declaration of variables

x=1;
clb=3/435;        %%% Calibration cm/pixels
imst=5;           %%% Analyses image 5 through 131
imend=131;
tr=40;            %%% Threshold value, pixels with average grey value 40 and below
                      indicates presence of ink

%%% Main program

for i=imst:imend
if i<=9
      fname=sprintf('5518 wf1/5518 weft1 00%g.jpg',i);      %%% fname= File name
   end

   if i>9 & i<=99
      fname=sprintf('5518 wf1/5518 weft1 0%g.jpg',i);
   end

   if i>99 & i<=999
      fname=sprintf('5518 wf1/5518 weft1 %g.jpg',i);
   end


   I = imread(fname);
   I=double(I);

   s=size(I);
   y=1000;

   for m=1:s(1)          %%%% m is row number and n is column number
      for n=1:s(2)
         if I(m,n)<=tr
            y=s(1)-m;
            break
         end
      end
      if y~=1000
         break
```

```
      end
   end

%%%%%%%%%%%%%%%%%%%%%%%%Store results in matrix R

R(x,1)=y*clb;

x=x+1;      %%%% Go to next row
end
```

APPENDIX B

MATLAB CODE FOR IMAGE ANALYSIS OF WICKING IN FABRIC

```
%%% Declaration of variables
x=1;
n=1;
cal=149;     %%% Calibration cm/pixels
imst=8;
imend=166;
tr=93;
%%% Main program

for i=imst:2:imend
  if i<=9
     fname=sprintf('3008/3008 wp1 00%g.jpg',i);
   end

   if i>9 & i<=99
     fname=sprintf('3008/3008 wp1 0%g.jpg',i);
   end

   if i>99 & i<=999
     fname=sprintf('3008/3008 wp1 %g.jpg',i);
   end

   if i>999
     fname=sprintf('sized flat/sized flat %g.jpg',i);
   end

   I = imread(fname);
   I=double(I);
   s=size(I);
   A=round(mean(I,2));

  for k=s(1):-1:5
     h=0;
     if A(k,1)>tr & A(k-1,1)>tr & A(k-2,1)>tr & A(k-3,1)>tr & A(k-4,1)>tr
        h=k;
        break
     end
  end

%%%%%%%%%%%%%%%%%%%%%Store results in matrix R
```

```
    R(x,1)=(s(1)-h)/cal;
    x=x+1;
end
```

APPENDIX C

MATLAB CODE FOR IMAGE ANALYSIS OF DROP SPREADING

```
%%% Declaration of variables
x=1;
n=1;
clb=1/114;
H=0;
L=0;
imst=7;
imend=284;
tr=30;

%%% Main program

for i=imst:imend

if i<=9
      fname=sprintf('Sized-2/sized-2 00%g.jpg',i);
   end

   if i>9 & i<=99
      fname=sprintf('Sized-2/sized-2 0%g.jpg',i);
   end

   if i>99 & i<=999
      fname=sprintf('Sized-2/sized-2 %g.jpg',i);
   end


   I = imread(fname);
   I=double(I);

   s=size(I);

   %%%%%%%%%%%%%%%%%%%%%%%%%%%%%%    Percent Area covered
   b=0;
   for m=1:s(1)
      for n=1:s(2)
         if I(m,n)<=tr
            b=b+1;
         end
      end
```

```
end
PA= b/(s(1)*s(2))*100;

%%%%%%%%%%%%%%%%%%%%%%%%%%%%%%%%%%%%length width
estimation

Vsummin=min(sum(I));
Hsummin=min(sum(I,2));

%%%%%%%%%%%%%%%%%%%%%Find vertical length VL in pixels

for k=1:s(2)
   if sum(I(:,k))==Vsummin
      Vmin=k;
      break
   end
end

for k=1:s(1)
   if sum(I(k,:))==Hsummin
      Hmin=k;
      break
   end
end


%%%%%%%%%%%%%%%%%%%%%Find vertical length VL in pixels
flag=0;
%%%%%%Finding upper point with lower pixel number

for r=Hmin:-1:1
   for c=1:s(2)
      if I(r,c)<=tr
         flag=1;
         break
      end
   end
   if flag==0;
      L=r;
      break
   end
   flag=0;
end


flag=0;
```

```
%%%%%%Finding lower point with higher pixel number
 for r=Hmin:s(1)
    for c=1:s(2)
       if I(r,c)<=tr
          flag=1;
          break
       end
    end
    if flag==0;
       H=r;
       break
    end
    flag=0;
 end

 VL=H-L;

 %%%%%%%%%%%%%%%%%%%%%%%%Find horizantal height in pixels
 flag=0;
 %%%%%%Finding right side point with lower pixel number

 for c=Vmin:-1:1
    for r=1:s(1)
       if I(r,c)<=tr
          flag=1;
          break
       end
    end
    if flag==0;
       L=c;
       break
    end
    flag=0;
 end


 flag=0;
 %%%%%%Finding lower point with higher pixel number
 for c=Vmin:s(2)
    for r=1:s(1)
       if I(r,c)<=tr
          flag=1;
          break
       end
    end
```

```
        if flag==0;
            H=c;
            break
        end
        flag=0;
    end

    HL=H-L;

    if (PA*(s(1)*clb*s(2)*clb/100))<=0.1
        HL=0;
        VL=0;
        PA=0;
    end

    %%%%%%%%%%%%%%%%%%%%%Store results
    R(x,1)=i;                                %%%%% Image number
    R(x,2)=VL*clb;                           %%%%% Vertical width of drop spread
    R(x,3)=HL*clb;                           %%%%% Horizontal width of drop spread
    R(x,4)=PA*(s(1)*clb*s(2)*clb/100);       %%%%%% Area of drop spread
    x=x+1;
end
```

APPENDIX D

MATLAB CODE FOR ESTIMATION OF GREY SCALE VALUE OF SOLID PRINT

```
I = imread('Cotton 3508-25-1.jpg');
I=rgb2grey(I);              %%% Convert image into grey scale image
s=size(I);

Sum=0;
for m=1:s(1)
    for n=1:s(2)
        Sum=Sum + I(m,n)
    end
end
GSV=Sum/(s(1)*s(2));     %%%% Calculate grey scale average
```

APPENDIX E

TGA ANALYSIS OF PIGMENT INK (TRIDENT FABRIC FAST ULTRA INK)

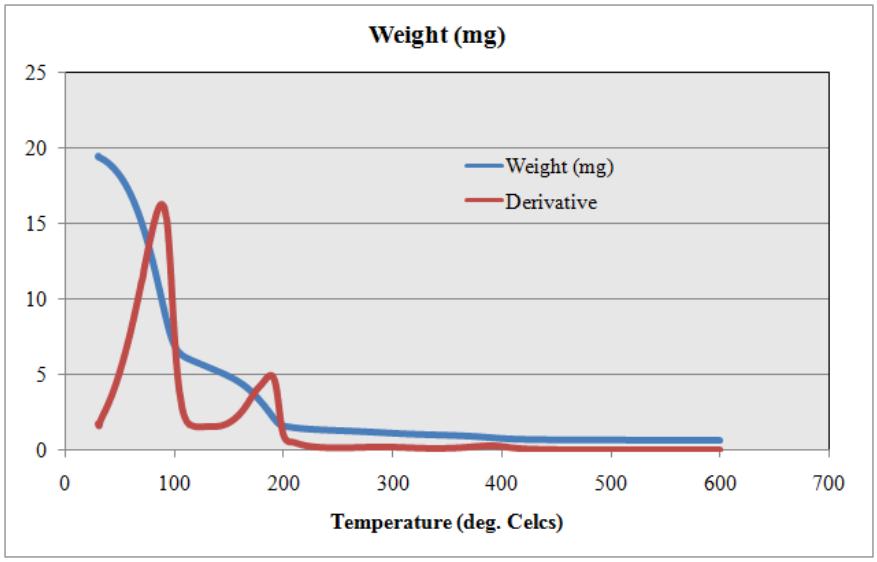

Figure 67: Temperature Vs. Sample weight TGA graph for Trident Ultra fast pigment ink

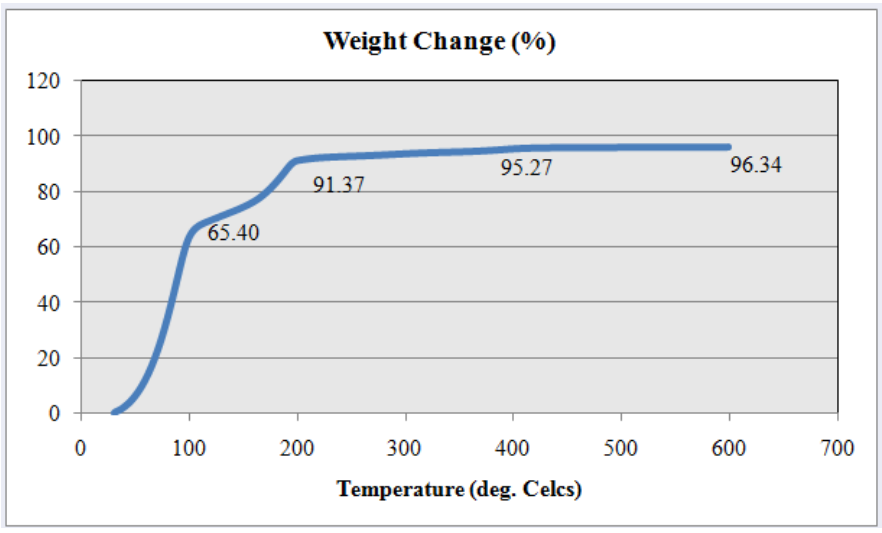

Figure 68: Temperature Vs. % weight change TGA graph for Trident Ultra fast pigment ink

APPENDIX F

WICKING FROM AN UNLIMITED RESERVOIR - CORRELATION COEFFICIENTS BETWEEN MEASURED WICKING PROPERTIES AND FABRIC CONSTRUCTION PARAMETERS

Table 25: Correlation between fabric construction parameters and wicking properties.

	Thickness T0 (um)	*Thickness Tm (um)*	*Areal Density (g/m2)*	*Bulk Density at To*	*Bulk Density at Tm*	*Yarn-warp-Wicking Rate K (cm/s0.5)*	*Yarn-weft-Wicking Rate K (cm/s0.5)*	*Fabric-warp-Wicking Rate K (cm/s0.5)*	*Fabric-weft-Wicking Rate K (cm/s0.5)*	*Warp-% Gain in wicking rate*	*Weft-% Gain in wicking rate*
Thickness T0 (um)	1.000										
Thickness Tm (um)	0.913	1.000									
Areal Density (g/m2)	0.759	0.857	1.000								
Bulk Density at To	-0.967	-0.807	-0.664	1.000							
Bulk Density at Tm	-0.947	-0.951	-0.717	0.902	1.000						
Yarn-warp-Wicking Rate K (cm/s0.5)	0.377	0.033	-0.220	-0.457	-0.211	1.000					
Yarn-weft-Wicking Rate K (cm/s0.5)	0.450	0.370	0.285	-0.454	-0.355	0.441	1.000				
Fabric-warp-Wicking Rate K (cm/s0.5)	0.758	0.499	0.296	-0.834	-0.636	0.779	0.752	1.000			
Fabric-weft-Wicking Rate K (cm/s0.5)	0.881	0.693	0.420	-0.890	-0.800	0.723	0.659	0.945	1.000		
Warp-% Gain in wicking rate	0.385	0.603	0.767	-0.350	-0.489	-0.624	0.180	-0.001	0.035	1.000	
Weft-% Gain in wicking rate	0.660	0.436	0.235	-0.716	-0.616	0.526	-0.172	0.500	0.608	-0.144	1.000

APPENDIX G

SOLID INK JET PRINTS ON FABRICS

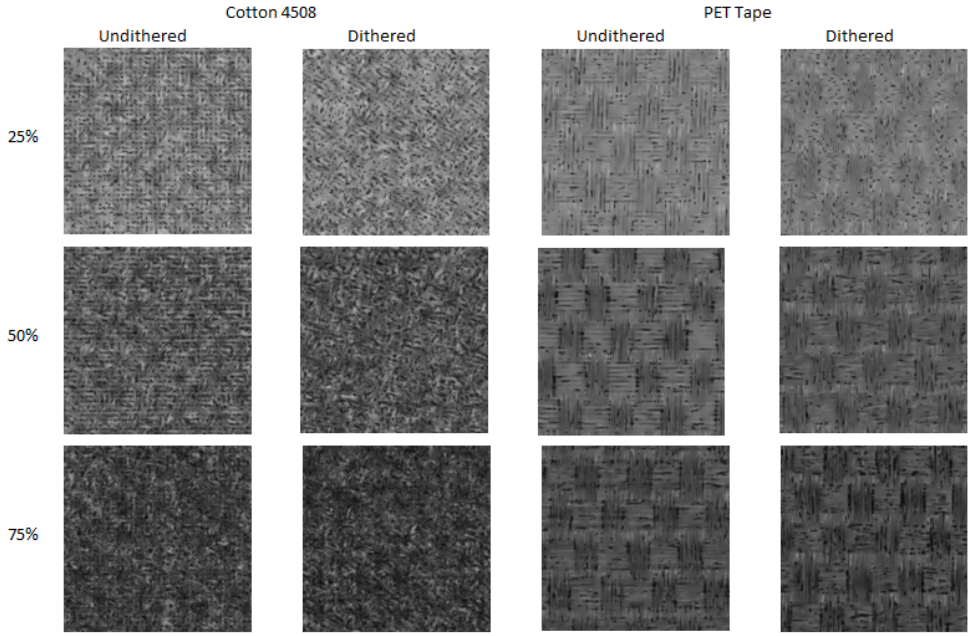

Figure 69: Dithered and undithered solid ink jet prints on fabrics; scanned images

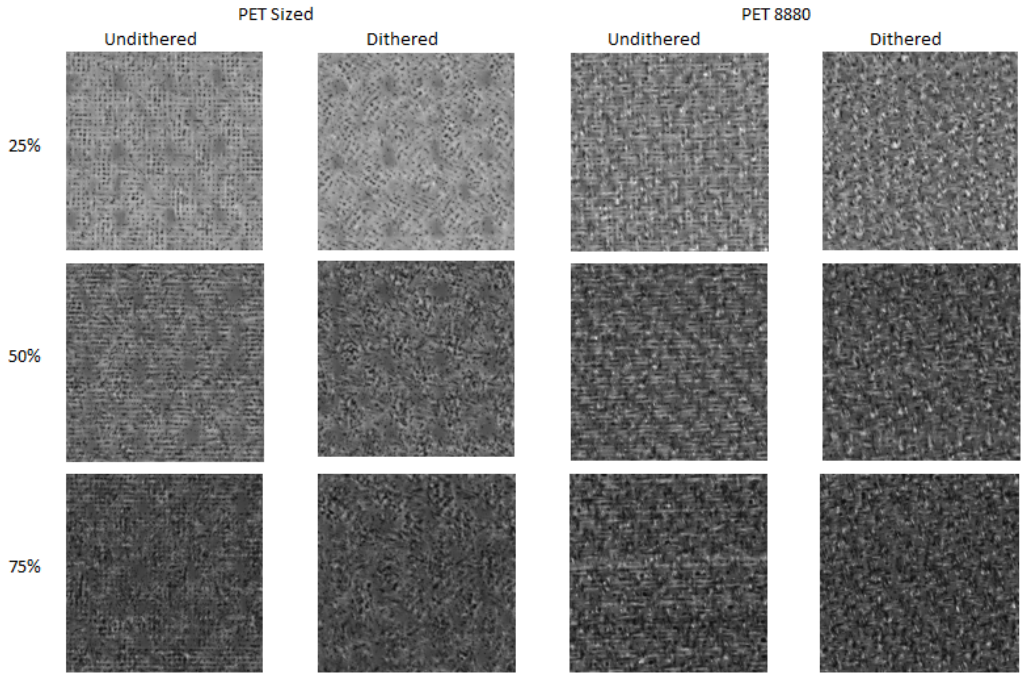

Figure 70: Dithered and undithered solid ink jet prints on fabrics; scanned images

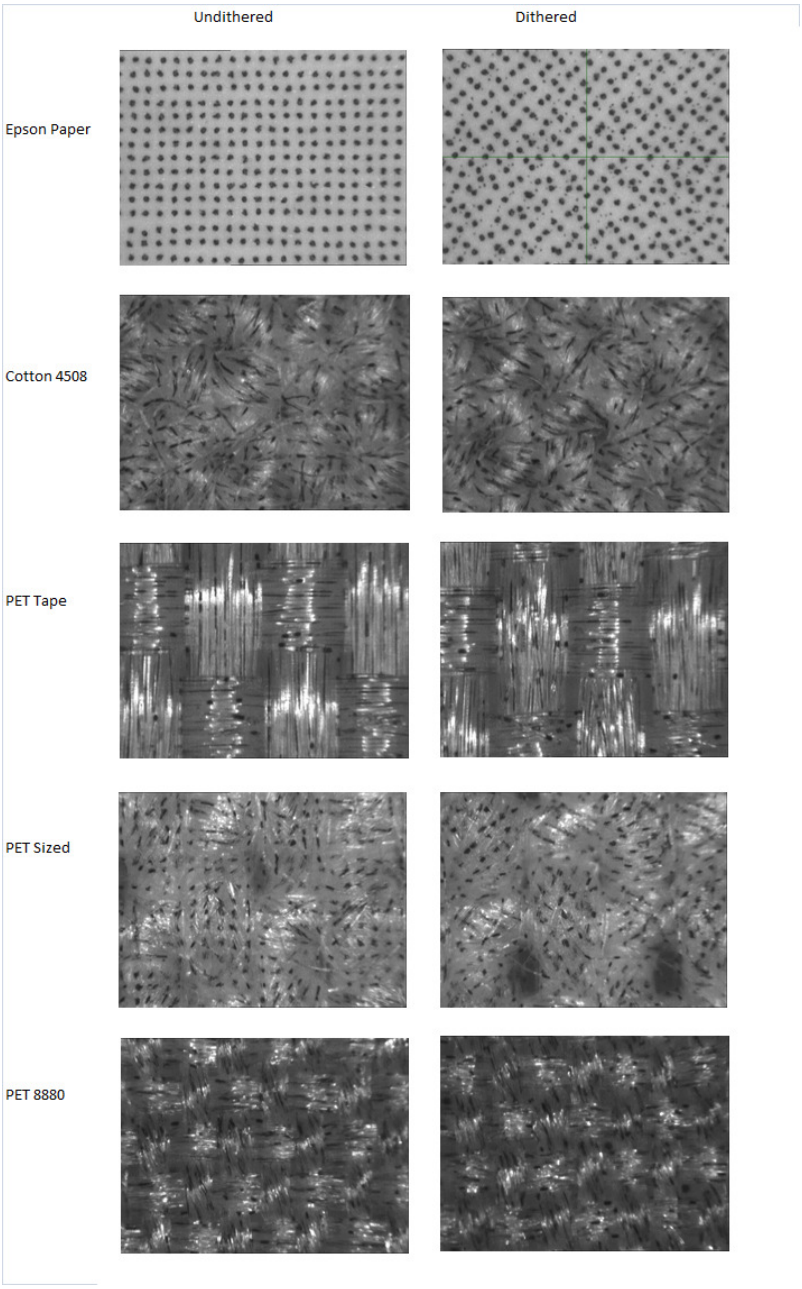

Figure 71: Dithered and undithered solid ink jet prints on fabrics (25% ink coverage); microscopic images

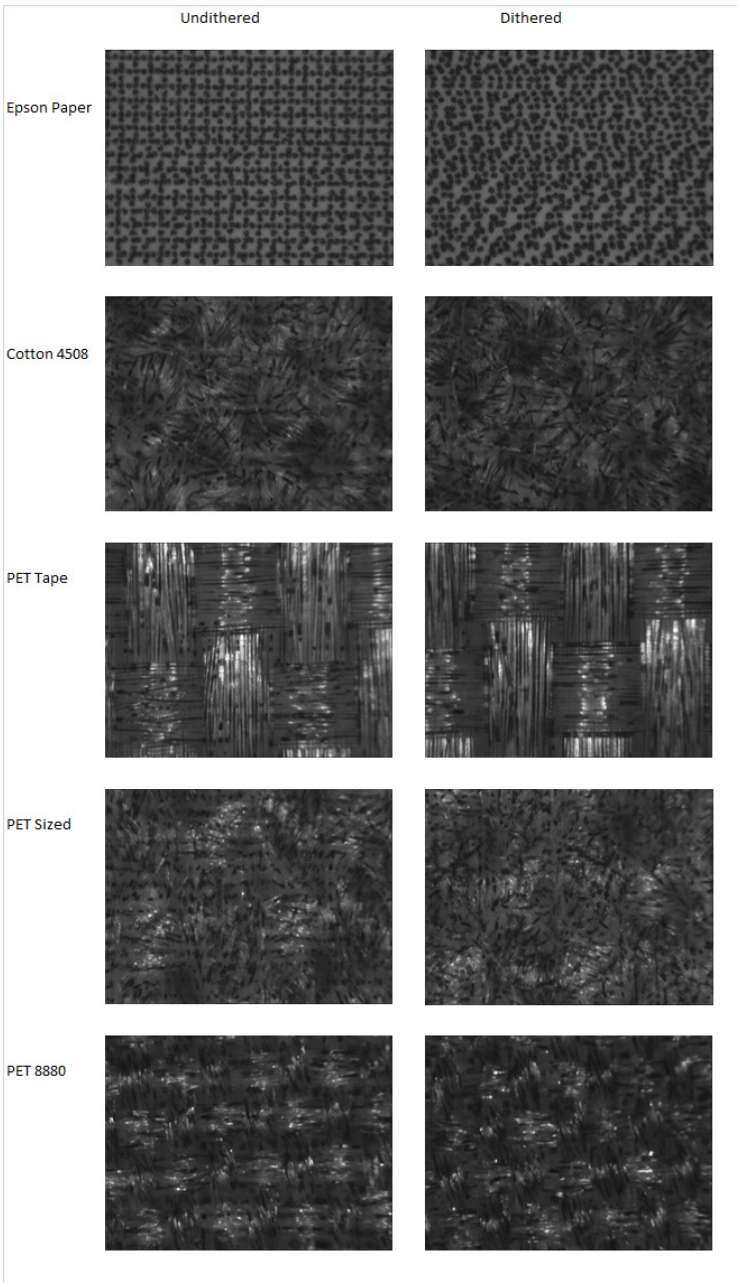

Figure 72: Dithered and undithered solid ink jet prints on fabrics (75% ink coverage); microscopic images

REFERENCES

1. Hollies, N., M.M. Kaessinger, and B. Watson, *Water Transport Mechanism in Textile Materials Part II: Capillary-Type Penetration in Yarns and Fabrics.* Textile Research Journal, 1957. **27**: p. 8.

2. Hsieh, Y.-L., *Liquid transport in fabric structures.* Textile Research Journal, 1995. **65**: p. 65.

3. Washburn, E.W., *The Dynamics of Capillary Flow.* Physical Reviews, 1921. **17**: p. 273.

4. Nyoni, A.B. and D. Brook, *Wicking mechanisms in yarns - the key to fabric wicking performance.* Journal of the Textile Institute, 2006. **97**: p. 119.

5. Perwuelz, A., P. Mondon, and C. Caze, *Experimental Study of Capillary Flow in Yarns.* Textile Research Journal, 2000. **70**: p. 333.

6. Hsieh, Y.L. and B. Yu, *Liquid wetting transport and retention properties of fibrous assemblies. I. Water wetting properties of woven fabrics and their constituent single fibres.* Textile Research Journal, 1992. **62**: p. 677.

7. Hsieh, Y.L., B. Yu, and M.M. Hartzell, *Liquid wetting transport and retention properties of fibrous assemblies. II. Water wetting and retention of 100% and blended woven fabrics.* Textile Research Journal, 1992. **62**: p. 697.

8. Pezron, I., G. Bourgain, and D. Quere, *Imbibition of a Fabric.* Journal of Colloid and Interface Science, 1995. **173**: p. 319.

9. Bayramli, E. and R. Powell, *The normal (transverse) impregnation of liquids into axially oriented fiber bundles.* Journal of Colloidal Interface Science, 1990. **138**: p. 346.

10. Bayramli, E. and R.L. Powell, *Experimental investigation of the axial impregnation of oriented fiber bundles by capillary forces.* Colloids and Surfaces, 1991. **56**: p. 83.

11. Zhang, Y., et al., *Modeling of capillary flow in shaped polymer fiber bundles.* Journal of Materials Science, 2007. **42**: p. 8035.

12. Rajagopalan, D., A.P. Aneja, and J.M. Marchal, *Modeling capillary flow in complex geometries.* Textile Research Journal, 2001. **71**: p. 813.

13. Liu, T., K.-f. Choi, and Y. Li, *Wicking in Twisted Yarns.* Journal of Colloid and Interface Science, 2008. **318**: p. 134.

14. Wiener, J. and P. Dejlová, *Wicking and wetting in textiles.* AUTEX Research Journal, 2003. **3**: p. 64.

15. Yoon, H.N. and A. Buckley, *Improved comfort polyester. I. Transport properties and thermal comfort of polyester/cotton blend fabrics.* Textile Research Journal, 1984. **54**: p. 289.

16. Hsieh, Y.-L., *Wetting Contact Angle Derivations of Cotton Assemblies of Varying Parameters.* Textile Research Journal, 1994. **64**: p. 553.

17. Patel, N. and L.J. Lee, *Modeling of void formation and removal in liquid composite molding. Part I: wettability analysis.* Polymer Composites, 1996. **17**: p. 96.

18. Minor, F.W., et al., *The Migration of Liquids in Textile Assemblies: Part II: The Wicking of Liquids in Yams.* Textile Research Journal, 1959. **29**: p. 931.

19. Chen, X., et al., *The wicking kinetics of liquid droplets into yarns.* Textile Research Journal, 2001. **71**: p. 862.

20. Minor, F.W., et al., *Pathways of Capillary Migration of Liquids in Textile Assemblies.* American Dyestuff Reporter, 1960. **49**: p. 37.

21. Kissa, E., *Capillary Sorption in Fibrous Assemblies. J.Colloid Interface Sci. 83 (1), 265-272 (1981).* Journal of Colloid and Interface Science, 1981. **83**: p. 265.

22. Kawase, T., et al., *Spreading of Liquids in Textile Assemblies. Part I: Capillary Spreading of Liquids.* Textile Research Journal, 1986. **56**: p. 409.

23. Kawase, T., et al., *Spreading of Liquids in Textile Assemblies, Part II: Effect of Softening on Capillary Spreading,.* Textile Research Journal, 1986. **56**: p. 617.

24. Adams, K.L. and L. Rebenfeld, *In-Plane Flow of Fluids in Fabrics: Structure/Flow Characterization.* Textile Research Journal, 1987. **57**: p. 647.

25. Arora, D., A.P. Deshpande, and S.R. Chakravarthy, *Experimental investigation of fluid drop spreading on heterogeneous and anisotropic porous media.* Journal of Colloid and Interface Science, 2006. **293**: p. 496.

26. Kumar, S.M. and A.P. Deshpande, *Dynamics of drop spreading on fibrous porous media.* Colloids and Surfaces A: Physicochemical and Engineering Aspects, 2006. **277**: p. 157.

27. Calvert, P., et al. *Soft structured sensors and connectors by inkjet printing*. in *ACS National Meeting*. 2006. Atlanta, GA, United States: American Chemical Society.

28. Sawhney, A., et al. *Piezoresistive sensors on textiles by ink jet printing and electroless plating*. in *Materials Research Society Symposium Proceedings*. 2006. Boston, MA, USA: Materials Research Society.

29. Ujiie, H., ed. *Digital Printing of Textiles*. 1st ed. Woodhead publishing in textiles, ed. H. Ujiie. 2006, CRC Press and Woodhead Pub.

30. Dawson, T.L., *Ink-jet printing of textiles under the microscope.* Journal of the Society of Dyers and Colourists, 2000. **116**: p. 52.

31. *ISO/IEC 13660, Information technology — Office equipment — Measurement of image quality attributes for hardcopy output —Binary monochrome text and graphic images*, 2001.

32. Fan, Q., et al. *Effects of Pretreatments on Print Qualities of Digital Printed Fabrics*. in *NIP 18, International Conference on Digital Printing Technologies*. 2002. San Diego, CA, USA.

33. Fan, Q., et al., *Fabric Pretreatment and Digital Textile Print Quality.* Journal of Imaging Science and Technology, 2003. **47**: p. 400.

34. Park, H., et al., *Image Quality of Inkjet Printing on Polyester Fabrics.* Textile Research Journal, 2006. **76**: p. 720.

35. Preparation/Finishing of Cotton Fabrics (Desizing, Scouring, Bleaching and DP Finishing), Lab Hand-out, PTFE Department, Georgia Institute of Technology.

36. http://www.dimatix.com/, Date accessed November 5, 2006.

37. Liu, T. and K.F. Choi, *Capillary rise between cylinders.* Surface and Interface Analysis, 2008. **40**: p. 368.

38. Chang, C.J., et al., *Effects of polymeric dispersants and surfactants on the dispersing stability and high-speed-jetting properties of aqueous-pigment-based ink-jet inks.* Journal of Polymer Science Part B-Polymer Physics, 2003. **41**: p. 1909.

39. Fu, Z., Rohm, and Haas, *Digital Printing of Textiles*, in *Digital Printing of Textiles*, H. Ujiie, Editor. 2006, CRC Press and Woodhead Pub. Ltd. p. 218.

40. Lee, H.K., M.K. Joyce, and P.D. Fleming, *Influence of pigment particle size and pigment ratio on printability of glossy ink jet paper coatings.* Journal of Imaging Science and Technology, 2005. **49**: p. 54.